ABSTRACT

REYNOLDS, WILLIAM LEONARD. Sustainable Service Rate Analysis at Signalized Intersections with Short Left Turn Pockets Using Macroscopic Simulation. (Under the direction of Dr. Nagui M. Rouphail).

A macroscopic simulation tool is developed and tested in order to quantify the effects of short turn pockets on the sustainable service rate of a signalized intersection. Unlike the theoretical signal capacity, the sustainable service rate includes queue interaction effects and is thus influenced by blockage and spillback at the entrance to a short turn pocket. Previous research on the topic has focused either on the probability of spillback from a short turn pocket or the operation of a system with a single approach lane. No macroscopic model currently available has the ability to analyze throughput reductions due to short turn pocket effects on a multilane approach. The model described herein utilizes a series of flow and density restrictions on cells of varying sizes on the approach to the intersection. Results indicate sensitivity of the model to turn pocket spillback, blockage, saturation flow rate, pocket length, lane utilization, phase sequence, phase overlap, permitted phasing, and time-dependent demand. A phase optimization procedure is also described to help efficiently allocate green time for a given set of turn pocket lengths and turn movement percentages. Outputs from the model compare favorably to results generated using microsimulation software, and recommendations are made regarding additional model enhancements and testing needs.

Sustainable Service Rate Analysis at Signalized Intersections with Short Left Turn Pockets Using Macroscopic Simulation

by
William Leonard Reynolds

A thesis submitted to the Graduate Faculty of
North Carolina State University
in partial fulfillment of the
requirements for the degree of
Master of Science

Civil Engineering

Raleigh, North Carolina

2010

APPROVED BY:

_____	_____
Dr. Nagui M. Rouphail Committee Chair	Dr. Billy M. Williams
_____	
Dr. George F. List	

DEDICATION

This thesis is dedicated to my ever-supportive parents, Charla and Tom Reynolds, and my loving and awe-inspiring wife, Johanna.

BIOGRAPHY

William Reynolds was raised in Culpeper, Virginia by parents Charla and Tom Reynolds. He earned a B.S. in both Environmental Science and Earth & Ocean Sciences in May, 2005, from Duke University, and was the recipient of the 2005 U.S. Forest Service Science Award. He entered the Civil Engineering program at North Carolina State University in 2007 and expects to graduate with an M.S. in May, 2010.

During his time at N.C. State, William served as a graduate research assistant on Project C-05 of the Strategic Highway Research Program under advisor Dr. Nagui M. Rouphail. Starting in the summer of 2009, he also worked with Triangle Transit on the proposed light rail system for the Triangle region. He was awarded membership into the honor society of Phi Kappa Phi for maintaining a 4.0 GPA throughout his graduate career and was named a 2010 CUTC Student of the Year. He is an active member of APA, TRB and ITE, and served as ITE's student chapter vice president from 2008-09. After graduation, he plans to move to Minneapolis, MN with his wife, Johanna.

ACKNOWLEDGMENTS

First and foremost, I would like to express my deepest gratitude to my advisor, Dr. Nagui M. Rouphail. His guidance, passion for the sharing of knowledge, tireless dedication to his students and colleagues, and profound curiosity has been inspirational over the past two and half years. His advice, support, and ideas made this research possible, and his questions made it stronger.

I would also like to extend a special thank you to thesis committee members Dr. Billy M. Williams and Dr. George F. List. Dr. Williams' ability to immediately absorb new ideas, share insight, and redirect focus makes him an invaluable resource, regardless of the problem. Dr. List's vision and broad outlook help frame almost any concept in a context difficult to see when too finely focused.

Dr. Xuesong Zhou and Mingxin Li deserve particular recognition for their role in developing the initial version of the simulation tool described in these pages. Dr. Zhou's creativity and keen intellect helped develop these ideas throughout the process, and Mingxin's spreadsheet implementation was the foundation for the final product from this research.

I would also like to thank the entire C-05 research team, including Wayne Kittelson, Brandon Nevers, Anxi Jia, Hyejung Hu, Nick Badal, and Li Jin. Their time and contributions set the framework for this project, and their ideas and feedback were invaluable.

Finally, I want to express a sincere thank you to Dr. Joseph Hummer and Dr. John Stone. They offered guidance and encouragement throughout my graduate program, and without them none of this would have been possible.

TABLE OF CONTENTS

LIST OF TABLES

LIST OF FIGURES

LIST OF VARIABLES

AVD	Approach Vehicle Distribution; Percentage of all vehicles on the approach in the letmost through lane (lane 1).
AVS	Average Vehicle Spacing. Distance between front bumpers of queued vehicles.
f_{LT}	Left turn adjustment factor.
$f_{Q\text{-}LT}$	Binomial variable; 1 when $k_{G\text{-}LT} = k_{jam}$, otherwise 0.
k_{LR}	Total density in the loading region (veh./mi./ln.).
k_G	Total density in the gating region (veh./mi.ln.)
$k_{G\text{-}LT}$	Density of left turning vehicles in the leftmost through lane of the gating region (veh./mi./ln.).
$k_{G\text{-}TH}$	Density of through vehicles in the gating region (veh./mi./ln.).
$k_{G\text{-}Lane1}$	Hypothetical density of the leftmost through lane in the gating region (veh./mi./ln.).
$k_{P\text{-}LT}$	Density in the left turn pocket region (veh./mi./ln.).
$k_{P\text{-}TH}$	Density in the through storage region adjacent to the pocket (veh./mi./ln.).
k_Q	Total density in the queue storage region (veh./mi./ln.).
$k_{Q\text{-}LT}$	Density of left turning vehicles in the leftmost through lane of the queue storage region (veh./mi./ln.).
$k_{Q\text{-}TH}$	Density of through vehicles in the queue storage region (veh./mi./ln.).
L_{P1}	Major Pocket length.
L_{P2}	Minor Pocket Length.
L_Q	Queue Storage Region Length.
L_{LR}	Loading Region Length.
Lane 1	Leftmost lane on the approach, upstream of the turn pocket entrance. Lane count proceeds from left to right (ie. with 3 lanes, lane 2 is the middle lane, lane 3 the rightmost approach lane.
LTS_{Lane1}	Left Turn Split; Within the leftmost through lane (lane 1), percentage of left turning vehicles.
M	Number of through lanes.
N	Number of exclusive left turn lanes.
n	Vehicle count.
n_{LR}	Total number of vehicles in the loading region.
$n_{LR\text{-}LT}$	Number of left turn vehicles in the loading region.
$n_{LR\text{-}TH}$	Number of through vehicles in the loading region.
n_G	Number of vehicles in the gating region.
$n_{G\text{-}LT}$	Number of left turning vehicles in the leftmost through lane of the gating region.
$n_{G\text{-}TH}$	Number of through vehicles in the gating region.
$n_{G\text{-}TH\text{-}Lane1}$	Number of through vehicles leftmost through lane of the gating region.
$n_{P\text{-}LT}$	Number of left turn vehicles in the left turn pocket region.

$n_{P\text{-}TH}$	Number of through vehicles in the through storage region adjacent to the pocket.
n_Q	Number of vehicles in the queue storage region.
$n_{Q\text{-}LT}$	Number of left turning vehicles in the leftmost through lane of the queue storage region.
$n_{Q\text{-}TH}$	Number of through vehicles in the queue storage region.
$n_{Q\text{-}TH\text{-}Lane1}$	Number of through vehicles in the leftmost through lane of the queue storage region.
p_{LT}	Percentage left turn demand on the approach.
p_{HV}	Percentage heavy vehicle demand on the approach.
p_{RT}	Percentage right turn demand on the approach.
p_{TH}	Percentage through demand on the approach.
s_o	Base saturation flow rate (veh./hr./ln.)
THVD	Through Vehicle Distribution; Percentage of through vehicles on the approach in the leftmost through lane (lane 1).
THS_{Lane1}	Through Split; Within the leftmost through lane (lane 1), percentage of through vehicles.
u_o	Base speed (mi./hr.)
v_{LR}	Output flow rate from the loading region (veh./hr.).
$v_{LR\text{-}LT}$	Left turn vehicle output flow rate from the loading region (veh./hr.).
$v_{LR\text{-}TH}$	Through vehicle output flow rate from the loading region (veh./hr.).
v_G	Output flow rate from the gating region (veh./hr.).
$v_{G\text{-}LT}$	Left turn vehicle output flow rate from the gating region (veh./hr.).
$v_{G\text{-}TH}$	Through vehicle output flow rate from the gating region (veh./hr.)
v_Q	Output flow rate from the queue storage region (veh./hr.).
$v_{Q\text{-}LT}$	Left turn vehicle output flow rate from the queue storage region (veh./hr.).
$v_{Q\text{-}TH}$	Through vehicle output flow rate from the queue storage region (veh./hr.).

1. INTRODUCTION

1.1 Background

Short turn lanes provide one method of improving both the performance and safety at a signalized intersection by creating a storage space for turning vehicles, removing them from the stream of through traffic. Insufficient bay length, however, may lead to either spillback or turn pocket blockage, which can reduce the effective operating capacity of an intersection, introduce significant delay, as well as create hazardous traffic conditions. It is therefore critical to both properly design turn pockets as well as periodically revisit signal timing plans as demand levels change in order to minimize or mitigate the occurrence of spillback and blockage.

When analyzing short turn pocket effects, it is helpful to discuss throughput in terms of the effective **sustainable service rate (SSR)** of an intersection:

SSR - The maximum sustainable throughput, by movement, that is able to proceed through a signalized intersection accounting for queue interaction and blockage effects.

Unlike signal capacity, a theoretical value based on the relationship between the saturation flow rate and the signal timing plan, SSR takes into account upstream signal metering effects and queue storage limitations. Just as queue interaction at closely spaced intersections may prevent an intersection from operating at signal capacity (Rouphail and Akcelik, 1998), turn

pocket blockage and spillback have the potential to reduce the maximum sustainable throughput from an intersection relative to the theoretical signal capacity.

1.2 Problem Statement

Although turn pocket analysis has taken on a variety of forms, there is no single widely-accepted model used today that is able to efficiently and comprehensively analyze turn pocket effects. For design purposes, NCHRP Report 279 (Neuman, 1985) recommends that the length of a left-turn bay should be designed to be twice the total length of the average number of arrivals of left turning vehicles per cycle. Due to its simplicity, this method has been widely used in the field, but by ignoring signal timing and departure rates, the method is subject to bias under very low and very high arrival rates. For capacity analysis purposes, the HCM (2000) simply treats short turn pockets as full-length exclusive lanes, therefore often overestimating capacity and underestimating delay.

Although not currently widely adopted into practice, a number of models have been developed to analyze turn pocket effects based on queuing theory and probabilistic analysis. These macroscopic models provide a reliable method of analyzing intersections with a single approach lane, but very little testing has been done on the behavior of these models when more than one through lane is present. One option is to apply a through vehicle distribution factor as an input variable and analyze each approach lane independently, but this ignores the critical lane interaction effects when a turn pocket is present. For example, when spillback occurs, it is very likely that through vehicles will change lanes to avoid queues if possible.

Microscopic simulation provides one method analyzing both through vehicle lane distribution values and sustainable service rates by movement at signalized intersections with one or more short left turn pockets and multiple approach lanes, but the time consuming nature of setting up, calibrating, and testing each intersection in a mircosimulation environment often makes analysis impractical. Futhermore, microsimulation results in this context depend on the validity of the lane changing algorithms contained within the software.

In short, a simplified model capable of predicting through vehicle lane changing behavior and SSR by movement inclusive of all turn pocket effects on multi-lane approaches is needed to make turn pocket analysis both accessible and practical. A robust yet computationally efficient model would help facilitate pocket design, aid in diagnosis when SSR values drop below signal capacity values, and assist with signal retiming and a variety of other mitigation strategies.

1.3 Objectives

The following list outlines the primary objectives of this research:

- Identify the primary input variables needed to develop a robust, macroscopic model capable of analyzing SSR at signalized intersections with multilane approaches.

- Calibrate baseline parameters and queue interaction modeling logic using field data.

- Develop a macroscopic simulation tool sensitive to the following operational parameters:
    1. Pocket spillback effects
    2. Pocket blockage and starvation effects
    3. Pocket length and total storage area
    4. Phase order and timing plans
    5. Saturation flow rates
    6. Lane changing behavior
    7. Time-dependent demand by movement

- Develop methodology to optimize green time allocation given a signal phasing plan.

- Generate recommendations for further research and model enhancements.

1.4 Organization

The following document is presented in six chapters. Chapter 2 provides a detailed literature review of the available short turn pocket analysis models, highlighting their strengths, shortcomings, and practical applicability. Next, in Chapter 3, two case studies are presented to provide field context for the problem, justify model requirements, and calibrate model parameters. Chapter 4 walks through the development of the model, outlining the assumptions, simplifications, and operational effectiveness. In Chapter 5, results are

generated, analyzed, and compared against both simulation and macroscopic models. A concluding section in Chapter 6 summarizes the research findings and conclusions and provides recommendations for further research.

2. LITERATURE REVIEW

2.1 Overview

The following literature review provides a detailed description of all available turn pocket analysis models, by model type and order of development. An introductory section first describes the concept of queue accumulation and discharge, as well as the basis of queuing theory within turn pocket analysis. Three sets of models are then discussed that were developed with design practice in mind, using queuing theory to predict *probability* of spillback and blockage under specific demand regimes for design purposes. The subsequent set of models described focus on capacity analysis, and while related to the first set, were largely developed under the assumption of continuous queue (i.e. oversaturated conditions), and therefore take on a slightly modified type of probabilistic analysis. Finally, a concluding section discusses the limitations of even the most robust macroscopic models available, and the need for additional research to make turn pocket analysis more practical and applicable for practitioners.

2.2 Concepts and Definitions

Before discussing individual models in detail, it will be helpful to first examine a standardized set of terminology for the accumulation and discharge of vehicles in queues at a signalized intersection. Originally based on the classical first-order model by Lighthill and Whitham (1955), a common analytical concept is the Cartesian plane, where vehicle arrivals and departures from the stop bar are plotted against time on the horizontal axis. As shown in

Figure 1, the area between the arrival and departure lines represents the queue of vehicles, called the QAP, or queue accumulation polygon (Viloria *et al*, 2000).

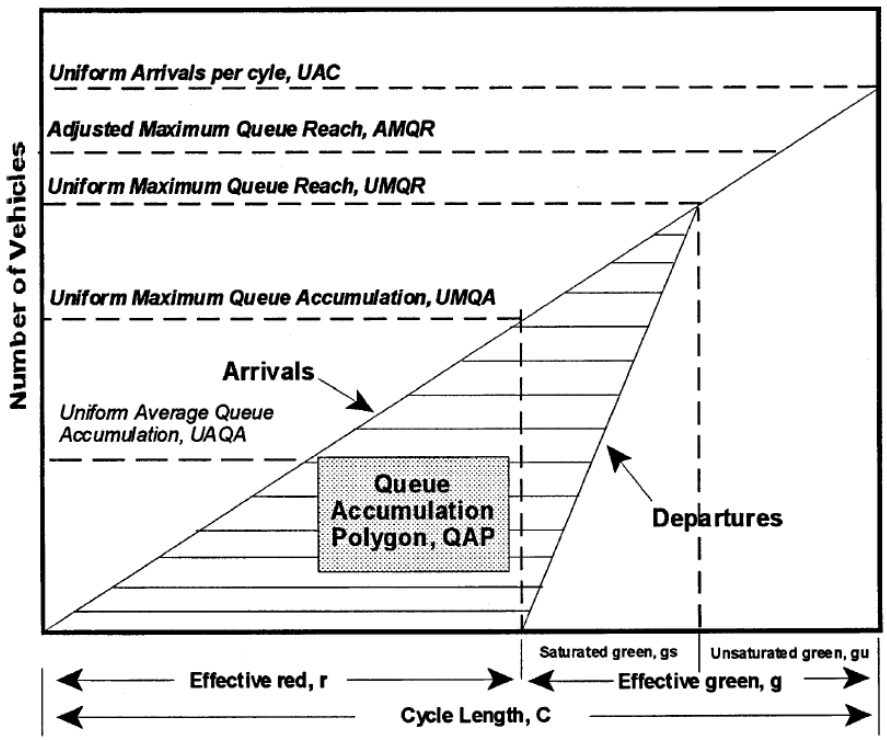

Figure 1 - Queue Accumulation and Discharge (Viloria *et al*, 2000)

Vehicles arriving on red must wait at the stop bar, and queues begin to build from this point based on the arrival rate of vehicles, or the Uniform Arrivals per Cycle (UAC). The Uniform Maximum Queue Accumulation (UMQA) refers to the total number of vehicles arriving on red, assuming uniform arrivals. For isolated intersections with fully random arrivals, the Uniform Average Queue Accumulation (UAQA) is simply half of the UMQA. Both of these terms are queue accumulation terms and therefore refer to the total number of vehicles actually contained with a queue.

Uniform Maximum Queue Reach (UMQR) refers to the position of the last queued vehicle relative to the stop bar at any point in time. Due to the fact that queues clear from the stop bar, queue reach continues to grow after the end of the red phase, reaching a maximum only when the queue has been fully served. Recognizing that the assumption of uniformity underestimates the effects of random arrivals and overflow from previous cycles, some models adjust the UMQR upward to produce a more realistic value called the Adjusted Maximum Queue Reach (AMQR).

Turn pocket analysis builds upon the concepts of queue accumulation, but must also investigate the relationship between queues as they interact due to the limited storage. Recent work by Kikuchi, Kronprasert and Kii (2007) provides perhaps the clearest description of the complicating effects of queue interaction in the context of queuing theory. Figure 2 shows an example of an approach with a three-branch fork, where a single feeder lane splits into 3 separate service channels. Spillback from any one of the three service channels has the potential to disrupt operation on one or both of the other lanes, preventing the use of any analysis technique that focuses solely on individual lanes. This presents an interesting problem in queuing theory due to the fact that vehicles cannot enter the desired channel despite the channel being open for service. This is a common operational problem in transportation, such as tracks splitting into multiple directions in a rail yard (Kikuchi, Kronprasert and Kii, 2007), and the following discussion of analysis methods based on queuing theory can provide some insight into the methods necessary to modify basic assumptions in order to apply to such transportation service channel bottleneck problems.

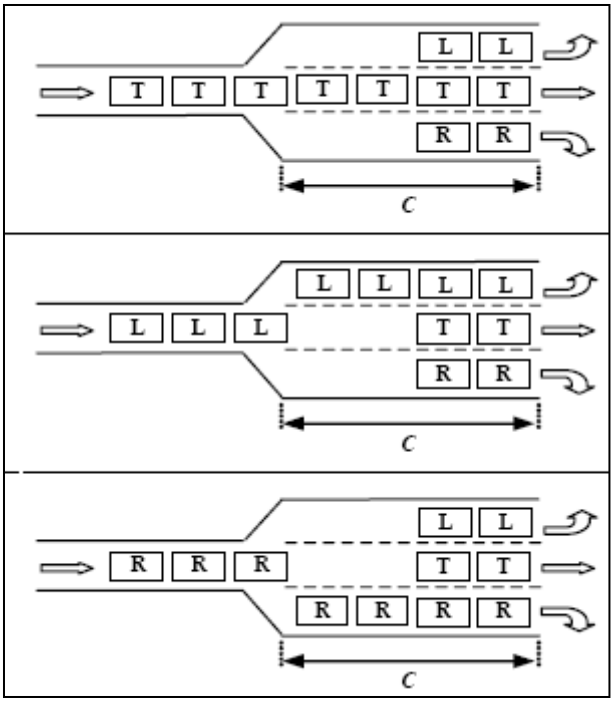

Figure 2 - Three-Branch Fork Example (Kikuchi, Kronprasert and Kii, 2007)

2.3 Bay Length Design Models

Oppenlander and Oppenlander

Basic queuing theory provides mathematical relationships between an input source, queue, and service mechanism. Most models assume all interarrival times as well as all service times are all independent and identically distributed. In transportation applications, it is often assumed that both the interarrival times and service times follow an exponential, or Markovian (M) distribution. By the common naming convention, these are simply called M/M/s models, referring to the distribution of interarrival times, the distribution of service times, and the number of servers, respectively. Other possible models in queuing theory include a degenerate distribution (D), an Erlang distribution (E_k), and any arbitrary general distribution (G).

Oppenlander and Oppenlander (1989) were among the first to apply queuing theory to turn pocket analysis. Simply, they modeled the queue within a turning pocket at a signalized intersection with a single, protected turn phase as a queue system with a Poisson arrival pattern, an exponential service distribution, and one server. In this basic M/M/1 model, the arrival rate is the average turn demand, and the service rate is the capacity of the turning lane. Percentile queue lengths, in number of vehicles, were then derived from the following queuing equation:

$$P_n = (1 - \lambda/\mu)\,(\lambda/\mu)^n$$

P_n = Probability of n vehicles in queue
λ = arrival rate (veh./hr.)
μ = service rate (veh./hr.)
n = number of vehicles in queue

By converting the arrival rate into passenger car equivalents and assuming constant vehicle spacing, the authors were able to develop a series of tables to serve as turn pocket design guidelines based on acceptable percentile queue lengths. Although each service channel was analyzed independently, the authors did recognize the need to check for blockage from the through lane, and advised using the larger of the two storage lengths calculated (turn pocket and adjacent through) when obtaining an appropriate pocket length.

By definition, such a model assumes a continuously serving queue based on the service capacity of the signal. This improperly represents the stop-and-go operation of a signalized intersection, and ignores the fact that most of the queue buildup at a signal occurs during the red phase. Subsequent studies by Qi *et al.* (2007) showed that this M/M/1 model

significantly underestimates maximum queue length due to this assumption regarding continuously serving queue.

Kikuchi

In an attempt to develop a more comprehensive set of guidelines for the design length of left turn lanes based on arrival and departure rates, Kikuchi *et al*. (1993) analyzed turn pockets from two aspects: (a) the probability of pocket spillback and (b) the probability of blockage by through vehicles in the adjacent lane. To begin, the authors determined the problem of pocket spillback to be largely related to turning volumes, protected phase green time, cycle length, and opposing volumes during the permitted phase, while the blockage problem was assumed to be related to through demand and through red time. A Discrete Time Markov Chain (DTMC) formulation was developed to model the number of turning vehicles in queue at the beginning of the protected phase, or the point at which queue lengths are most likely to be longest. Unlike the M/M/1 formulation, such an approach is able to account for both random fluctuations in arrival patterns as well as the effects of signal timing on total queue length.

The system described is defined in terms of states and time points, with the states representing the number of vehicles waiting to turn at each time point. A one-step transition probability matrix representing the probability of a change in queue length from one time point to the next can be populated by each of the elements calculated as follows based on Poisson arrival:

$$P_{\alpha}^{\beta} = \frac{(\lambda_l \beta)^{\alpha} e^{-\lambda_l \beta}}{\alpha!}$$

P_{α}^{β} = Probability α vehicles arrive during β
β = Duration of phase or cycle of interest
λ = Arrival rate of turning vehicles (veh/s)

The probability that a given number of vehicles are queued in the pocket can be calculated using the steady state equation of the Markov chain, and with a tolerable probability of overflow, a recommended lane length can then be calculated. This value is then compared to the value calculated using arrivals of through vehicles on red to obtain a final recommendation, with independent tolerances of overflow and blockage.

This highly innovative approach provided a robust analytical tool, and the authors continued with the approach in subsequent analyses to model double left turn pockets (Kikuchi *et al*, 2004), the three-branch fork described previously (Kicuchi *et al*, 2007), and short right turn pockets with right on red allowed (Kikuchi and Kronprasert, 2008). But the approach is not without shortcomings. Most notably, the model assumes that all queued vehicles are able to clear the intersection each cycle. While the authors provided the disclaimer that the analysis was applicable only during undersaturated conditions, subsequent research showed that even with left turn v/c ratios between 0.60 and 0.80, left turn queue carryover can occur about 20% of the time (Qi *et al*, 2007). In these cases, the model will underestimate back of queue and therefore produce shorter lane length estimates than by other methods. Finally, the model must ignore any other lane interaction effects that arise when more than one through lane is present. This shortcoming is common to essentially all current analytical turn pocket models, but it is nonetheless important as any multi-through

lane analysis requires an assumption of constant demand on the turn pocket-adjacent through lane, which ignores lane utilization that may be dependent upon the presence of the turn pocket.

Qi

Recognizing the significance of leftover queue in determining the design length of turn pockets, Qi *et al*. (2007) developed a model for estimating queue in two parts: (a) the queue formed during the red phase and (b) the queue carryover from previous cycles. Although the model assumes a v/c ratio of less than one, the authors determined that even in undersaturated conditions, queue carryover provides a significant portion of the total queue. The influencing factors affecting turn pocket operation taken into account included turning volume, opposing volume, cycle length, phasing, turning vehicle headway, and vehicle mix. Figure 3 shows the modeling assumptions, with queue carryover included on the arrival and departure curve.

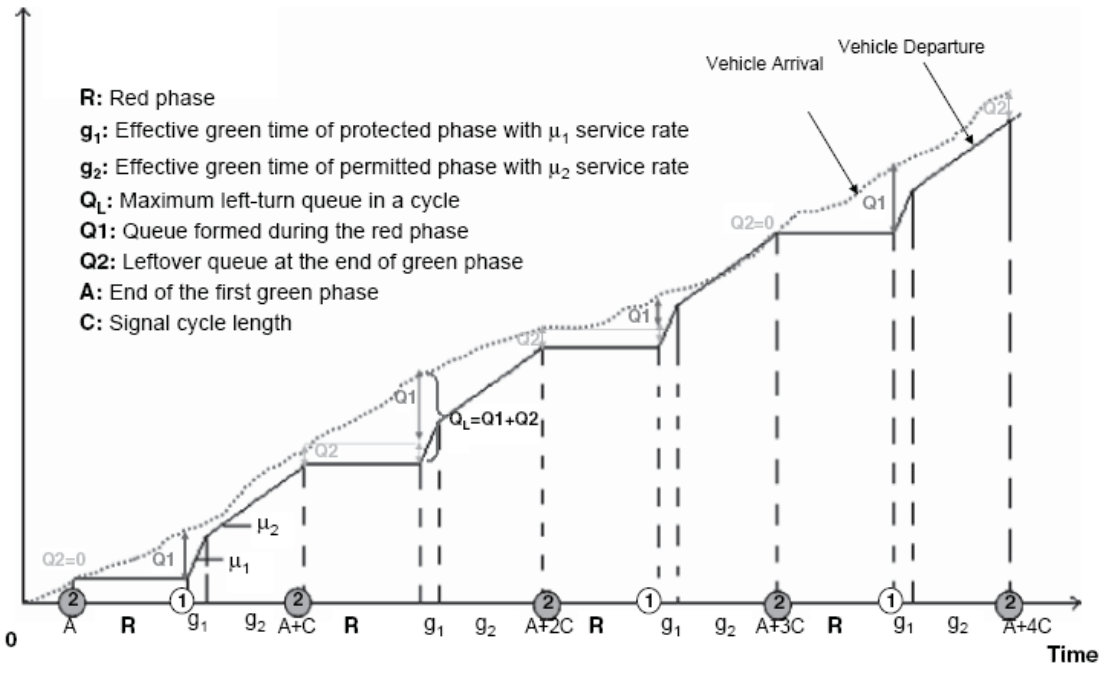

Figure 3 - Cumulative vehicle arrival and departure curve (Qi et al., 2007)

Under the assumption of Poisson arrivals at rate λ_l, the probability that a maximum number of turning vehicles (Q_1) will arrive during the red phase (R) can be estimated by:

$$P \text{ (arrivals during } R \leq Q_1) = \sum_0^{Q_1} \frac{(\lambda_l R)^k e^{-\lambda_l R}}{k!}$$

To estimate the maximum leftover queue length, Q_2, a one-step transition matrix, P, is derived using a DTMC system. Part I from Figure 4 indicates that all vehicles will be discharged from the green phase, calculated by the following equation, where *m* refers to the per-cycle capacity of the intersection, *i* the leftover queue length, and C the total cycle length:

$$P_{ij} = \sum_0^{m-i} P_k^C$$

Part II indicates that queue carryover will occur, calculated as follows, with *j* referring to the carryover queue in the next cycle:

$$P_{ij} = P^{C}_{m+j-i}$$

Finally, the elements of Part III are all equal to zero, as it is impossible to discharge more vehicles than *m*, the maximum per-cycle capacity of the signal. By assuming that the intersection represents a stable system, the steady state equation can be solved to obtain an estimate of the maximum leftover queue length, Q_2, at a given level of probability. Q_L, or the maximum total queue length at a given probability level, is then simply the summation of the arrival queue, Q_1, and leftover queue, Q_2.

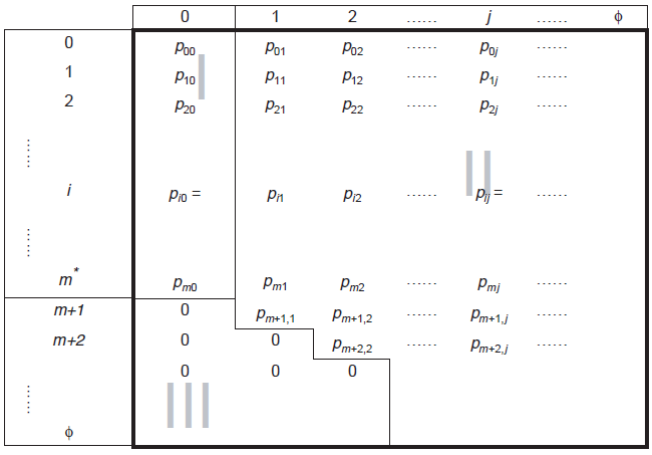

Figure 4 - One-step transition matrix (Qi et al., 2007)

The approach, although similar to the methods developed by Kikuchi *et al.* (1993), represents a significant improvement over previous models when queue carryover occurs. The authors conducted a field survey of 14 intersections, and found that the model

outperformed all existing methods in predicting left-turn queue lengths compared to actual observations.

As with previous methods, however, the Qi model requires individual lane analysis, preventing investigation of interaction between back of queue in different lanes. The model also assumes constant demand by lane and is unable to account for changes in lane utilization related to queue buildup in the turn pocket. These effects are more closely related to capacity and delay analysis, however, and the Qi model likely provides the single strongest analytical method of predicting queue length by lane. As noted, the approach is only valid in undersaturated conditions, but such is an assumption is valid when using any analytical model to predict queue lengths within a reasonable certainty for turn pocket design purposes.

2.4 Capacity Analysis Models

While the queue length models discussed above all focus on predicting percentile back of queue values for turn pocket design purposes, capacity models typically start with an assumption regarding pocket length, and use signal timing and demand levels in order to predict total intersection capacity, inclusive of turn pocket spillback and blockage effects. Capacity models therefore focus on oversaturated conditions, with an assumption of essentially continuous queue. In these cases, turn percentages and the relationship between signal timing and pocket length become the primary influencing factors on approach capacity.

Tian & Wu

Starting with an assumption of continuous queue, Tian and Wu (2006) developed a detailed capacity estimation procedure to determine the total approach capacity of an intersection with a single through lane feeding a single short right turn pocket. For model development purposes, the authors ignored right turn on red, and analyzed a single timing plan where both the right and through movements proceeded simultaneously (full overlap). With a continuous queue, it can be assumed that either pocket spillback or blockage will occur every cycle, simplifying the analysis to focus on the total expected number of vehicles in each lane at the end of the red phase.

If *x* denotes the total number of vehicles contained within both lanes, plus the blocking vehicle, the value can only vary between N+1 and 2N+1, where N denotes the length of the pocket in vehicles. The value follows a negative binomial distribution, and when blockage occurs due to a through vehicle, the expected value is calculated as follows, where p_t refers to the proportion of through vehicle demand:

$$E(x) = \sum_{x=N+1}^{2N+1} x \left[\binom{(x-1)}{N} (1-p_t)^{x-(N+1)} p_t^{n+1}\right]$$

It then follows that the expected number of vehicles in the right turn pocket, $E_r(x)$, is simply:

$$E_r(x) = E(x) - (N+1)$$

Using the same methodology, $E_t(x)$ can be determined in the case of spillback from the turn pocket. Additionally, the probability of spillback is calculated as:

$$Pr_r = \sum_{n_r=N+1}^{2N+1} \binom{(2N+1)}{n_r} (1-p_r)^{2N+1-n_r} p_r^{n_r}]$$

The probability of blockage by the through lane is calculated in the same manner using Pr_t.

With the probability of each blocking scenario, along with the expected number of vehicles in each lane for both cases, capacity analysis is conducted in two parts. During the first portion of green, c_1', each lane is able to process simultaneously, and the flow rate from each lane is determined by the expected number of vehicles contained within each lane at the beginning of the green phase. The second portion of green, c_2', consists of the total green time minus the total time needed to clear N vehicles. During this time, capacity is calculated based on HCM shared lane analysis methods.

In order to reduce the scope of the analysis, the authors included a number of simplifying assumptions that limit the practical applicability of the model. Right turns on red were ignored altogether, which is only valid when blockage results from queue buildup in the through lane. If blockage occurs as a result of pocket spillback, however, right turns on red significantly complicate the analysis required, as the red phase acts in a similar manner to an exclusive right turn phase with a low saturation flow rate. Pedestrians and heavy vehicles were also ignored, and both may affect the queue clearance time of the turn pocket, thereby affecting capacity. Additionally, the model only deals with one geometric condition with a single phasing sequence, and cannot be used with any other phasing pattern. If multiple

through lanes exist, it is feasible to apply a lane distribution factor and analyze the rightmost through lane only, but such a method ignores the effects of lane interaction and the ability of through vehicles to temporarily change lanes to bypass pocket spillback. Despite these shortcomings, the model provided the basis for a number of subsequent analysis methods.

Zhang & Tong

Starting with the same assumptions used by Tian and Wu, Zhang and Tong (2008) used a probabilistic approach to determine capacity in two specific scenarios: (a) left turn capacity when blockage from the through lane prevents full utilization of a leading left protected phase, and (b) through lane capacity when spillback prevents utilization of the through green phase preceding a lagging left phase. The analysts treated each situation independently, and calculated the probability of each case using the negative binomial distribution with an assumption of Poisson arrivals. Capacity for scenario (a) was calculated in two parts, using the expected number of vehicles in the left turn lane when blockage occurs, and the left turn saturation flow rate when no blockage occurs. The capacity of the leftmost through lane from scenario (b) was calculated using the same method.

Although the model was able to improve upon the HCM methodology for capacity analysis when blockage and spillback occur, the practical applicability of the model is very limited due to the fact that the analysts only examined a fully exclusive left turn phase with no overlap. Furthermore, the authors provided no discussion of the relationship between left turn capacity and green time relative to pocket length. In fact, the assumption was that when blockage occurs, the capacity is equal to the expected number of vehicles contained within

the left turn pocket, ignoring cases where insufficient green time is provided to clear the pocket. Finally, as with previous models, the method requires a constant ratio of through traffic to left turn traffic, which may not be valid when multiple through lanes exist as traffic will often change lanes to bypass queues.

Wu

In a follow-up paper to the original capacity model discussed, Wu (2008) developed a series of models to examine the total approach capacity of signalized intersections under various phasing plans with one through lane and a single short left turn pocket. To maximize the applicability of the model, the author first enumerated the following boundary conditions to be contained within the model:

- The capacity of a short turn lane is less than or equal to the capacity of a full lane.
- Approach capacity is equal to the capacity of a single, full lane if the flow rate of one of the two movements (q_l or q_t) is equal to 0.
- The capacity of the approach is equal to the capacity of a shared lane when turn pocket length goes to 0.
- The ratio of flow rates remains constant for all turn pocket lengths.

The fourth condition is perhaps the least intuitive, and arises due to the assumed geometry, where a single though lane acts as the feeder lane for both the turn pocket and the adjacent through lane.

Using the distribution function of queue lengths from a waiting stream, total approach capacity, C_m, can be expressed by the following equation, regardless of the phase sequence:

$$C_M = \frac{1}{\sqrt[1+f(N_k)]{\frac{a_L}{C_L}^{1+f(N_k)} + \frac{a_T}{C_T}^{1+f(N_k)}}}$$

N_k = Pocket length in vehicles
$f(N_k)$ = Monotony ascending function of Nk
a_L = Ratio of left turn flow
a_T = Ratio of through flow ($1-a_L$)
C_L = Left turn capacity per cycle time
C_T = Through lane capacity per cycle time

When the green times of both the through phase and the protected left turn phase fully overlap, the ideal capacity of each lane (C_L and C_T) can be calculated using the effective green time and saturation flow rate (HCM methods). When the green times are fully exclusive of one another (leading or lagging left), each of the maximum capacity values must be calculated using the following equations:

$$C_L = \frac{1}{\frac{a_L a_T}{2+a_L {N_k}^3}+\frac{1}{C_L}}; \; C_T = \frac{1}{\frac{a_L a_T}{2+a_T {N_k}^3}+\frac{1}{C_T}}$$

In the final step of model development, the author used VISSIM (PTV, 2008) to obtain a calibrated model parameter, $f(N_k)$, for both the fully exclusive and full overlap models. Any phasing plan with partial overlap can then be calculated by using a weighted average of the fully exclusive phase and the full overlap phase, based on the total overlap time, ΔG.

To date, the models provide the most robust set of analytical tools to analyze approach capacity with short lane effects taken into account. Due to the assumption of continuous queue, the models can be applied to any phase sequence with a single turn pocket and an adjacent through lane. For example, while the author dealt explicitly with a leading left phase when developing the fully exclusive model, a lagging left phase uses the same equations, producing the same results. In other words, in terms of capacity, there is no difference between a lagging left phase and leading left phase in oversaturated conditions with a single through lane. The relative difference between these two phasing patterns arises when attempting to minimize delay to each movement in undersaturated conditions.

One limitation of the model is the inability to easily account for left turn phases that include both a protected and permitted phase. The author has recently produced a detailed analysis of the capacity of a shared lane with a permitted phase (Wu, 2009), however, and it may be possible to synthesize this work to produce a more robust model. Additionally, the model only deals with a single approach lane, limiting the practical applicability to situations with multiple through lanes where vehicles have the ability to bypass queues. Further study will be needed to obtain a reliable lane distribution model that takes into account short turn pocket effects, which could then be used in conjunction with this model to analyze multi-lane approaches.

2.5 Macroscopic Software

SIDRA

The Signalized and Unsignalized Intersection Design and Research Aid (SIDRA) program (Ackelik & Associates, 2004), a micro-analytical traffic evaluation tool, was among the first to develop a highly detailed queue-length analysis procedure, intended primarily for design purposes. The program effectively performs percentile back of queue calculations based on demand levels and signal capacity, which can be used to anticipate blockage or spillback effects. In undersaturated conditions, SIDRA can be very useful for analyzing queue lengths relative to storage capacity, but the model stops short of analyzing queue interaction. In other words, analysts have the tools necessary to predict pocket spillback as well as pocket blockage by queues from the through lanes, but the complicated relationship between back of queue interaction in adjacent lanes is largely left up to interpretation. As such, SIDRA is currently unable to provide valuable sustainable service rate estimations in oversaturated conditions as the software does not specifically translate a high probability of spillback into an impedance factor within the adjacent lane.

In an effort to standardize the practice of queue-length analysis, the HCM 2000 included a detailed analysis procedure based on the methods developed for the SIDRA package (Viloria *et al*., 2000). HCS+ therefore performs similar calculations to those contained within the full SIDRA INTERSECTION model, providing back of queue and delay estimates, but fails to reduce throughput due to a blockage or spillback.

Synchro

Synchro is a macroscopic analysis and optimization tool that uses HCM 2000 methods for capacity analysis, but also incorporates a term for blocking delay within the delay calculations. As such, for timing plan optimization, Synchro does have the ability to account for turn pocket spillback blockage analytically. However, the tool was developed for signal timing purposes, and is unable to explicitly reduce the effective operating capacity of an intersection due to queue interaction.

As an example of the critical difference between delay estimation and throughput analysis inclusive of turn pocket effects, consider an intersection with two left turn bays of different lengths. For truly effective sustainable service rate estimates in oversaturated conditions, the critical point of interest would be the position of the turn pocket entrance relative to the stop bar, as once queues extend beyond this point, queue interaction impedes flow. In SYNCHRO, this point is not provided as an input, as the package only asks for the "average length of the lanes" in order to determine the total storage within the turn pocket area. For delay purposes, this value is likely sufficient for predicting blocking delay when the turn pocket region reaches storage capacity, but for throughput calculations with continuous queues, the position of the pocket entrance become critical.

2.6 Mesoscopic Software

DYNASMART-P

DYNASMART-P is a mesoscopic modeling platform that allows for network-level analysis while still maintaining individual vehicle identity, therefore acting as a bridge between microscopic and macroscopic simulation. It is able to maintain efficiency by tracking vehicle trajectories while using macroscopic traffic flow characteristics on individual links. Reynolds *et al*. (2010) documented the implementation of a gating mechanism within DYNASMART-P at the entrance to short left turn pockets, improving upon the model's capabilities for handling mid-link perturbations. The improvements enable sensitivity to turn pocket spillback, blockage, signal timing, and phase sequencing on multilane approaches by generating a vertical queue at the entrance to the turn pocket when blockage occurs.

The logic contained within this research paper is heavily used in this thesis, and represents a starting point for the development a macroscopic simulation tool. Due to the need for computational efficiency when analyzing entire networks, DYNASMART-P updates vehicle positions every 6 seconds, however, limiting reliability for very short turn pockets where vehicles are able to clear both the turn pocket and the intersection during the time step. The model also ignores short right turn pocket effects, recommending this addition as a need for further research. Perhaps most importantly, however, the enhancements to DYNASMART-P described in the paper are not available in any commercially distributable version of the software, preventing practical use in the field of the concepts described.

2.7 Summary

As has been shown, there is no single macroscopic model or software package that is capable of analyzing the sustainable service rate of intersections with short left turn pockets in oversaturated conditions with multiple approach lanes. The vast majority of turn pocket analysis has focused on delay and back of queue estimation in undersaturated conditions, and as a result, the HCM currently includes a fairly robust back of queue estimation procedure. Only a relatively small number of models have been developed for capacity analysis in oversaturated conditions, however, and none of these examined approaches with multiple through lanes.

Of the models and software packages discussed, only Wu's analytical models will be used for comparison purposes in this research. None of the queuing theory macroscopic models or macroscopic software packages provides any estimate of throughput inclusive of blockage effects, and therefore provides little use for capacity analysis purposes. Of the macroscopic capacity analysis models, Wu's models can be used with a variety of pretimed phasing patterns, providing the most flexibility of use. Basic assumptions will need to be made regarding initial lane distributions as Wu's equations deal only with the interaction between the leftmost through lane and the turn pocket, but these equations certainly represent the state-of-the-art of macroscopic turn pocket capacity analysis procedures.

In addition to recognizing the deficiencies of available models, prior to model development, it is necessary to obtain field-validated parameters used as the foundation of any macroscopic model. Additionally, it is critical to observe driver behavior in the field in the presence of turn pocket effects to aid in the development of lane changing logic for a

model capable of analyzing multi-lane approaches. In the following chapter, two sets of field data will be used to examine vehicle spacing in queue, vehicle positioning at the onset of blockage, observed saturation flow rates, pocket storage capacity with permitted phasing, as well as through vehicle lane distribution and lane changing behavior on the approach to the entrance of a turn pocket at heavily congested intersections. These calibrated parameters and behavioral observations will then provide the foundation for model development in Chapter 4.

3. CASE STUDIES

3.1 Objectives

This chapter documents observations of driver behavior and vehicle interaction effects at two congested sites with short left turn pockets with the goal of developing a real-world conceptual foundation that can be used for model development. As extremely oversaturated conditions with effectively continuous queues are very difficult to observe in the field, the field data collection focused primarily on parameter calibration rather than actual capacity observations for comparison purposes.

The following characteristics were observed in the field:

- Vehicle spacing in queue
- Saturation flow rates
- Storage capacity of turn pocket with permitted phase (due to sneakers)
- Position of blocking vehicle relative to the stop bar
- Through vehicle lane distribution upstream of the turn pocket entrance

The overall magnitude of observations necessary for model comparison purposes excludes any option to collect real-world capacity observations, and microsimulation will be used for final comparison. But with valid field observations of the parameters outlined above, any model developed will be tied directly to real world conditions.

Two sources of real-world observations were selected for this study: NGSIM data from Atlanta, GA, and actual peak hour observations of a congested intersection in Raleigh,

NC. The NGSIM dataset provides a rare opportunity to generate actual vehicle trajectories, which were used to observe all parameters of importance outlined above. Field data collected from an intersection in Raleigh, NC, included less detail due to cost and time limitations, and therefore focused on calibration of vehicle spacing, lane utilization, and the position of the blocking vehicle relative to the stop bar. Each source of real-world data, including collection and analysis procedures, are discussed in detail in the following sections.

3.2 NGSIM – Atlanta, GA

3.2.1 Dataset

Sponsored by FHWA, the Next Generation Simulation (NGSIM) program (2008) set out to create a group of detailed datasets that could be used freely by the research community for algorithm development and validation purposes. The Peachtree Street dataset from Atlanta, Georgia in particular provides one method to examine turn pocket blockage and lane distribution using highly detailed, real-world data from one easily accessed source with no need for field data collection. Generated using a series of video cameras mounted on buildings along a 2,100-foot north-south stretch of Peachtree Street in downtown Atlanta, the 30-minute bi-directional dataset provides detailed vehicle trajectory data at 1/10 second intervals, along with vehicle length information and signal timing data. By translating the vehicle-based data into time-space trajectory diagrams, the data can be used to track lane-by-lane queue buildup and dissipation, providing insight into the onset of blockage of the entrance to the left turn pockets.

The dataset is split into two 15-minute analysis periods collected on November 8, 2006: 1) 12:45 p.m. to 1:00 p.m. and 2) 4:00 p.m. to 4:15 p.m. The corridor includes one stop-controlled intersection as well as 4 signalized intersections. Excluding the entry segments where queues extend beyond the reach of the cameras, there are 2 short left turn pockets over the 0.4-mile section of urban arterial, both located at the intersection of Peachtree Street and 12th St. NE. The following analysis therefore focuses on both the northbound and southbound approaches to this intersection, as shown below in Figure 5, with each turn pocket labeled with the number '11.'

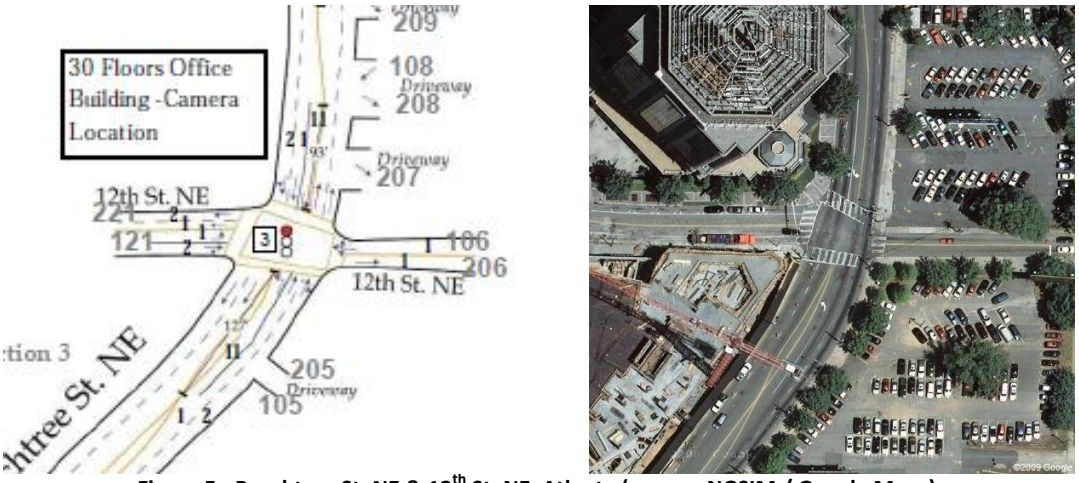

Figure 5 - Peachtree St. NE & 12th St. NE, Atlanta (source: NGSIM / Google Maps)

3.2.2 Analysis Methodology

The first step in translating the vehicle movement information into workable trajectory data was to import each of the 15-minute datasets into a spreadsheet tool capable of processing approximately 500,000 lines of data (Excel 2007). With the data separated into 23 columns, filter tools were then applied to extract the data of interest for each approach.

On the northbound approach, for example, the data was filtered to only include vehicles within Section 3 (northbound approach to 12th St.) or Intersection 3 (Peachtree & 12th St.) traveling northbound (Direction 2). To remove mischaracterized data, which is common, a redundant filter was applied to only include data from the 'Local Y' column of interest (distance measured from the entry point of the system along Peachtree Street). Once filtered, each of the four reduced dataset files (2 time periods with 2 approaches each) contained approximately 30,000 to 50,000 lines of data.

Next, a trajectory graph was constructed using time along the x-axis (Frame ID, in 1/10 seconds) and distance along the y-axis (Local Y, in feet) for each vehicle ID (series). It was helpful to perform this step first before separating the trajectories by lane due to the time consuming nature of adding nearly 200 series to any time-space graph. After each graph was developed, individual vehicles were tracked manually and removed from the graph at the point of a lane change or turning movement. Although the dataset provides "Lane ID" to aid in this process, this column often misrepresents the location of the vehicle, and "Local X" (distance from centerline, in feet) was often needed in conjunction with this information to determine the point of a lane change. Within the actual intersection, it was also common to pick up vehicle observations as they turned onto Peachtree Street, and care was taken to remove these vehicles from the trajectory diagrams.

Although trajectory data for the rightmost through lane on each approach provided valuable information regarding queue spacing, observed saturation flow rates, and arrival types, the primary focus was on queue buildup in the leftmost through in relation to the entrance to the turn pocket. As the approach to the turn pocket consists of what is essentially

a shared lane, all left turning vehicles were included in the leftmost through lane trajectory graph and shown as dotted lines to clearly distinguish them from through vehicles. This allowed for direct observation of these vehicles relative to the through queue.

After adding signal timing information to each of the trajectory graphs, analysis was conducted graphically. Average vehicle queue spacing was obtained by measuring the distance between the fronts of each queued vehicle, as indicated by a horizontal trajectory. Saturation flow rate measurements were taken at the stop bar by measuring the time headways between vehicles discharging from a queue; as per the HCM 2000, the first 3 vehicles to discharge were ignored due to start up lost time. Counts were taken every cycle to determine the total number of vehicles in queue, as well as the total number of vehicles within each lane arriving on green that did not need to slow or stop at the back of queue. Finally, counts were taken at three distinct points on each approach to vehicle lane distribution values (AVD) at the stop bar, the entrance to the turn pocket, and 200 feet upstream of the entrance to the turn pocket. Taken together, all of this information provided the basis necessary to compare observed queue buildup to HCM 2000 predictions and calibrate saturation flow rate and spacing parameters from field data.

3.2.3 Visualization of Data

The results of the data analysis procedure discussed above are provided for the leftmost through lane in Figure 6 (12:45 – 1:00 pm) and Figure 7 below (4:00 – 4:15 pm). The signal indication is provided for reference, with one single, through/permitted-left phase per cycle. Running as part of a coordinated, actuated system, the cycle length remains

essentially constant at approximately 95 seconds per cycle at midday and 100 seconds per cycle during the afternoon peak. Data is therefore available for effectively 9 full cycles during each 15-minute interval.

For reference, left turning vehicles are shown as dotted lines and through vehicles in varying shades of gray, with an arrow indicating direction of travel. The thick, black horizontal line represents the entry point to the turn pocket on each approach. Queues extending beyond this line effectively generate blockage of the turn pocket for any left turning vehicles arriving after the onset of blockage. At midday, blockage is rare, but becomes increasingly common during the afternoon peak hour. Due to limited left turn demand, there were only 2 observed cases in which a left turning vehicle arrived after the onset of blockage, and in both cases, the vehicles essentially ignored pavement markings to access the pocket.

In addition to clearly portraying the buildup and dissipation of queues, the trajectories provide visual representations of lane changing, density, platooning and varying arrival types, as well as the disrupting effects of vehicles turning onto and off of urban arterials. With queues extending nearly 300’ back on the southbound approach during the afternoon peak hour, the importance of coordination and effective signal timing plans become visually apparent.

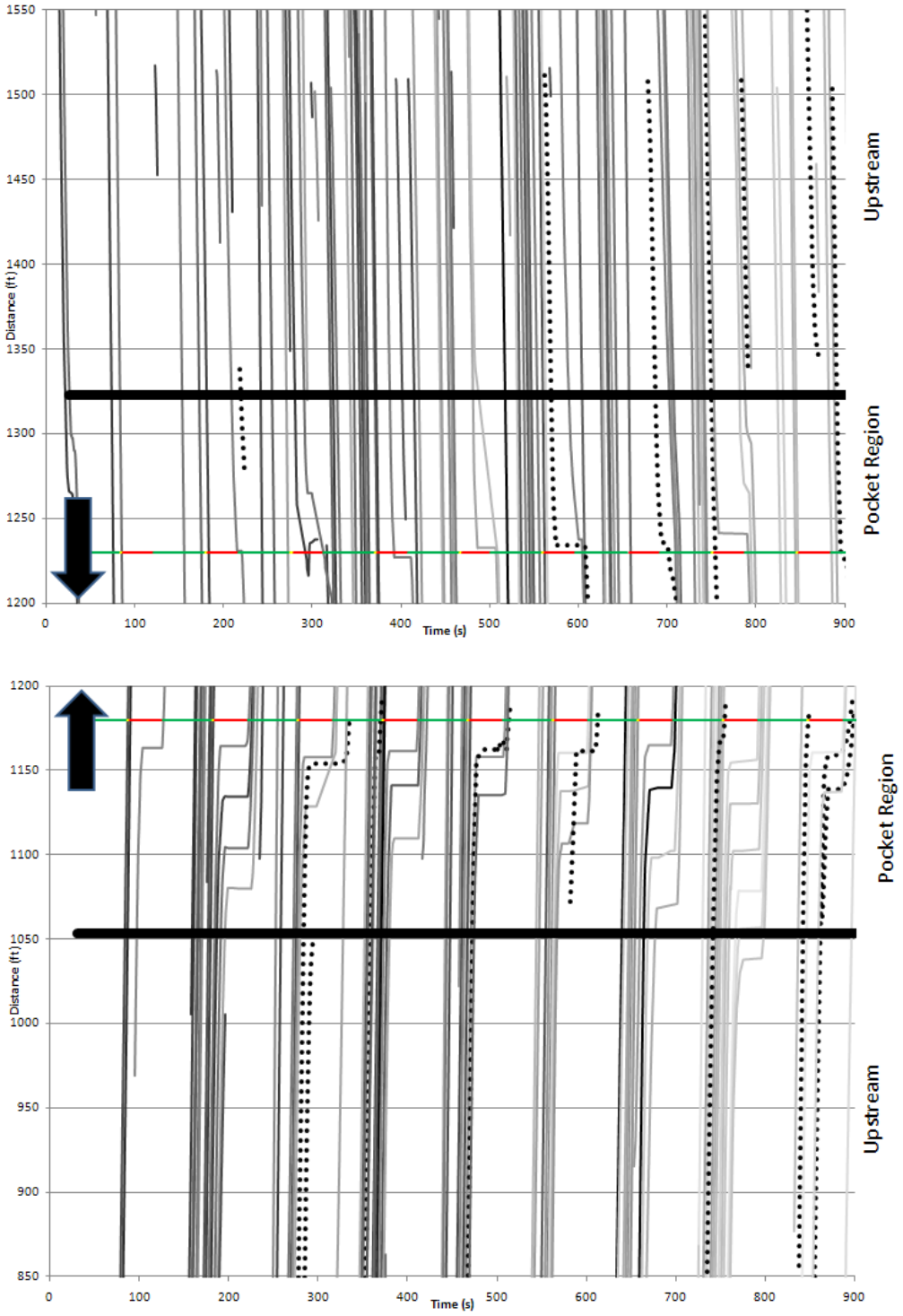

Figure 6 - Southbound (top) and northbound (bottom) trajectories (12:45 - 1:00 pm)

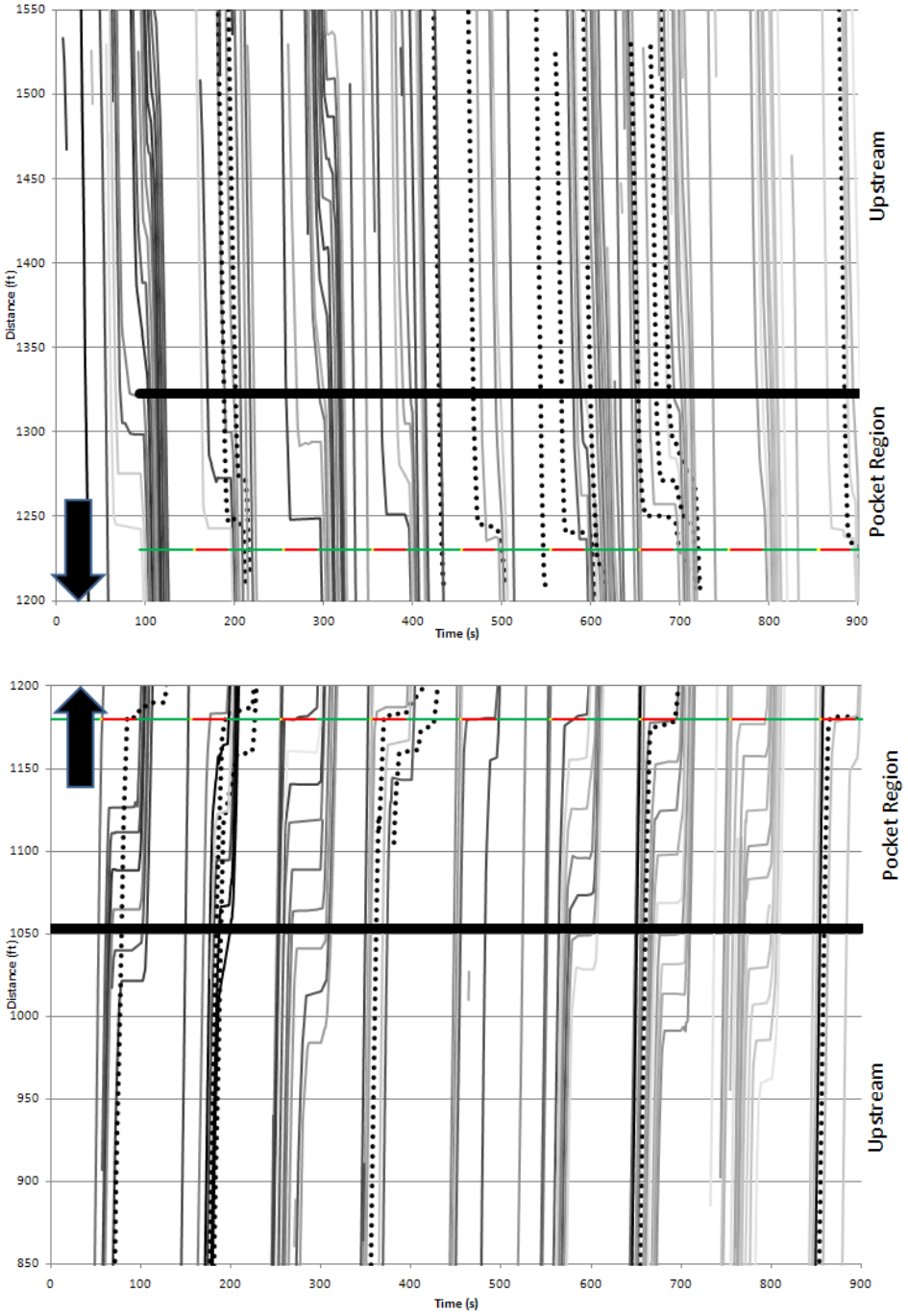

Figure 7 - Southbound (top) and northbound (bottom) trajectories (4:00 - 4:15 pm)

3.2.4 Observations and Demand Characteristics

While several interesting trends emerge from the data simply from visual inspection, careful measurement provides detailed information that can be used for comparison purposes. Demand characteristics as well as traffic flow observations for the leftmost through lane on each approach are provided in Table 1. Although not shown, the rightmost through lane on each approach serves less demand than the leftmost through lane, with the approach vehicle distributions (AVD) shown in the table at three points along each approach:

AVD = (leftmost through lane demand in passenger car equivalents) /
(total approach demand in passenger car equivalents)

As a result, the onset of blockage can be expected to occur at a greater frequency than would be expected under with equal lane distribution. Detailed lane distribution analysis is provided in the following section. In addition to demand and approach lane distribution (AVD) values, percentage heavy vehicles (HV%), percent left turn demand (p_L), percent right turn demand (p_R), observed progression factor (R_P), total blockage during time, total number of cycles with blockage, observed average queue spacing, and observed saturation flow rates are provided in Table 1.

Table 1 - NGSIM Peachtree Street Dataset Demand Characteristics and Observations

		Demand (veh/hr)				g/C	Lane Utilization (%PCE)			R_P	Blockage Time	Cycles with Blockage	Avg. Queue Spacing	Obs. Sat. Flow
		Approach vph	P_{HV}	P_L	P_R		Entry	Pocket Entrance	Stop Bar					
12:45 - 13:00	NB	576	3%	6%	2%	0.60	57%	61%	61%	1.09	28	1	24	-
	SB	540	2%	2%	7%	0.60	65%	59%	54%	1.37	0	0	-	-
16:00 - 16:15	NB	528	5%	5%	2%	0.61	59%	65%	60%	0.53	188	6	25	1635
	SB	720	0%	6%	5%	0.61	58%	54%	52%	0.60	60	2	28	1523
Weighted Avg.													25	1596

As the effective g/C ratio remains essentially constant throughout both analysis periods (g/C = 0.61), the progression factor (R_P) is one of the most critical variables for predicting queue length. Calculated as the percentage of arrivals on green divided by the g/C ratio, there is clearly more effective progression at midday that during the afternoon peak hour. This more than any other single variable leads to a greater number of cycles that include a period of blockage during the afternoon peak hour. In fact, although very little changes in the northbound direction in terms of demand or discharge capacity between the two analysis periods, poorer progression in the afternoon leads to nearly 3 total minutes of blockage out of the 15 minute analysis period. As will be discussed, this blockage causes two left turning vehicles to essentially cross the median to bypass the queue and access the turn pocket.

In addition to these operational statistics, the data also provides valuable observations needed to calibrate any turn pocket analysis model. Vehicle spacing is one such parameter, and it is critical when attempting to estimate total turn pocket storage capacity to have an accurate estimate of this value. After removing cycles that contain queued heavy vehicles due to their variability of length, a weighted average of all observations in both through lanes

leads to an estimate of 25', a commonly cited value. Saturation flow rate was also calculated, although the rightmost through lane was excluded in order to remove the effects of right turning vehicles. In a central business district with 5% trucks, the HCM predicts a saturation flow rate of 1,629 vph, which is only slightly greater than the estimate below, obtained using 45 observations from the dataset.

3.2.5 Lane Distribution Analysis

Lane distribution analysis is critical for any turn pocket model with multiple approach lanes, as throughput in oversaturated conditions is directly linked to the methods by which through vehicles use available queue space. As mentioned, if through vehicles heavily favor the leftmost through lane, blockage of the turn pocket may occur more frequently than under a move even lane distribution. However, lane distribution ratios are typically related not only to geometry, but also to demand levels, which is a critical distinction when attempting to translate observed values into expected values in oversaturated conditions.

Figure 8 shows the percentage of all approach vehicles in the leftmost through lane (AVD), in passenger car equivalents, at three points along the approach to the intersection. The first point is located 200' upstream of the turn pocket entrance, serving as the entry lane distribution value. The second point is located at the entrance to the turn pocket, including left turning vehicles. The final point represents the stop bar, and therefore does not include left turning vehicles, which occupy the turn pocket at this point along the link.

Although all of the observations shown in the graph depict a favoring of the leftmost through lane, the most critical observation that can be taken from the data is the shift in AVD

as demand increases to afternoon peak levels. At 12:45 p.m., demand levels are relatively low, with only a few vehicle arrivals per cycle. At these low levels of congestion, drivers are largely free to choose a lane with little regard for other vehicles. The favoring of the leftmost through lane is therefore likely due to outside influences, such as maintaining distance from bicyclists and pedestrians on the sidewalk. Under congested traffic conditions, however, it would be reasonable to expect drivers to favor efficiency and speed over other outside influences. This hypothesis is supported by afternoon AVD observations. As traffic demand increased (although still far below saturated conditions), favoring of the leftmost through lane was reduced, dropping to just over 50% at the stop bar.

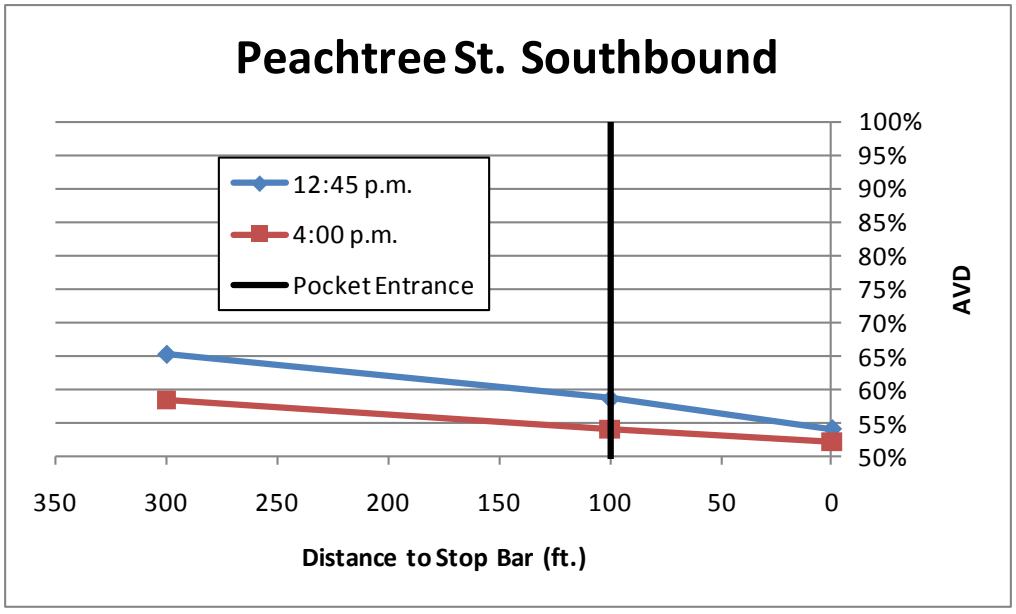

Figure 8 - Southbound Approach Veh. Distribution (% of Total Vehicles in Lane 1)

Unlike the southbound approach, which is unlikely to be strongly affected by turning movements at subsequent intersections, observations on the northbound approach are likely

biased by prepositioning as drivers anticipate the opening of an additional through lane immediately after the intersection, as well as heavy left turn demand at the upcoming 14th St. intersection (approximately 17% of all demand during the 4:00 p.m. period). Combined, these factors seem to indicate that lane distribution cannot be analyzed independently, and likely play a role in the heavy favoring of the leftmost through lane, as shown in Figure 9. However, it is interesting to note that unlike the previous example, demand levels actually drop by around 10% in the afternoon dataset, and the percentage of approach vehicles in the leftmost through lane is higher under lower demand levels. As before, the points shown represent entry, turn pocket entrance, and stop bar approach vehicle distribution values, respectively.

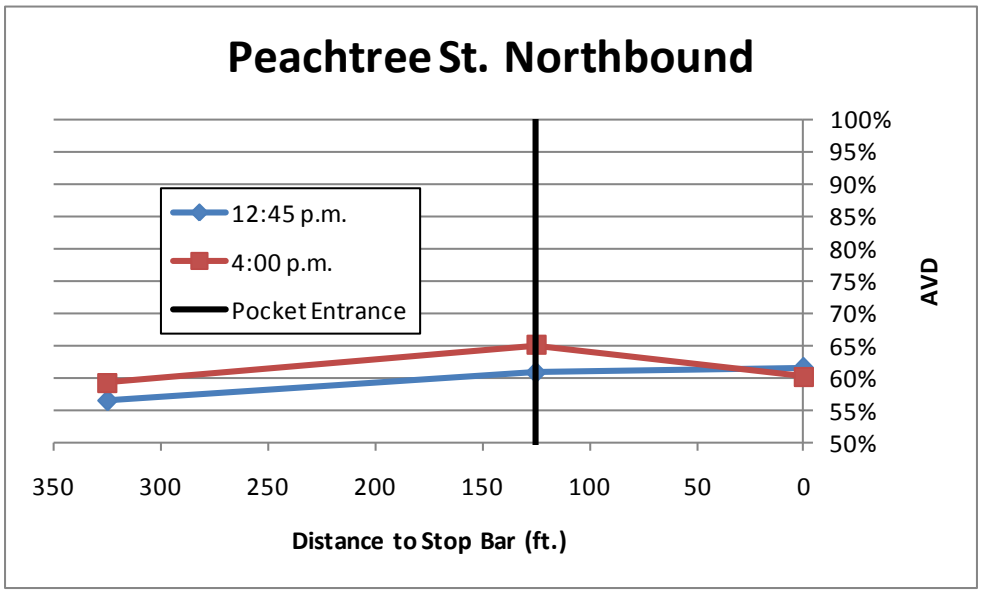

Figure 9 - Northbound Approach Veh. Distribution (% of Total Vehicles in Lane 1)

3.2.6 Queue Length Analysis

Using much of the information from Table 1 as input values, average and 95th percentile HCM 2000 queue length predictions were obtained for each lane and compared to actual observations of average and maximum queue lengths obtained from the dataset. This comparison is provided below in Table 2, with the difference (in vehicles) provided below each comparison. Observations or predictions that exceed the available approach turn pocket storage capacity are highlighted in red, using an assumption of 25' per vehicle.

Table 2 - Queue Length Observations vs. HCM 2000 Predictions

Queue Analysis		Turn Pocket				Lane 1 (Leftmost Through Lane)				Lane 2 (Rightmost Through Lane)			
		Average		95th Percentile		Average		95th Percentile		Average		95th Percentile	
		Obs.	Pred.	Obs.	Pred.	Obs.	Pred.	Obs.	Pred.	Obs.	Pred.	Obs.	Pred.
12:45 - 13:00	NB	0.56	0.57	2.00	1.42	3.00	4.53	6.00	9.08	2.44	2.94	4.00	6.33
		0		1		-2		-3		0		-2	
	SB	0.20	0.30	1.00	0.77	1.20	2.08	3.00	4.70	1.20	2.17	3.00	4.89
		0		0		-1		-2		-1		-2	
16:00 - 16:15	NB	0.78	0.72	2.00	1.79	6.00	6.12	10.00	11.59	3.67	3.75	8.00	7.78
		0		0		0		-2		0		0	
	SB	0.78	1.04	3.00	2.50	4.89	6.06	13.00	11.51	3.22	4.65	6.00	9.27
		0		0		-1		1		-1		-3	

With even a limited dataset that only includes 9 consecutive cycles on each approach, average back of queue values were found to follow HCM 2000 predictions very closely. In fact, the greatest deviation from the predicted average queue length is only 1.5 vehicles, a fairly modest difference in terms of relative significance. As HCM values are very sensitive to the progression factor, the observed differences may be due to assumptions regarding arrival time in calculating the progression factor. Perhaps most importantly, HCM

predictions concerning the onset of blockage follow observed data very closely. In the afternoon peak, it is both predicted and observed in the data that the average cycle will produce pocket blockage. Due to limited left turn demand on each approach, the blockage fails to produce any observable effects, but clearly even a slight increase in left turn demand will lead to a significant increase in blockage events.

3.2.7 Blockage

The final goal of the analysis was to document conditions leading to the onset of blockage. Although there were two cycles in which left turning vehicles arrived after through vehicles had queued beyond the marked entrance to the turn pocket, there is no raised median along Peachtree Street, allowing vehicles to cross the centerline as needed. This was likely the case for two northbound vehicles between 4:00 and 4:05 p.m. Using the trajectory data of the preceding vehicle as well as an estimate of vehicle spacing in queue, however, it is possible to make some assumptions regarding each vehicle's potential path were a raised median present. The blue dotted lines in Figure 10 below provide a likely trajectory for each vehicle as they approached the turn pocket and found the entrance blocked by queued through vehicles with no way to bypass the queue.

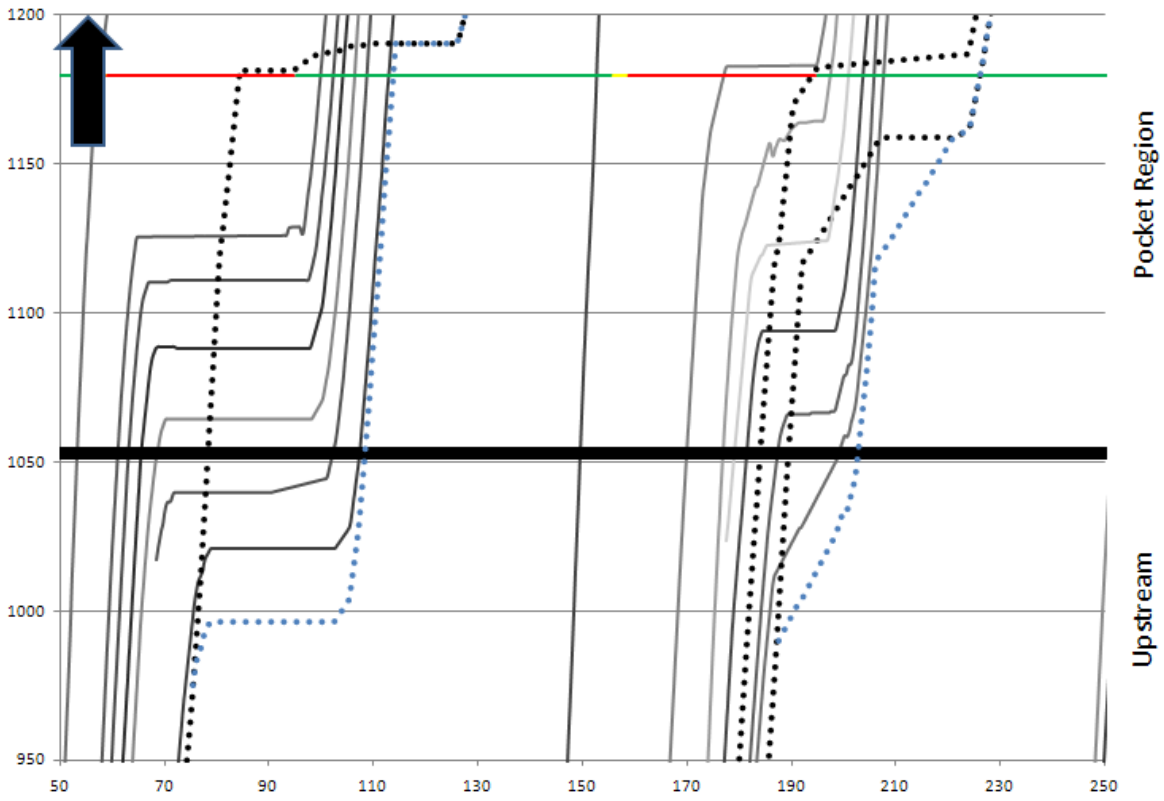

Figure 10 - Estimated Trajectories of Blocked Left-Turning Vehicles

By measuring the time needed to accelerate back to their original speeds, respective delays of 30 seconds and 14 seconds could be expected with a median in place. In both cases, due to delay caused by permitted left turns, the assumed blockage delay was insufficient to generate actual discharge delay, as the vehicles would have been able to reach the stop bar before an acceptable gap was available in the opposing traffic stream. Delay to access the stop bar is not always insignificant, however, and in cases with protected left phasing, this delay may very well lead to a cycle failure for the left turning vehicle, equating to a minimum delay of over 100 seconds.

In oversaturated conditions, delay is not of particular interest, but the fact that the left turning vehicles would have remained in the leftmost through lane were a raised curb present is certainly a component that affects both discharge and lane distribution values. These blocked vehicles would contribute to an overall reduction in the processing efficiency within the lane, and affect available queue storage space and lane choice of drivers. Ultimately, however, the conditions of interest depend on a raised curb to prevent premature access to the blocked turn pocket.

3.2.8 Analysis Conclusions

High resolution vehicle trajectory data, although cumbersome, provides one of the most effective methods of examining queue buildup, lane distribution, vehicle spacing, saturation flow rates, arrival types and platoon ratios. Overlaying left turning vehicle trajectories with through vehicles in the leftmost through lane, as shown above, highlights the importance of modeling the approach segment upstream of the entrance to the turn pocket as a shared lane, and demonstrates the concept of blockage for vehicles unable to enter an available turn pocket due to queued through vehicles. Although limited left turn demand on each approach prevented a robust analysis of the effects of blockage on left turning vehicles, the data was sufficient to provide estimates of vehicle spacing, saturation flow rates, and average queue length based on demand, signal timing, and observed arrival types. Comparison with HCM 2000 equations demonstrated a close fit for the undersaturated conditions observed.

Although HCM equations provide an effective method of estimating average back of queue in undersaturated conditions, turning movement ratios and lane distribution play more critical roles for determining sustainable service rates in oversaturated conditions. Analysis of undersaturated conditions is inherently different from observations obtained in oversaturated conditions, but the following observations will likely provide critical insight when developing a capacity-based turn pocket model:

- **Vehicles spacing in queue** – 25 feet; this value is necessary for determining turn pocket storage capacities.
- **Base saturation flow rate** – 1900 pc/hr/ln; this number greatly influences discharge rates during green, and field observations validate this number, when used in conjunction with appropriate reduction factors.
- **Position of blocking vehicle –** The lack of a raised curb prevented direct observation of this value, highlighting the importance of physical barriers for objective turn pocket capacity analysis.
- **Approach Vehicle Distribution** – Undersaturated conditions and upstream and downstream conditions prevented direct observation of an appropriate value, but observations did support the hypothesis that outside factors tend to diminish as demand levels increase.

3.3 Brier Creek Parkway – Raleigh, NC

3.3.1 Location

The intersection of Brier Creek Parkway and Little Brier Creek Lane in Raleigh, NC was selected for analysis due to the presence of both spillback and starvation from opposing directions during the P.M. peak hour. Located at the entrance to Brier Creek Commons, a large shopping complex featuring restaurants, retail, and a movie theater, and less than 1500' feet from Highway 70, a major east-west commuter corridor in the Triangle, the intersection experiences heavy peaking due to both commuters and evening shoppers.

With a curbed median, heavy demand, and a 200' and a 275' short left turn pocket on the northbound and southbound approaches, respectively, the intersection provides an optimal environment to measure vehicle spacing in queue and observe vehicle positioning at the onset of both pocket blockage and spillback. As the system operates under actuated control with queues clearing every cycle, no capacity measurements could be taken directly, but observations could prove to be valuable for model development.

3.3.2 Geometry

The northbound approach includes 2 through lanes, a 200' short left turn pocket, and a 200' short right turn pocket. The actuated signal system includes a leading protected left turning movement and a permitted left / through phase. Right turn on red into the shopping center is permitted. Crosswalks are marked and signalized across all lanes, although pedestrian traffic is relatively light and does not tend to impede traffic flow. The closest upstream signalized intersection is Brier Creek Parkway and Lumley Road, approximately

3200’ away. The intersection with Highway 70, approximately 1500’ downstream, includes dual left and right turn pockets, as well as two through lanes (6 total lanes).

The southbound approach includes two through lanes, a single 275’ short left turn pocket, and a 200’ short right turn pocket. As on the opposite approach, the actuated control includes a leading protected left phase as well as a permitted left / through phase. Crosswalks are marked, and right-turn-on-red onto Brier Leaf Lane is permitted.

3.3.3 Data Collection

On November 19, 2009, data collection was carried out of 4:00 p.m. to 5:30 p.m. to capture as much of the peak hour effects available during daylight conditions. Due to very low demand on both approaches during the initial half hour of data collection, only the period from 4:30 p.m. to 5:30 p.m. is reported here.

On each approach, a camera was placed just upstream of the entrance to the left turn pocket, pointed toward the signal heads to capture signal timing, approach vehicle distributions at the turn pocket entrance, and lane-by-lane queue counts. The position of each synchronized camera relative to the intersection is shown below in Figure 11 and Figure 12. Due to the large amount of data needed for analysis, video was used as the primary collection tool, used in conjunction with field notes and observations made during the data collection period.

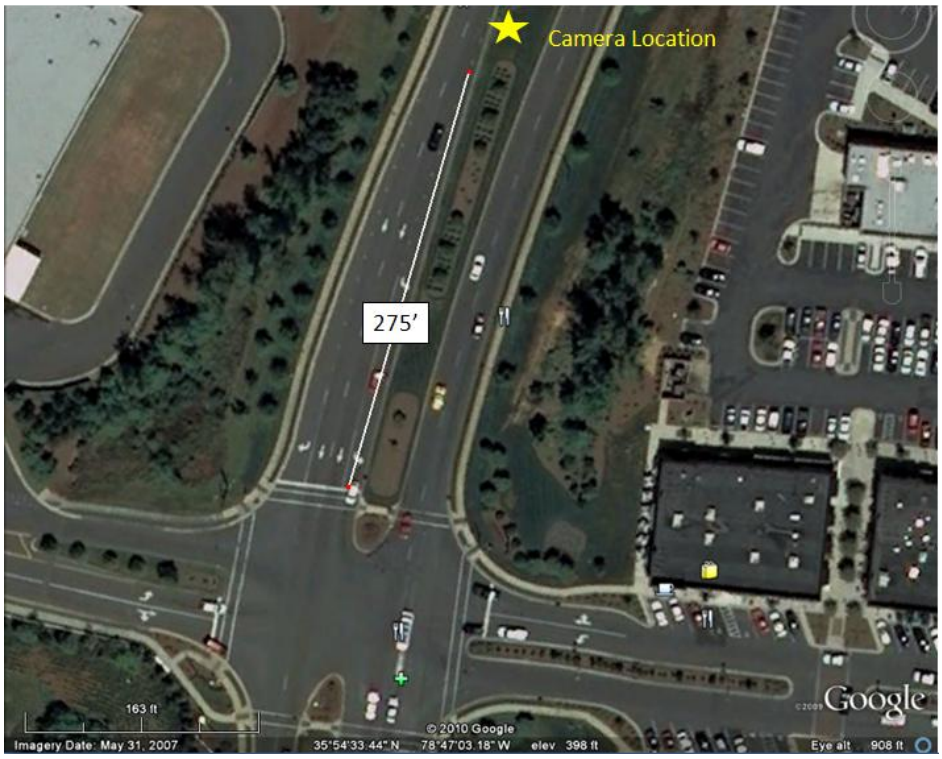

Figure 11 - Brier Creek Parkway Southbound Approach

Figure 12 - Brier Creek Parkway Northbound Approach

3.3.4 Signal Timing and Demand Characteristics

Table 3 below provides a summary of the average signal timing data and demand observations for the period from 4:30 p.m. to 5:30 p.m. As the system runs under actuated control, phase times varied widely, and the averages are reported in the table. On the southbound approach, a total of 18 cycles included a protected left turn phase, with a maximum observed phase time of 39 seconds. On the northbound approach, due to limited left turn demand, only 6 cycles included a protected left phase, with a maximum observed phase time of 13 seconds. In all cases, when a protected left turn phase was called, the phase began prior to or in conjunction with the through phase (leading left actuated control).

Table 3 - Demand and Signal Timing Characteristics

Brier Creek Parway			Northbound	Southbound
Signal	Time	sec.	3602	3602
	Cycles	sec.	31	31
	Average Cycle	sec.	116	116
	Average Through Green	sec.	63	79
	Average Protected Left	sec.	2	15
	Average Yellow	sec.	4	4
Demand	Total Demand	veh.	1065	1007
	Vehicles/Hour	veh./hr.	1064	1006
	Through Capacity	veh./hr.	2053	2579
	Through d/c	ratio	0.42	0.24
	Left Demand	veh.	112	378
	Through Demand	veh.	869	612
	Right Demand	veh.	84	17
	Left Demand (%)	%	11%	38%
	Right Demand (%)	%	8%	2%
	HV (%)	%	0.5%	0.3%

On both approaches, the through movement was well undersaturated, and all through queues cleared each cycle with no observations of cycle failure for this movement. Overall

demand levels were similar for each approach, although left turn demand on the southbound approach was nearly 3 times greater than on the northbound approach do to the presence of Brier Creek Commons. For this same reason, right turn demand levels on the northbound approach were nearly five time higher than on the southbound approach, although he presence of a short right turn pocket and the availability of right-turn-on-red made these vehicles largely irrelevant in terms of left and through movement queue analysis.

3.3.5 Queue Length Analysis

In order to obtain measurements of average vehicle spacing in queue as well as the position of each blocking vehicle at the onset of a spillback or blockage event, queue counts in both the turning bay and the leftmost through lane were taken and recorded for each observed event.

Blockage

A total of 7 turn pocket blockage events were observed over the evening peak hour on the northbound approach (11% left turn demand), defined as an event in which a queued vehicle physically blocks the entrance to the left turn pocket. Figure 13 provides a snapshot of one of these events recorded in the field. Notice that the critical vehicle is the through vehicle queued beyond the entrance to the turn pocket, as this is the vehicle that prevents entry.

Figure 13 - Blockage Event on the Northbound Approach

Table 4 provides a summary of the 7 observed blockage events, providing the time of the event, the number vehicles in the pocket, and the number of queued vehicles in the leftmost through lane at the onset of blockage. In all cases on the northbound approach, which includes a 200' left turn pocket, the blocking vehicle was the 9th vehicle to join the back of queue. As shown in Figure 13, 8 vehicles effectively occupied the space adjacent to the turn pocket in each case. It was the 9th vehicle that initiated the blockage event however. This support Wu's assumption that if the turn pocket is 'n' vehicles in length, blockage will occur upon the arrival of 'n+1' through vehicles (Wu, 2008).

Table 4 - Summary of Turn Pocket Blockage Events

	Vehicle Count	
Onset of Blockage	Left Turn Bay	Leftmost Through Lane
4:57:47 PM	0	9
5:05:03 PM	2	9
5:09:46 PM	1	9
5:13:53 PM	4	9
5:23:37 PM	3	9
5:26:41 PM	5	9
5:29:20 PM	0	9

Ignoring the final blocking vehicle, the 7 observations of blockage demonstrated that in each case, 8 vehicles occupied 200' of queue space adjacent to the turn pocket. These observations directly support the queue space value of 25' per vehicle calculated from the NGSIM dataset. The actual onset of blockage depends upon the shape of the entrance region to the pocket, but the values support the use of 25' per vehicle in a short turn pocket model.

Spillback

On the southbound approach (38% left turn demand), a total of 8 pocket spillback events were recorded, defined as the point at which queued left turning vehicles begin to physically block the vehicles from freely using the leftmost through lane. Figure 14 provides a snapshot of a spillback event recorded in the field. As can be seen, the actual onset of spillback depends on the angle of entry of the last one or two vehicles, leading to slightly greater variability in the determination of the onset of spillback.

Figure 14 - Spillback Event on the Southbound Approach

With a 275' pocket, spillback most frequently occurred upon the arrival of the 12th left turning vehicle, as shown in Table 5. As with the blockage events, these observations support the concept of defining spillback as the arrival of 'n+1' left turning vehicles, as 'n' vehicles will typically fully occupy the pocket, but will not cause any impedance to through vehicles. Although in 2 cases, the final vehicle to enter the pocket failed to fully clear from the through lanes and therefore created some degree of impedance on the lane, but on average, 12 vehicles were required.

Table 5 - Summary of Turn Pocket Spillback Events

Onset of Spillback	Vehicle Count	
	Left Turn Bay	Leftmost Through Lane
4:46:07 PM	11	0
4:49:41 PM	11	0
4:54:57 PM	12	0
5:08:32 PM	12	0
5:12:48 PM	12	0
5:18:39 PM	12	0
5:22:49 PM	12	0
5:28:19 PM	12	0

Consistent with the observations from turn pocket blockage events, left turning vehicles required approximately 25' of space in queue, calculated based on the 11 vehicle pocket storage capacity of the 275' short turn pocket. The last couple of vehicles tended to 'creep' forward a few more feet, but this trend was not sufficient to reduce the overall average queue space required.

3.3.6 Approach Vehicle Distribution Analysis

In addition to queue counts, careful lane distribution counts were taken to provide insight into the behavior of vehicles in the presence of short left turn pocket effects. Table 6 provides a summary of these observations. The first two values provide the overall approach vehicle distribution (AVD) of all approach vehicles in passenger car equivalents, taken at the entrance to the turn pocket on each approach. This value is comparable to the lane distribution values discussed with the NGSIM data, as it refers to the percentage of all vehicles utilizing the leftmost through lane on the approach to the intersection over the entire peak hour period. The through vehicle distribution values (THVD), on the other hand, refer

exclusively to the lane choice of through vehicles at the entrance to the turn pocket, excluding both left and right turning vehicles. To provide slightly greater detail, this value was also calculated for the cycles that included either a blockage or spillback event. The final percentage reflects the percentage of vehicles arriving on green to give a sense for the progression of the system and the amount of vehicles impacted by spillback and blockage events.

Table 6 - Lane Distribution Analysis

Brier Creek Parkway	Northbound	Southbound
AVD (%PCE)	47%	68%
THVD (%)	45%	50%
THVD (%) with Blockage/Spillback	40%	41%
Arrivals on Green	54%	66%

On the northbound approach, there was a slight favoring of the rightmost through lane over the hour. Although it is difficult to extract each of the factors that may play a role in this effect, it is interesting that through vehicles were more likely to choose the rightmost through lane on cycles that included a blockage event. This may be due to drivers observing the blockage event, and opting to use the rightmost through lane if possible to minimize the effects to the left turn vehicles. The sample size is certainly limited, but such observations support the concept of efficient use of queue space by drivers.

On the southbound approach, overall lane distribution values heavily favored the leftmost through lane (lane 1), due largely to the presence of approximately 38% left turn demand on the approach. Despite this heavy left turn volume, it is interesting to note that, over the entire hour, through vehicles were no more likely to select the rightmost through lane over the left one. Total through demand levels were far below saturated values,

however, with very good progression, meaning that very few through vehicles would have had a need to choose the rightmost through lane. On cycles in which spillback events were observed, through vehicles did in fact favor the rightmost through lane, possibly to avoid queues. Furthermore, as spillback is defined as the complete blockage of the leftmost through lane, during spillback events, all through vehicles were forced to use the rightmost through lane if available, often changing lanes to do so. In other words, although the observations were muted due to limited through demand, observed lane distribution values tend to support dynamic lane choice, with drivers reacting to spillback events to more efficiently use available capacity and queue space.

3.3.7 Analysis Conclusions

Several critical observations were made over the peak hour analysis period. As with the NGSIM data, all observation occurred in undersaturated conditions and care must be taken when attempting to extrapolate these values into expectations in oversaturated conditions. However, it is unlikely that general trends in behavior or jam density values will drastically change due solely to longer queues. The following observations provide additional support and validations to observations extracted from the NGSIM data:

- **Vehicles spacing in queue** – 25 feet; this value was observed in both the left turn pocket itself, as well as the through storage region adjacent to the turn pocket.
- **Position of blocking vehicles –** The presence of a curbed median allowed for several direct observations of impedance during both blockage as well as spillback events,

supporting the common assumption of ‘n+1’ vehicles needed to initiate either spillback or blockage.

- **Approach vehicle distribution** – Although vehicle distribution values are likely largely dependent upon the level of saturation, variations in observations tend to support the concept of dynamic lane choice, where drivers attempt to more efficiently use available lane capacity in response to a variety of short turn pocket effects.

4. MODEL DEVELOPMENT

4.1 Model Requirements

Based on previous work and field observations, measurements or estimates of sustainable service rates inclusive of short turn pocket effects within a macroscopic simulation model require that the platform be sensitive to seven basic parameters and vehicle interaction effects:

1. Pocket spillback and the corresponding reduction in through vehicle throughput.
2. Pocket blockage and starvation and the corresponding reduction in left throughput.
3. Pocket storage area and length.
4. Phase order and timing plans.
5. Saturation flow rates.
6. Lane switching behavior.
7. Demand by movement.

As noted previously, no single macroscopic model includes all seven of these model requirements, limiting their practical applicability. Probabilistic bay length design models, as found in the work by Kikuchi *et al*. (1993), focus on pocket storage and signal timing, but are unable to reduce discharge rates when spillback is predicted. Similarly, available macroscopic software packages, such as SIDRA and Synchro, include built in logic for queue buildup but fail to account for back of queue interactions when spillback and pocket blockage occur. Capacity models, as exemplified by Wu's work (2008), achieve nearly all of these

objectives, but are unable to account for lane changing as turn pocket effects emerge, limiting their effectiveness when more than one approach lane upstream of the turn pocket is present.

4.2 Conceptual Definitions

Field observations provided a clear picture of the operation of congested approaches with a short left turn pocket, and these observations were used heavily in developing the logic for the proposed macroscopic model. As such, it is helpful to first discuss the critical dimensions in the context of actual vehicles before shifting to a macroscopic, flow-based analysis.

Pocket blockage, or starvation, occurs when through vehicles physically prevent access to the turn pocket, despite available queue storage space. Due to the tapering of a typical turn pocket, however, blockage will only occur after the arrival of the n+1 through vehicles in the case a single approach lane (M = 1). When multiple through lanes are present (M >1), field observations indicate that through vehicles tend to shift lanes, if possible, to delay the onset of pocket blockage. The basic assumption follows that turn pocket blockage will occur after the arrival of $M*(L_{P1}/AVS) + M$ through vehicles, and the vehicle that generates the blockage event is said to occupy the "gate." Figure 15 provides an example of the onset of a blockage event, where M = 2 and $L_{P1}/AVS = 2$ such that pocket blockage occurs after the arrival of 2*2 + 2 = 6 through vehicles.

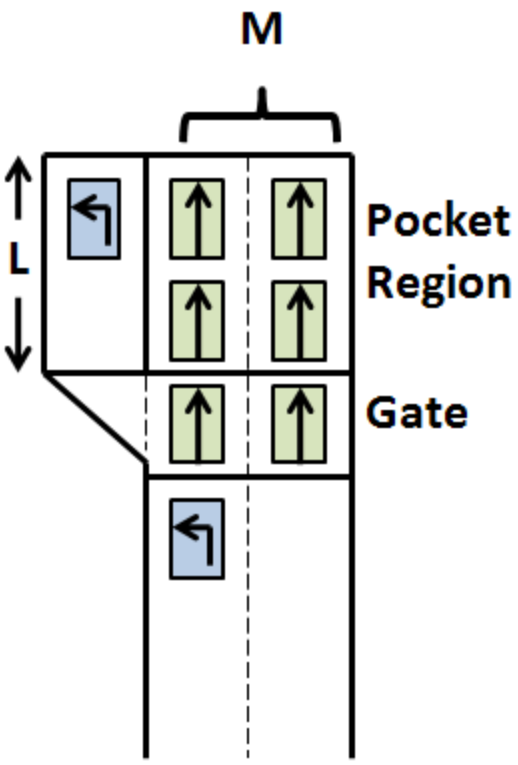

Figure 15 - Pocket Blockage: M*n+M Through Vehicles

Spillback, on the other hand, occurs when queued turning vehicles begin to impede flow within the through lanes, in much the same way that a turning vehicle will impede flow within a shared through/turn lane at a signalized intersection. While blockage will only occur after the gate is fully occupied by through vehicles, spillback occurs upon the arrival of n + 1 left turning vehicles, as one turning vehicle more than can be stored in the pocket will begin to affect operation in the leftmost through lane. Figure 16 provides an example of the onset of pocket spillback, where 1 turning vehicle arriving at the gate will begin to affect through vehicle operation.

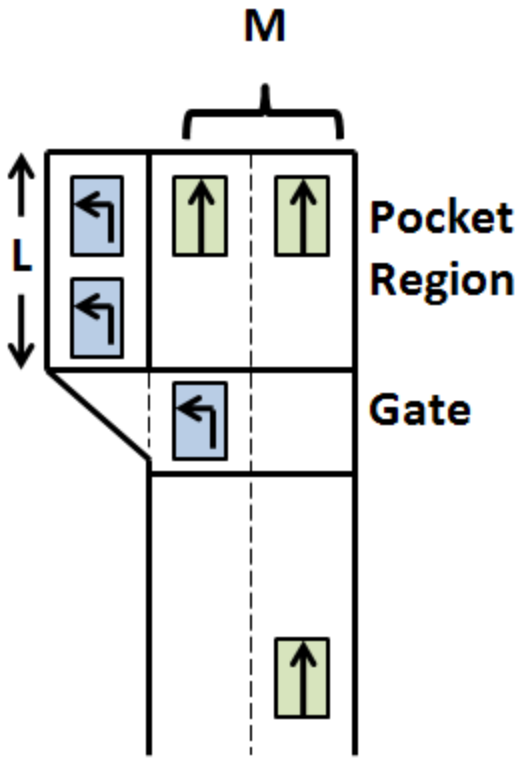

Figure 16 - Pocket Spillback: n+1 Turning Vehicles

4.3 Modeling Framework

Maintaining a macroscopic, flow-based model, requires a shift in thinking from individual vehicles to density and capacity-based constraints on a fluid-like system. Following from the logic developed in Daganzo's cell transmission model (1993), the intersection approach was broken down into a series of "cells," whose sizes can be calibrated based on field observations. By applying the desired constraints on the input and output from each cell based on the simulation interval, the macroscopic model is able to perform similar to a microscopic simulation with an exponentially decreased computational burden.

Figure 17 demonstrates the concept of a cell-based approach to an intersection with a single short left turn pocket and two through lanes. The "pocket" ($_P$) refers to the independent left turn pocket and adjacent through vehicles storage region immediately upstream of the stop bar. The "gate" ($_G$), as previously discussed, defines the critical cell where both spillback and pocket blockage occur. The "queue storage region" ($_Q$) can be of user-defined length and serves as a filter for vehicles entering the gate. As the ratio of turning vehicles dynamically adjusts based on both output and input, this region is also critical for lane utilization analysis. Finally, the "loading region" ($_{LR}$) serves to store the remaining approach vehicles in an essentially unconstrained, infinite queue.

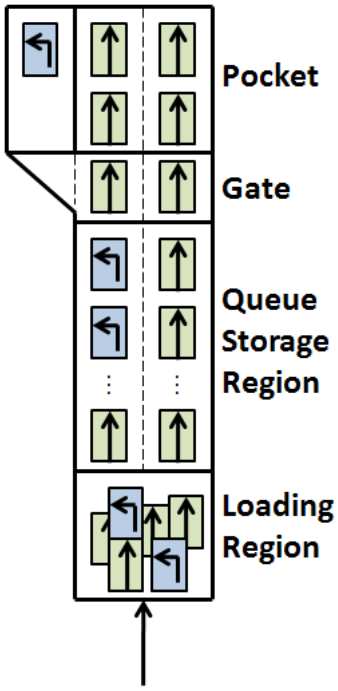

Figure 17 - Cell-based System

In a macroscopic environment, however, individual vehicles as well as queue discipline is eliminated for more efficient computational speed, and each of the constraints on the system is based on cell density, speed and flow relationships, as well was saturation flow rate assumptions. The actual effects of spillback and starvation therefore occur not upon the arrival of a discrete number of vehicles, but instead in terms of cell density. Figure 18 provides a conceptual illustration of how the macroscopic model treats both a) spillback and b) starvation. Blockage by individual vehicles has effectively been replaced by flow and density-based constraints on the system, consisting of multiple interacting cells.

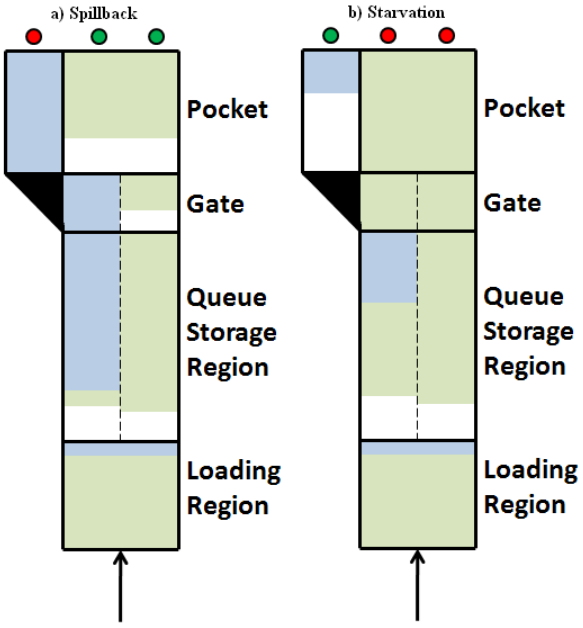

Figure 18 - Effective Macroscopic Operation

4.4 System Constraints

The following section describes in detail each of the regions defined in the cell-based system described above. Starting from the pocket region ($_P$), where signal timing largely

dictates output, moving backwards to the loading region ($_{LR}$), each constraint applied to the model will be discussed. In each cell, the constraints will be discussed in terms of flow rates, but the default time step used throughout (Δt) is 0.25 seconds, placing a global constraint of 0.132 vehicles per lane able to pass between cells in a single time step (0.25*1900/3600).

4.4.1 Pocket Region ($_{P}$)

The pocket region consists of two independent cells: the left turn pocket and the adjacent through vehicle storage region. The two cells are of equivalent length (L_{P1}), but experience no interaction, receiving proportional input from the gating cell ($_{G}$). The total storage capacity of each region depends on the number of lanes (through = M, left = N) in each region, as well as the length of the secondary left turn pocket (L_{P2}), if one is present.

Figure 19 describes two constraints on the through region of the pocket during effective green time. The model assumes infinite receiving capacity downstream of the stop bar, and output is therefore a function of the (1) saturation flow rate, as well as (2) the number of vehicles available for discharge (speed * density). Default values or calculations for each parameter are provided below the figure.

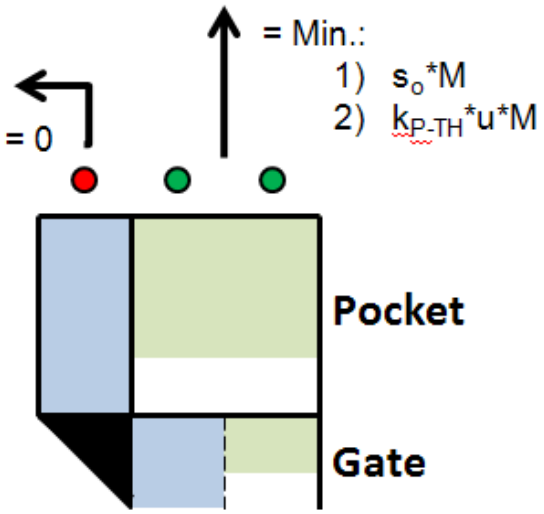

Figure 19 - Pocket Region Through Vehicle Outflow Constraints

s_o = 1900 vph
k_{P-TH} = (n_{P-TH}) / $(L_{P1}$*M)
u_o = 30 mph

Figure 20 depicts the two constraints on the left turning pocket during effective green time. Again, the primary constraints are the (1) saturation flow rate and (2) the number of vehicles available for discharge. The only significant difference between the through and left constraints is the presence of f_{LT} in the turn pocket constraint calculation. This factor represents a simple geometric constraint during a protected left phase, but takes on a much more complicated calculation procedure during a permitted left phase, as described in HCM 2000 Chapter 16 Appendix C.

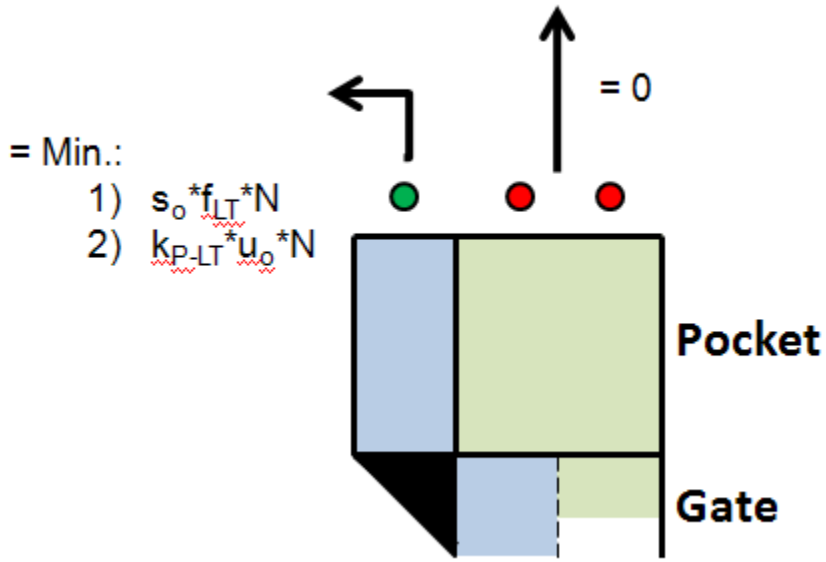

Figure 20 - Pocket Region Left Turning Vehicle Outflow Constraints

k_{P-LT} = (n_{P-LT}) / $(L_{P1}+L_{P2})$ / N
f_{LT} = 0.95 (Protected)
= See HCM 2000 Exhibit C16-9 (Permitted)

4.4.2 Gate ($_G$)

The gate, by definition, is equivalent in length to the space needed per vehicle in queue. This value, called AVS (average vehicle spacing), is taken to be 25' based on the field observations described in Chapter 3. L_G in miles is therefore simply AVS / 5,280. The total storage capacity of the gate, in vehicles, is therefore simply M, the total number of through lanes. Unlike the downstream segments, however, the gate is able to store both through and left turning vehicles. A basic lane distribution assumption was therefore built into the model, calculated as an equivalent distribution of all vehicles among lanes after

converting to passenger car equivalents to account for the slight disutility introduced to the system by turning vehicles (f_{LU}). However, left turning vehicles may only occupy the leftmost through lane (lane 1).

It should be noted that this logic, on the surface, may seem slightly different from the assumption described in section 4.2, where all through vehicles will first occupy the rightmost through lanes. The gate is treated in this manner to allow for an approximation of the through vehicle distribution (THVD) discharging from the gate, which would not be possible if all vehicles are assumed to occupy the rightmost through lane when operating under jam density. Instead, the assumption of left turn priority on the leftmost through lane (lane 1) will be handled by input from the upstream cell, as described in section 4.4.3.

Figure 21 demonstrates the three constraints placed on left turn output from the gate. The first term represents the (1) saturation flow rate (1900 vph), weighted by the proportion of left turning vehicles in the leftmost through lane ($LTS_{G\text{-}Lane1}$). The second term (2) calculates the number of left turning vehicles available for movement during the time step. It should be noted that $k_{G\text{-}LT}$ is simply the number of left turning vehicles in the gating region divided by L_G and not the actual density of the leftmost through lane, which includes both left ($n_{G\text{-}LT}$) and through vehicles ($n_{G\text{-}TH\text{-}Lane1}$) in the leftmost through lane. The final constraint represents (3) the receiving capacity of the downstream left turn pocket region. In the calculation shown, L_{P1} and L_{P2} are converted to miles, and Δt in hours, giving the number the expected value of vph.

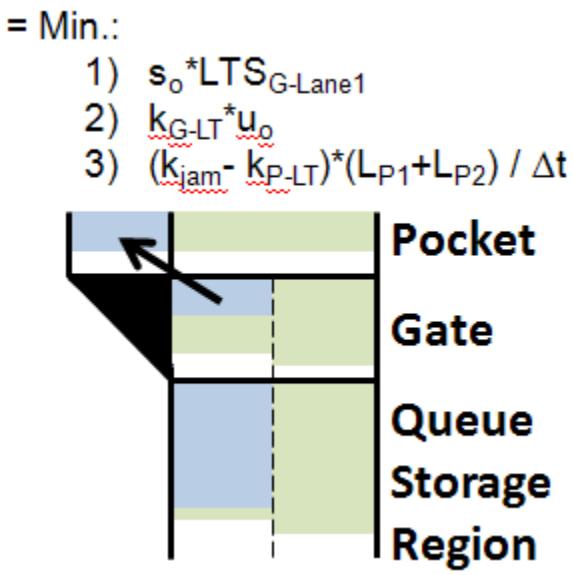

Figure 21 - Gating Region Left Turning Vehicles Outflow Constraints

$LTS_{G\text{-}Lane1}$	= $n_{G\text{-}LT}$ / ($n_{G\text{-}LT}$ + $n_{G\text{-}TH\text{-}Lane1}$)
$n_{G\text{-}TH\text{-}Lane1}$	= MAX (0, [($n_{G\text{-}LT}$/f_{LU} + $n_{G\text{-}TH}$)/M] – $n_{G\text{-}LT}$/f_{LU})
$n_{G\text{-}LT}$	= LT Vehicles in Gating Region
$n_{G\text{-}TH}$	= TH Vehicles in Gating Region
f_{LU}	= 0.95
$k_{G\text{-}LT}$	= $n_{G\text{-}LT}$ / L_G
k_{jam}	= 1 / L_G = 211.20 veh./mi./ln.
Δt	= 0.25 seconds = 0.0000694 hours

Figure 22 describes the four constraints placed on through vehicle output from the gate. The first term represents the (1) saturation flow rate (1900 vph) multiplied by the number of lanes, minus the observed left turning vehicle outflow calculated above ($v_{G\text{-}LT}$). The second term ensures that even when the left turn output drops to zero, (2) through vehicle outflow from the leftmost through lane is weighted by the proportion of through vehicles contained within the lane ($THS_{G\text{-}Lane1}$). The third term calculates the (3) number of through vehicles within the gate available for movement during the time step. The final

constraint represents the (4) receiving capacity of the downstream through pocket region. In the calculation shown, L_{P1} is in miles and Δt in hours.

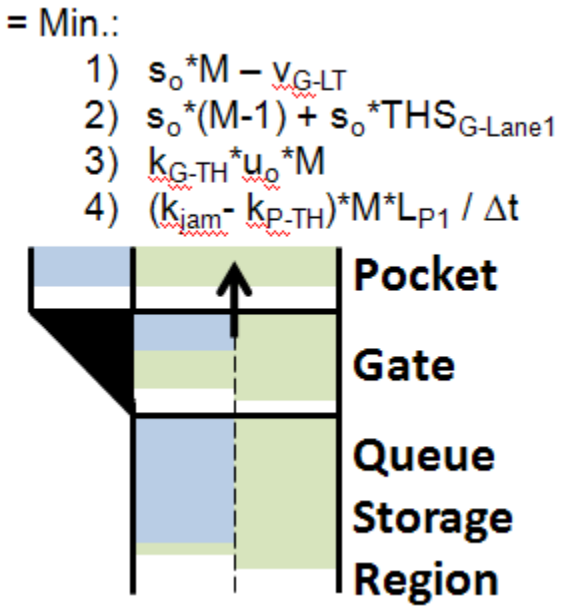

Figure 22 - Gating Region Through Vehicle Outflow Constraints

v_{G-LT} = LT gating region output flow rate, from Figure 21.
$THS_{G-Lane1}$ = $n_{G-TH-Lane1}$ / (n_{G-LT} + $n_{G-TH-Lane1}$)
k_{G-TH} = n_{G-TH} / (L_G*M)

4.4.3 Queue Storage Region ($_Q$)

The queue storage region defines a region of finite length where vehicles are able to queue upstream of the gating region. As the number of vehicles able to queue within the region is finite, the region has the potential to limit input from the upstream cell. More importantly, however, the region enables a mechanism by which left turning vehicles can generate a continuous queue. As observed in the field, when spillback occurs, through

vehicles queued upstream of the gate will switch out of the leftmost through lane, leaving a continuous queue of left turning vehicles. Output from the queue storage region is therefore not simply proportional to the vehicles contained within the region, but influenced by lane discipline.

A critical variable defined in this region, called $k_{G\text{-}Lane1}$, refers to the *hypothetical* density of the leftmost through lane (lane 1) within the downstream gate. As mentioned in the previous section, the lane distribution of through vehicles discharging from the gate is based on an equivalent lane distribution using passenger car equivalents contained within the region. However, through vehicles tend to move out of the leftmost through lane if possible to prevent premature pocket blockage, making the actual instantaneous density within the leftmost through lane irrelevant in terms of *hypothetical* density when placing constraints on discharge rates from the queue storage region upstream. When more than M-1 through vehicles are present in the region, however, $k_{G\text{-}Lane1}$ will exceed $k_{G\text{-}LT}$ by definition, as a certain number of through vehicles must still occupy the leftmost through lane. Therefore, the hypothetical density in the leftmost through lane in the gating region can be said to be greater than or equal to $k_{G\text{-}LT}$, the density of left turn vehicles within the gate's leftmost through lane, and less than or equal to the instantaneous density in the leftmost through lane:

$$k_{G\text{-}Lane1} = [n_{G\text{-}LT} + MAX\ (0, n_{G\text{-}TH} - (M - 1))] / (L_G)$$

$$k_{G\text{-}LT} \leq k_{G\text{-}Lane1} \leq (n_{G\text{-}LT} + n_{G\text{-}TH\text{-}Lane1}) / L_G \leq k_{jam}$$

Figure 23 demonstrates the three constraints placed on left turn output from the queue storage region. The first term represents the (1) saturation flow rate (1900 vph), weighted by the proportion of left turning vehicles in the leftmost through lane ($LTS_{Q\text{-}Lane1}$). The second term calculates the (2) number of left turning vehicles available for movement during the time step. The final constraint represents the (3) hypothetical receiving capacity of the gating region's leftmost through lane, weighted by the proportion of left turning vehicles in the queue storage region's leftmost through lane ($LTS_{Q\text{-}Lane1}$).

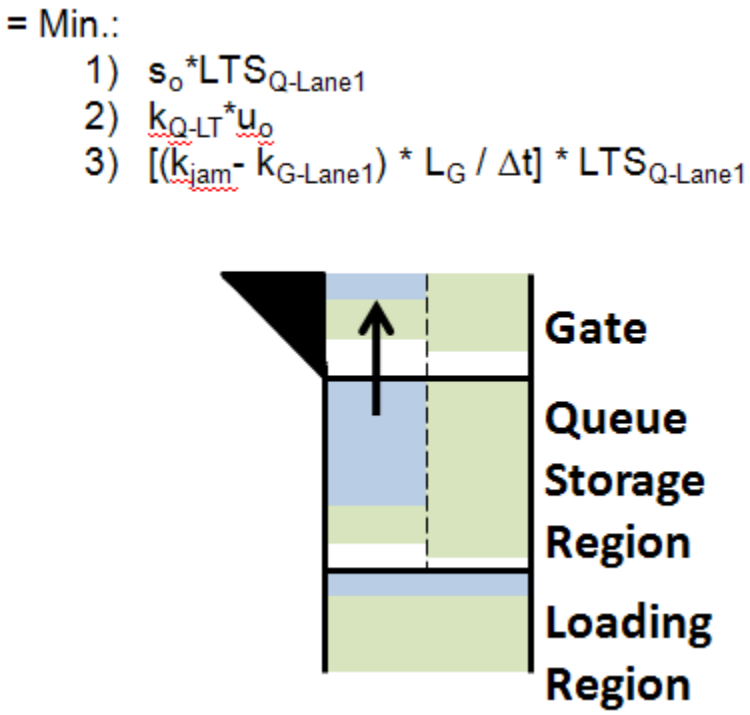

Figure 23 - Queue Storage Region Left Turning Vehicles Outflow Constraints

$LTS_{Q\text{-}Lane1}$ = $n_{Q\text{-}LT} / (n_{Q\text{-}LT} + n_{Q\text{-}TH\text{-}Lane1})$
$n_{Q\text{-}TH\text{-}Lane1}$ = $MAX\ (0, [(n_{Q\text{-}LT}/f_{LU} + n_{Q\text{-}TH})/M] - n_{Q\text{-}LT}/f_{LU})$
$n_{Q\text{-}LT}$ = LT Vehicles in Queue Storage Region
$n_{Q\text{-}TH}$ = TH Vehicles in Queue Storage Region

$k_{Q\text{-}LT}$ = $(n_{Q\text{-}LT}) / (L_Q)$
L_Q = 0.0947 miles (Default queue storage area length = 500 feet)
$k_{G\text{-}Lane1}$ = $[n_{G\text{-}LT} + MAX (0, n_{G\text{-}TH} – (M - 1))] / (L_G)$

Figure 24 describes the four constraints placed on through vehicle output from the queue storage region. The first term represents the (1) saturation flow rate (1900 vph) multiplied by the number of lanes, minus the observed left turning vehicle outflow calculated above ($v_{Q\text{-}LT}$). The second term calculates (2) free flow output from the rightmost through lanes and adds the saturation flow rate from the leftmost lane weighted by the proportion of through vehicles in the leftmost through lane. The third term calculates the (3) number of through vehicles within the gate available for movement during the time step. The final constraint represents the (4) total receiving capacity of the gating region, minus the previously calculated left turn output from the queue storage region.

= Min.:

1) $s_o * M - v_{Q\text{-}LT}$
2) $s_o * (M-1) + s_o * LTS_{Q\text{-}Lane1}$
3) $k_{Q\text{-}TH} * u_o * M$
4) $[(k_{jam} - k_G) * M * L_G / \Delta t] - v_{Q\text{-}LT}$

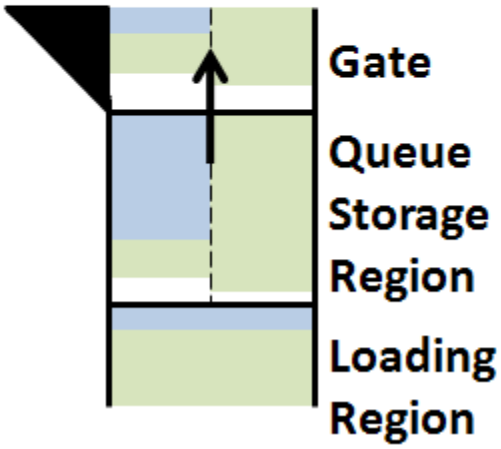

Figure 24 - Queue Storage Region Through Vehicle Outflow Constraints

$v_{Q\text{-}LT}$ = LT queue storage region output flow rate, from Figure 23.
$k_{Q\text{-}TH}$ = $n_{Q\text{-}LT} / (L_Q * M)$
k_G = $(n_{G\text{-}LT} + n_{G\text{-}TH}) / (L_G * M)$

4.4.4 Loading Region ($_{LR}$)

The final component of the model is the loading region, where vehicles are loaded into the system and stored when there is no capacity available in the queue storage region. Although the user is able to define a length of the region in order to account for travel time over the link, there is no specific storage capacity constraint placed on the region. The user is able to observe density within the region, and therefore predict if spillback will occur from

the loading region, but the model prevents any adjustments to the loading pattern as the region begins to exceed the storage capacity.

Figure 25 depicts the three constraints on the total output from the loading region. Unlike the downstream cells, the constraints on this section start with the total output constraints, and then add additional restrictions to both the left and through vehicles in subsequent steps. As with all previously defined constraints, the system is limited by the (1) saturation flow rate, (2) available vehicles, and the (3) total downstream density. An additional factor is introduced, $f_{Q\text{-}LT}$, which is a 0 or 1 variable that tracks the density of queued left turning vehicles in the queue storage region. When this density reaches jam density, the total number of lanes discharging vehicles from the loading region drops by one to reflect the influence of spillback from the queue storage region.

It should be noted that in order to normalize the entire segment length, regardless of the length of the turn pocket, the user is asked to input the total length of the segment. The length of the loading region, L_{LR}, is therefore calculated as the total segment length, minus the length of each of the three downstream cells.

= Min.:

1) $s_o*(M - f_{Q\text{-}LT})$
2) $k_{LR}*u_o*M$
3) $(k_{jam} - k_Q)*M*L_Q / \Delta t$

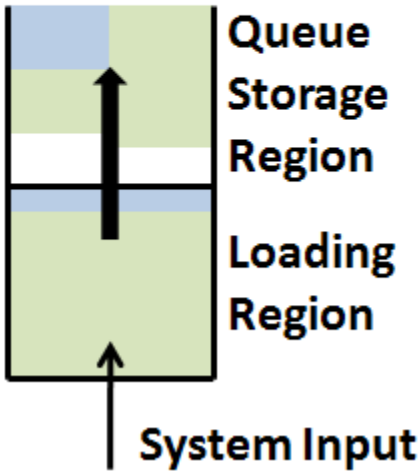

Figure 25 - Loading Region Total Vehicle Outflow Constraints

$f_{Q\text{-}LT}$ = IF ($k_{Q\text{-}LT} = k_{jam}$, then 1, otherwise 0)
k_{LR} = $(n_{LR\text{-}LT} + n_{LR\text{-}TH}) / (L_{LR}*M)$
L_{LR} = $L_{Segment} - L_{P1} - L_G - L_Q$
k_Q = $(n_{G\text{-}LT} + n_{G\text{-}TH}) / (L_Q*M)$

Figure 26 demonstrates the additional constraints placed on the left turn output from the loading region. Following from the assumption that only after entering the queue storage region will left turning vehicles preposition in order to access the turn pocket, the (1) total left turn vehicle output is simply proportional to the total output. However, an additional constraint is placed on left turn output to ensure that (2) discharging vehicles do not overload the storage capacity of the leftmost through lane within the queue storage region.

= Min.:

1) $v_{LR} * n_{LR\text{-}LT} / (n_{LR\text{-}LT} + n_{LR\text{-}TH})$
2) $(k_{jam} - k_{Q\text{-}LT}) * L_Q / \Delta t$

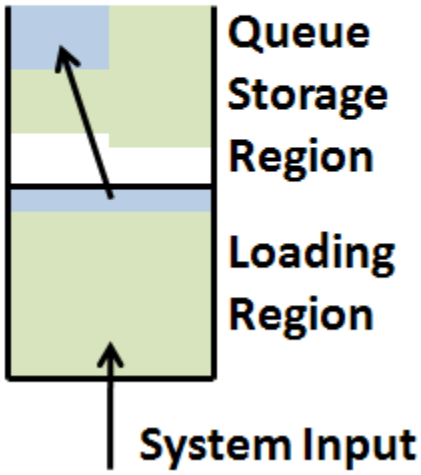

Figure 26 - Loading Region Left Turning Vehicles Outflow Constraints

v_{LR} = Total loading region output flow rate, from Figure 25.
$n_{LR\text{-}LT}$ = LT Vehicles in Loading Region
$n_{LR\text{-}TH}$ = TH Vehicles in Loading Region

Finally, Figure 27 calculates the total through vehicle output from the loading region. This value is simply constrained by the (1) remaining flow rate after applying the additional left turning vehicle constraints, and the (2) total number of through vehicles available to move.

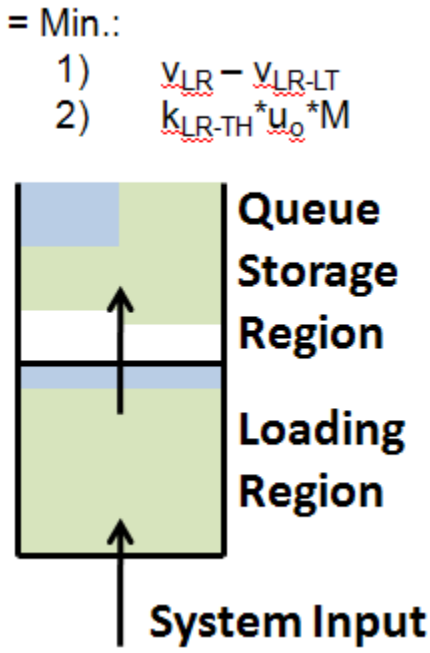

Figure 27 - Loading Region Through Vehicle Outflow Constraints

v_{LR-LT} = Left Turn loading region output flow rate, from Figure 26.
k_{LR-TH} = $(n_{LR-TH}) / (L_{LR} * M)$

Table 7 provides a summary of output constraints by region, as described in detail above. The primary constraints are numbered for reference, and calculated constraints based on the primary constraints are shown for consistency.

Table 7 - Summary of Output Constraints by Region

Region	LT Output	TH Output	Total Output
Pocket	1. $s_o*f_{LT}*N$ 2. $k_{P\text{-}LT}*u_o*N$	1. s_o*M 2. $k_{P\text{-}TH}*u_o*M$	$v_{P\text{-}LT} + v_{P\text{-}TH}$
Gate	1. $s_o*LTS_{G\text{-}Lane1}$ 2. $k_{G\text{-}LT}*u_o$ 3. $(k_{jam}- k_{P\text{-}LT})*(L_{P1}+L_{P2}) / \Delta t$	1. $s_o*M - v_{G\text{-}LT}$ 2. $s_o*(M\text{-}1) + s_o*THS_{G\text{-}Lane1}$ 3. $k_{G\text{-}TH}*u_o*M$ 4. $(k_{jam}- k_{P\text{-}TH})*M*L_{P1} / \Delta t$	$v_{G\text{-}LT} + v_{G\text{-}TH}$
Queue Storage	1. $s_o*LTS_{Q\text{-}Lane1}$ 2. $k_{Q\text{-}LT}*u_o$ 3. $[(k_{jam}- k_{G\text{-}Lane1}) * L_G / \Delta t] * LTS_{Q\text{-}Lane1}$	1. $s_o*M - v_{Q\text{-}LT}$ 2. $s_o*(M\text{-}1) + s_o*LTS_{Q\text{-}Lane1}$ 3. $k_{Q\text{-}TH}*u_o*M$ 4. $[(k_{jam}- k_G)*M*L_G / \Delta t] - v_{Q\text{-}LT}$	$v_{LR\text{-}LT} + v_{LR\text{-}TH}$
Loading	1. $v_{LR} * n_{LR\text{-}LT} / (n_{LR\text{-}LT} + n_{LR\text{-}TH})$ 2. $(k_{jam}- k_{Q\text{-}LT}) * L_Q / \Delta t$	1. $v_{LR} - v_{LR\text{-}LT}$ 2. $k_{LR\text{-}TH}*u_o*M$	1. $s_o*(M - f_{Q\text{-}LT})$ 2. $k_{LR}*u_o*M$ 3. $(k_{jam}- k_Q)*M*L_Q / \Delta t$

4.5 User Interface

As a spreadsheet-enabled macroscopic simulation model, the user must simply enter the desired demand, geometric, and signal timing information within the spreadsheet before pressing "calculate" to run the simulation. Figure 28 provides the input information required to run the spreadsheet analysis. Although the simulation runs for a total of 2 hours to allow for various amounts of loading time, the demand is entered in vehicles per hour. This demand is then loaded directly into the loading region in equivalent units each time step. Within the signal timing dialog, the user must first calculate the effective green time before placing these values into the spreadsheet, accounting for lost time offline. The only other timing information needed then is the total cycle length and starting time of each phase. The calibration parameters, shown in gray, include default values used throughout the analysis

described in the following chapter. The critical gap parameters (t_c, t_f, t_L) are used exclusively to the calculate f_{LT} when a permitted left turning phase is present, following the HCM 2000 procedure.

	Parameter	Unit	Value
Demand	Left Turn Demand	vehicles/hour	380
	Through/Right Demand	vehicles/hour	1520
	Opposing Demand	vehicles/hour	0
Geometry	Pocket Length (L_{P1})	feet	100
	Left Turn Pockets (N)	integer	1
	Secondary Pocket Length (L_{P2})	feet	0
	Approach Lanes (M)	integer	2
	Opposing Lanes	integer	2
	Approach Segment Length ($L_{Segment}$)	miles	1
Signal Timing	Effective Green Time - Protected Left	seconds	25.25
	Effective Green Time - Permitted Left	seconds	-
	Effective Green Time - Through	seconds	46.75
	Effective Green Time - Opposing Through	seconds	0.00
	Start Time - Protected Left	seconds	0.00
	Start Time - Permitted Left	seconds	-
	Start Time - Through	seconds	29.25
	Start Time - Opposing Through	seconds	0.00
	Cycle Length	seconds	120
Calibration	Base Saturation Flow Rate (s_o)	pc/hour/lane	1900
	Speed (u_o)	miles/hour	30
	Vehicle Spacing (AVS)	feet	25
	Lane Width	feet	12
	Queue Storage Region Length (L_Q)	feet	500
	Opposing Platoon Ratio (R_{po})	ratio	1
	Critical Gap (t_c)	seconds	4.5
	Follow-Up Headway (t_f)	seconds	2.5
	Opposing Lane Group Lost Time (t_L)	seconds	4
	Opposing Lane Utilization Factor (f_{LUo})	factor	0.95
	Left Turn Adjustment Factor (f_{LT})	factor	0.95

Figure 28 - User Input Dialog

Figure 29 provides a depiction of five basic phasing sequences that will be used in Chapter 5, all with a cycle length of 120 seconds. In each case, protected left g/c is equal to 0.21 (25.25 seconds), and through movement g/c is equal to 0.39 (26.75 seconds). Phase order and degree of overlap is varied while holding these values constant to provide four distinct phasing patterns. The values shown represent the necessary values needed to input into the model. For reference, Figure 28 represents the correct implementation of phase sequence a), as shown in Figure 29. The through phase effectively starts 4 seconds after the completion of the protected left phase. The opposing movement is not shown as the duration is irrelevant when protected-only phasing is used.

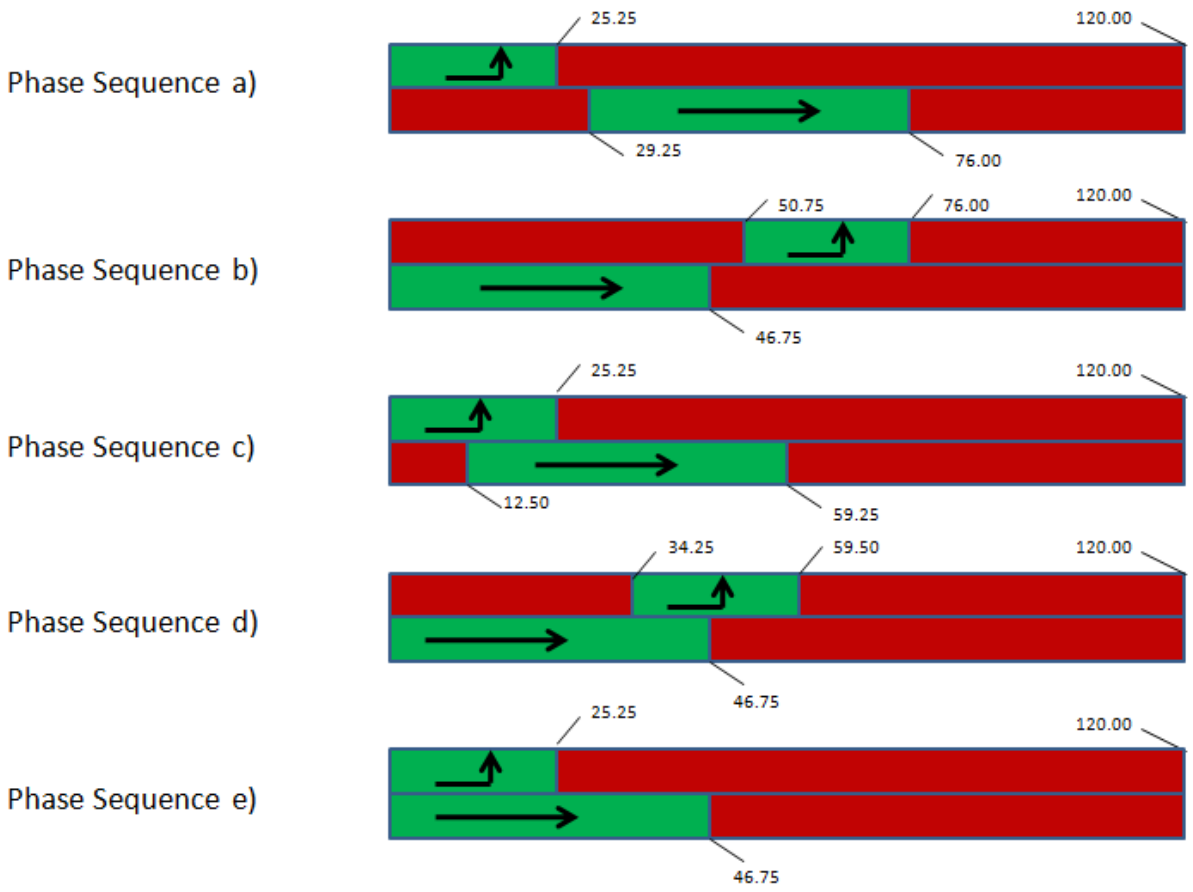

Figure 29 - Phase Sequence Input Example

Table 8 provides a snapshot of the output provided by the model. Sustainable service rates (SSR) by movement are provided for 5 one-hour-long floating time windows over the 2 hour simulation period. SSR divided by the calculated signal capacity (SSR/c) is also provided for each movement. The next three values show the through vehicle distribution values (THVD) at three points along the approach: discharge from (1) the loading region, (2) the queue storage region, and (3) the gate, respectively. $LTS_{G\text{-}Lane1}$ provides the proportion of the left turning vehicles in the leftmost through lane within the gate, expressed as a ratio of the total number of vehicles using the leftmost through lane within the gate. The final value,

SSR_L/SSR_{Total}, reflects the total percentage of left turning vehicles discharging from the intersection.

Table 8 - Model Output

	SSR						Through Vehicle Distribution			Lane Split	Output Ratio
Time Window	SSR_{LT}	SSR_{LT}/c_{LT}	SSR_{TH}	SSR_{TH}/c_{TH}	SSR_{Total}	SSR_{Total}/c_{Total}	$THVD_{LR}$	$THVD_Q$	$THVD_G$	$LTS_{G\text{-}Lane1}$	SSR_L/SSR_{Total}
0-60	229	0.60	993	0.67	1222	0.67	0.37	0.23	0.10	0.70	0.19
15-75	248	0.65	993	0.67	1241	0.67	0.37	0.22	0.09	0.74	0.20
30-90	248	0.65	993	0.67	1241	0.67	0.37	0.22	0.09	0.74	0.20
45-105	248	0.65	993	0.67	1241	0.67	0.37	0.22	0.09	0.74	0.20
60-120	248	0.65	993	0.67	1241	0.67	0.37	0.22	0.09	0.74	0.20

The final piece of information provided to the user describes operation within the loading region, as shown in Table 9. As noted above, the loading region is unconstrained, and may exceed jam density for a poorly operating intersection. This information is available to the user to determine if spillback into the region has occurred, as well as the maximum observed percentage of left ($n_{LR\text{-}LT}$ / n_{LR}) and through ($n_{LR\text{-}TH}$ / n_{LR}) vehicles contained within the region at any point over the 2 hour simulation period. If the maximum observed density by movement is below jam density, the actual maximum will be shown. If this value exceeds jam density, ">kjam" will appear to indicate spillback through the region.

Table 9 - Loading Region Information

Max. $k_{LR\text{-}LT}$	148
Max. $k_{LR\text{-}TH}$	>kjam
Max. k_{LR}	>kjam
Max. $n_{LR\text{-}LT}/n_{LR}$	20%
Max. $n_{LR\text{-}TH}/n_{LR}$	80%

5. ANALYSIS OF RESULTS

5.1 Overview

This chapter provides a detailed analysis of a select set of results in order to demonstrate the model's sensitivity to a variety of parameters, as well as provide a comparison against results generated using microscopic simulation (VISSIM) and Wu's capacity model, adjusted using a constant lane distribution adjustment factor. In general, the basic case study used throughout the following analysis focuses on an intersection with a single, 100' left turn pocket, 2 approach through lanes, 20% left turn demand (left = 380 vph, through = 1520 vph), exclusive leading left phasing, effective green times for the left and through movements of 0.21 and 0.39 g/C, respectively, and a 120 second cycle (Phase sequence a) from Figure 29). Sensitivity to each parameter is demonstrated by varying one of these default values while holding the remaining values constant. Each of these values can be referenced in Figure 29 from Chapter 4. For ease of visualization, wherever possible, blue represents left turning vehicles while green represents through vehicles.

5.2 Stabilization

Analysis of sustainable service rates, by definition, requires that observed throughput values are able to reach a point of stabilization. In other words, as SSR analysis is most interested in the maximum sustainable number of vehicles that can proceed through an intersection over a specified period of time, it is critical that this value reaches and maintains a relatively stable peak value. In oversaturated conditions, queue lengths are time dependent,

but in many cases, throughput values are able to stabilize after an initial loading period, and can thus be referred to as sustainable service rates.

Figure 30 and Figure 31 provide illustrations of throughput stabilization over time, for both left turn and through vehicle throughput, respectively. Each point represents total throughput by movement over the previous 60 minutes, divided by signal capacity for the movement. With a mile-long segment length, there is an initial loading period, where left turn throughput values have yet reach a maximum value. After 15 minutes, however, hourly throughput values appear to stabilize in almost every case, effectively reaching the sustainable service rate of interest, inclusive of turn pocket and lane interaction effects.

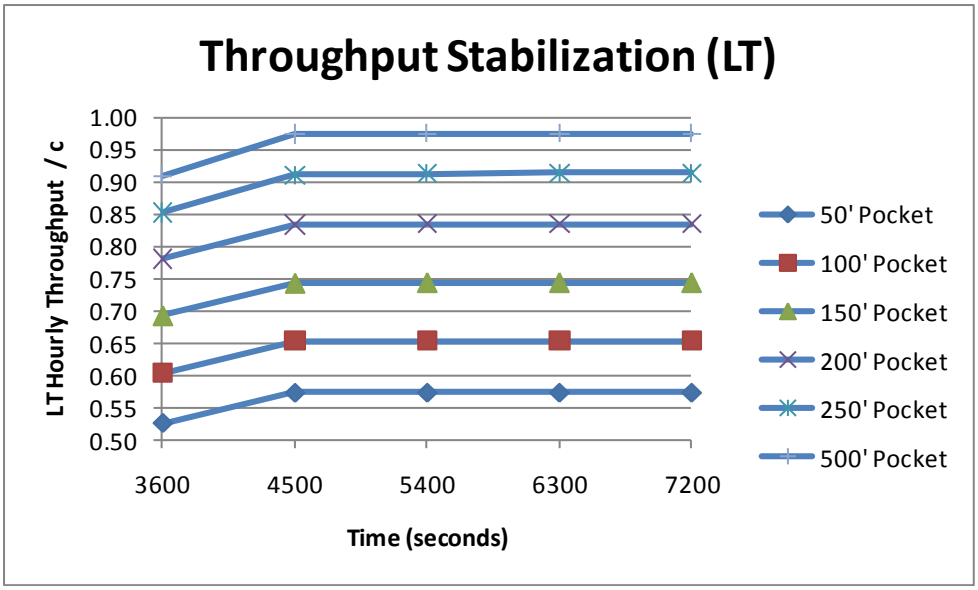

Figure 30 - Left Turn Throughput Stabilization

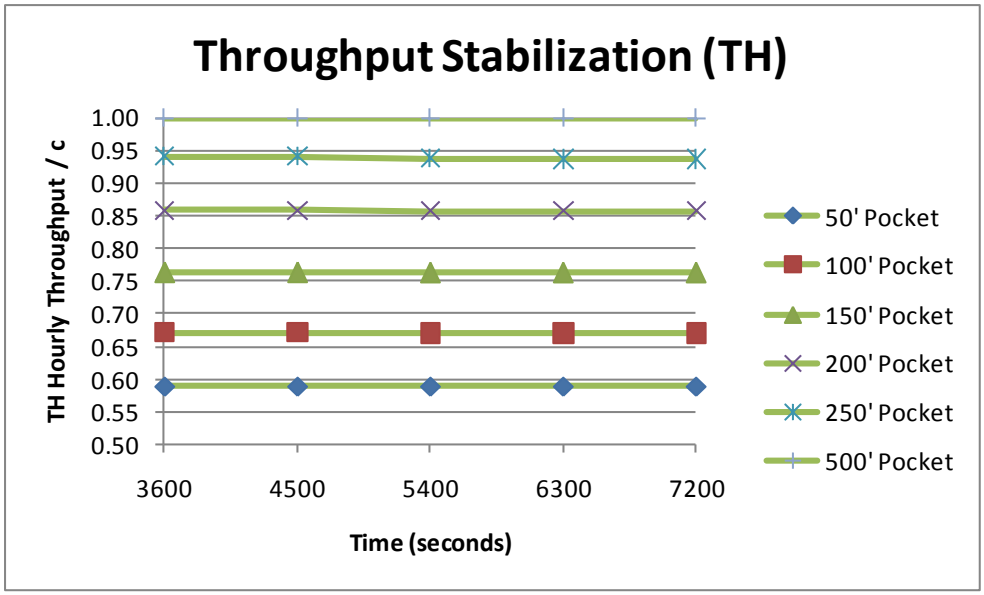

Figure 31 - Through Vehicle Throughput Stabilization

5.3 Queue Storage Region Length

Before critically analyzing model results, it is important to examine the sensitivity of the model to the length of the queue storage region, developed as a mechanism to allow for a

continuous queue buildup of left turning vehicles upstream of the gate. Figure 32 provides a sensitivity analysis for both a 50' and 100' turn pocket with varying queue storage lengths. As shown, with queue storage region lengths less than 10 vehicles, SSR values are highly sensitive to the length of this region. When the region begins to exceed around 15 vehicles, however, the sensitivity of SSR values to the queue storage diminish rapidly.

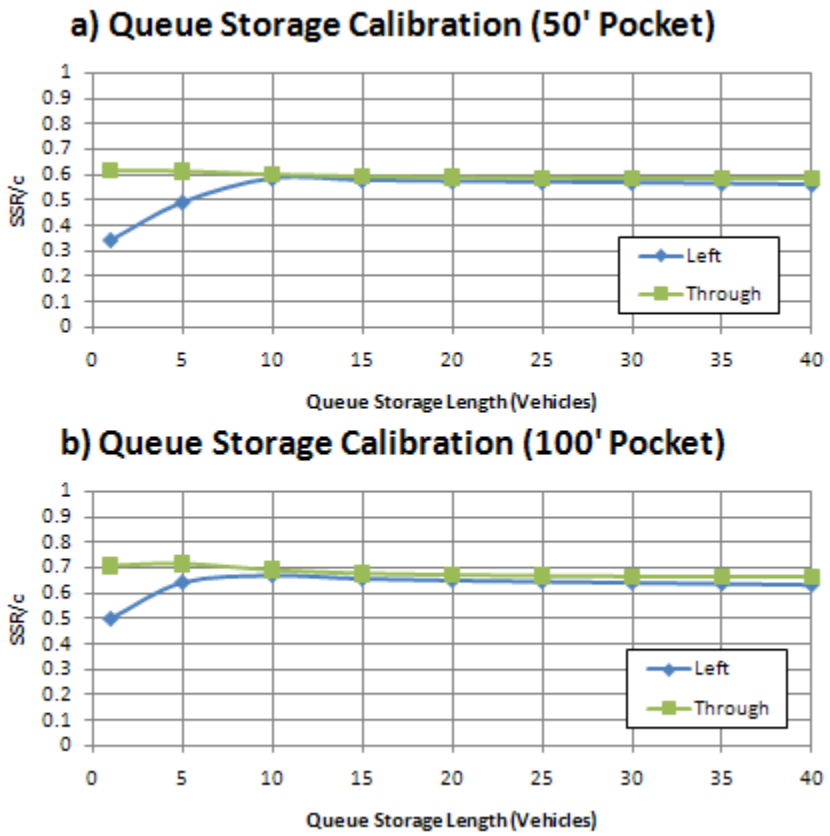

Figure 32 - Queue Storage Region Calibration for a 50' & 100' Pocket

These observations can be explained by the relationship between the signal timing plan, the pocket length and the length of the queue storage region. With very short turn pockets, a significant proportion of vehicles able to discharge from the intersection originate

within the queue storage region at the beginning of the phase. For the timing plan shown, the signal capacity of the left turn movement is greater than 12 vehicles per cycle. This means that the percentage of left turning vehicles in the queue storage region has a significant effect on discharge proportions. When the length of the turn pocket plus the queue storage region begins to exceed the per cycle signal capacity, sensitivity to the actual length becomes much less significant.

To test this hypothesis, sensitivity of SSR to the queue storage region was analyzed for a 500' pocket. As shown in Figure 33, when the turn pocket is able to store the entire per cycle capacity, sensitivity to the queue storage region length becomes essentially insignificant.

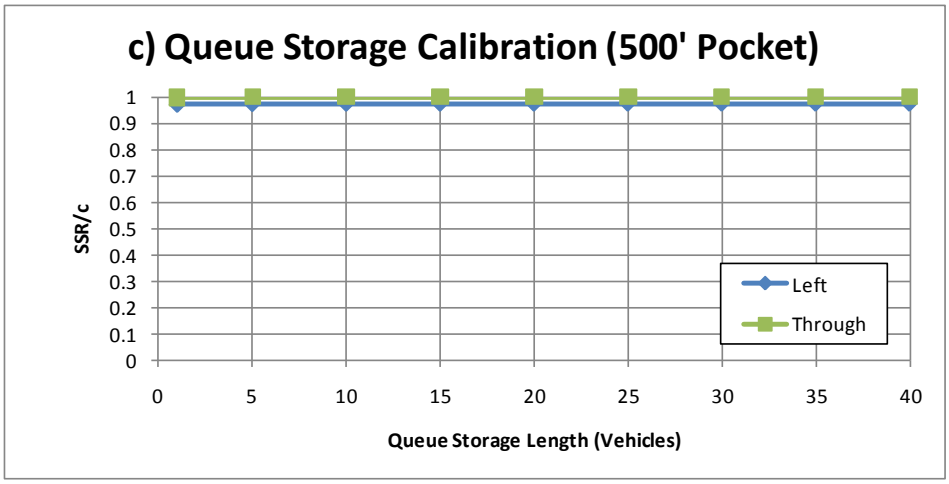

Figure 33 - Queue Storage Region Sensitivity with a 500' Pocket

Based on this analysis, it was determined that a 500' queue storage region is sufficient, even with very short turn pockets. It should be noted, however, that with excessively long green times for the left turning movement, this value may need to be re-

analyzed. For consistency, however, the queue storage region is held constant at 500' for the entire following analysis.

5.4 Pocket Length

From a practical standpoint, pocket length analysis is one of the most critical components to this research, as this single parameter enables the practitioner to determine the relative effectiveness of extending the pocket length as a way of improving the operation of congested intersection. Figure 34 demonstrates the sensitivity of the model to pocket length, assuming constant signal capacity and demand values. Under the scenario described, with 20% left turn demand, there is clearly much to be gained by extending a very short turn pocket. In fact, a 50' turn pocket would only be able to effectively operate at around 60% of signal capacity. Sustainable service rates begin to reach near-capacity conditions with pockets greater than around 250' feet, suggesting there is little to be gained by extending the pocket beyond this point.

It is interesting to note the degree to which pocket length sensitivity is tied to the signal timing plan. In the case described, the signal capacity for the left turn pocket is around 12 vehicles per cycle, which is approximately the number of vehicles able to queue within a 300' short turn pocket. The results therefore follow closely with intuitive expectations that an efficient signal system operating at capacity should allow the entire turn pocket to clear each cycle.

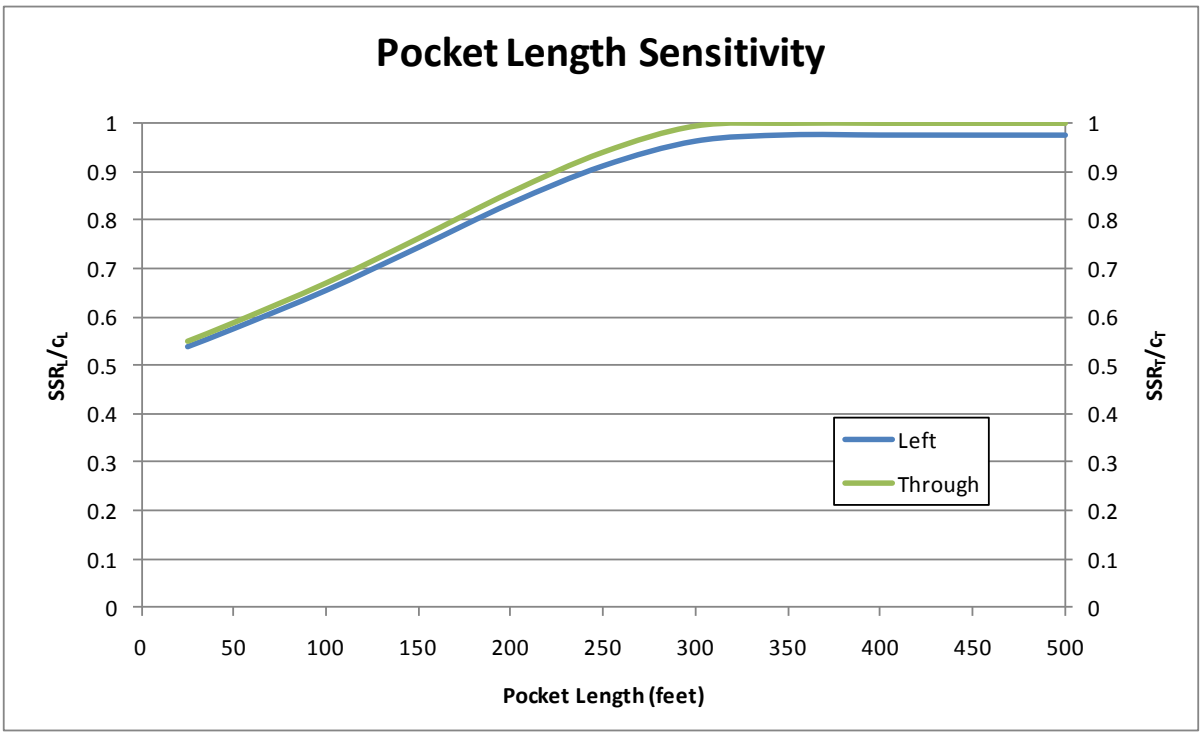

Figure 34 - Pocket Length Sensitivity

5.5 Demand Levels

In addition to pocket length analysis, an effective macroscopic simulation model must also allow the user to track the onset of turn pocket effects based on demand levels. In undersaturated conditions, prior to the onset of any short turn pocket effects, it would be expected that all intersections should have the ability to process all incoming demand. As turn pocket effects begin to impede flow, however, throughput values would be expected to converge to a stable, sustainable value, regardless of the degree of oversaturation. Figure 35 and Figure 36 demonstrate this trend, with throughput values equivalent to demand until turn pocket effects begin to have a disrupting effect on the system.

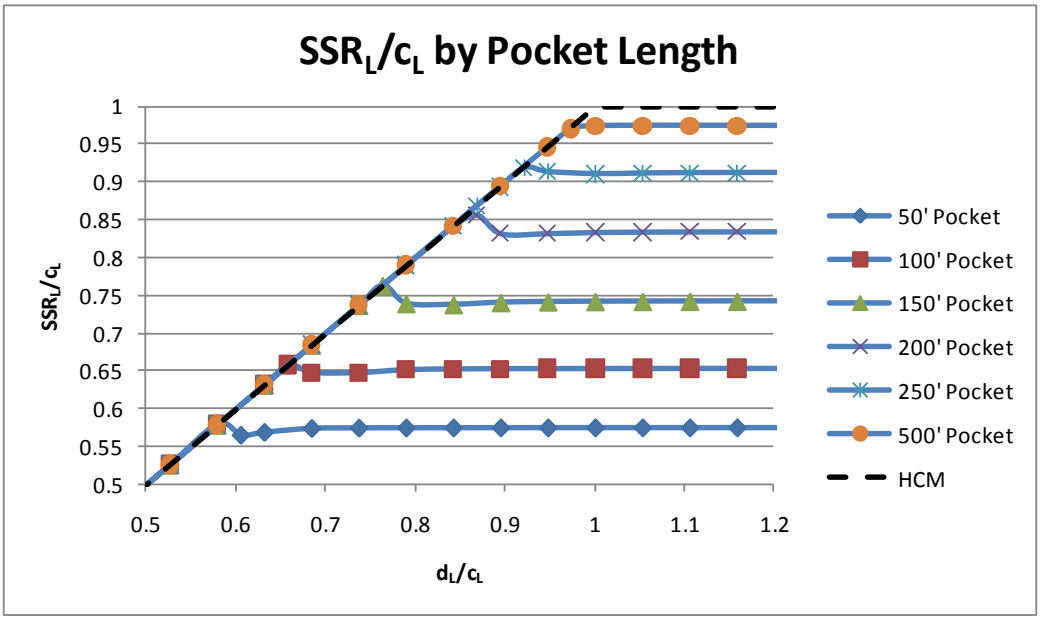

Figure 35 - Left Turn Throughput Demand Sensitivity

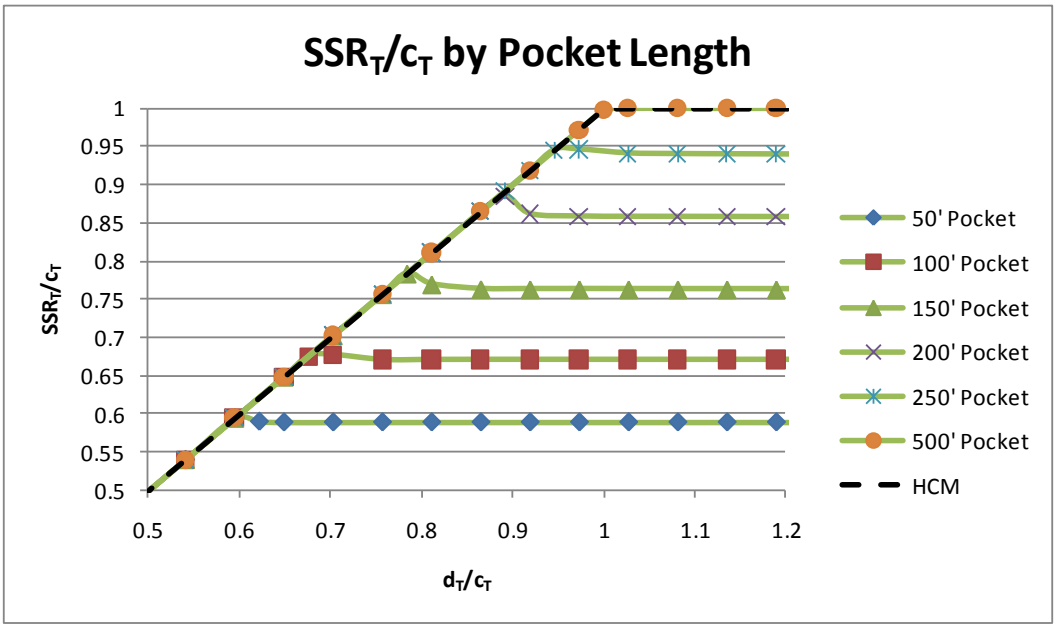

Figure 36 - Through Vehicle Throughput Demand Sensitivity

In several cases, increasing demand actually *decreases* throughput slightly. The 200' pocket case provides the clearest example of this drop in throughput, where stable SSR

values are actually lower the maximum observable throughput. The drop is slight, typically less than about 3% of signal capacity, but the trend is consistently present. The most likely explanation for this drop is the disrupting effects of spillback and starvation effects. When demand levels are just below those necessary to generate spillback or blockage, the system is able to process all incoming demand. Additional demand placed on the system introduces short turn blockage effects, however, causing a slight drop in throughput back to sustainable service levels. This case indicates the importance of distinguishing between observed throughput values, which are demand dependent, and the sustainable service rate of the intersection, which is a stable condition independent of total demand levels.

5.6 Phase Sequence

Phase order and the total amount of phase overlap are two components of the signal timing plan that significantly affect the extent of short turn pocket effects. Even with full overlap of the protected left and through phase, in cases where the per-cycle capacity is greater than the storage capacity of the short turn pocket, a portion of the cycle will operate below signal capacity due to the nature of the shared approach lane. However, it would be expected that phase overlap would suppress short turn pocket effects by limiting blockage time.

Figure 37 and Figure 38 demonstrate the sensitivity of the macroscopic simulation model to both phase order and degree of overlap. A depiction of each phase described is provided in Figure 29 from Chapter 4. For all five phase sequences shown, the total amount

of green time is constant for each movement, but the order is varied. For lead-overlap and lag-overlap (c & d), half of the protected left phase occurs overlaps the through movement. With full overlap (e), both the left and through movements begin simultaneously, although the through movement remains green after the end of the protected left phase. To normalize the observations, only the period from 3600 to 4500 seconds is shown, and each movement therefore has the same total effective green time over the 15-minute simulation interval.

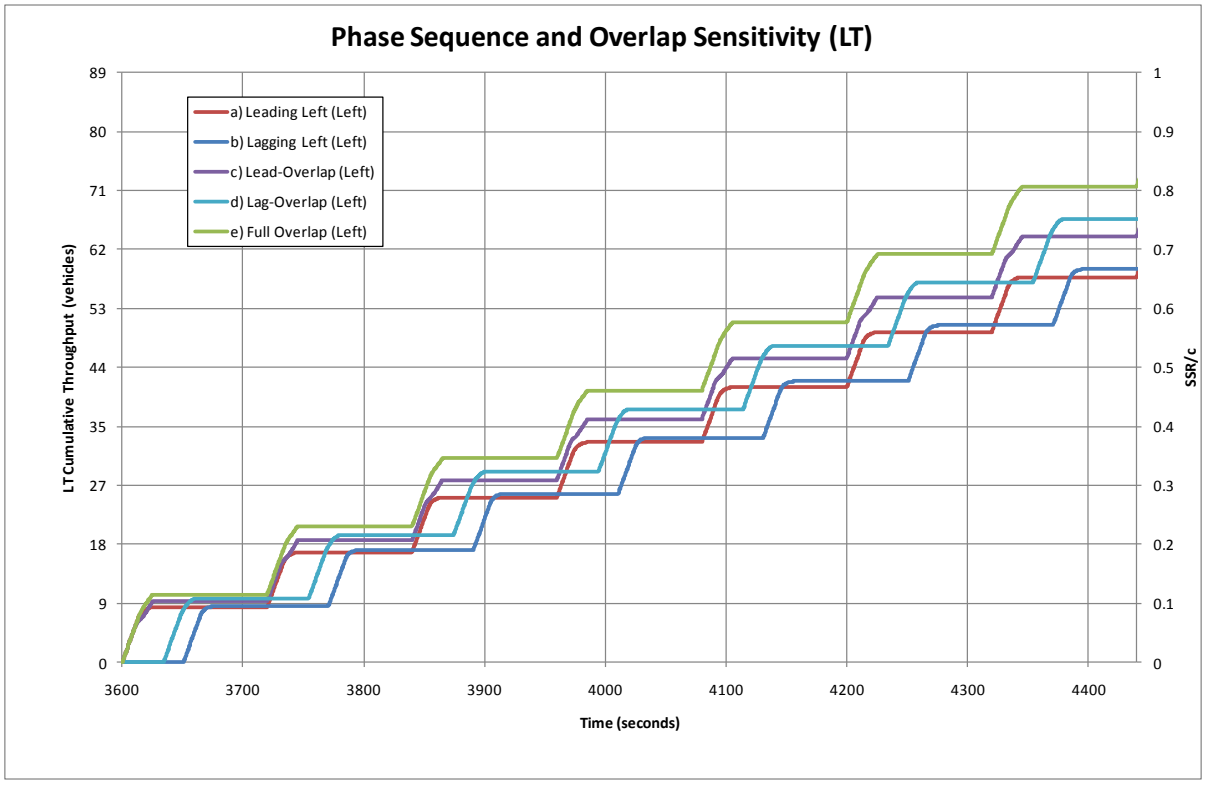

Figure 37 - Phase Sequence and Overlap Sensitivity (LT Throughput)

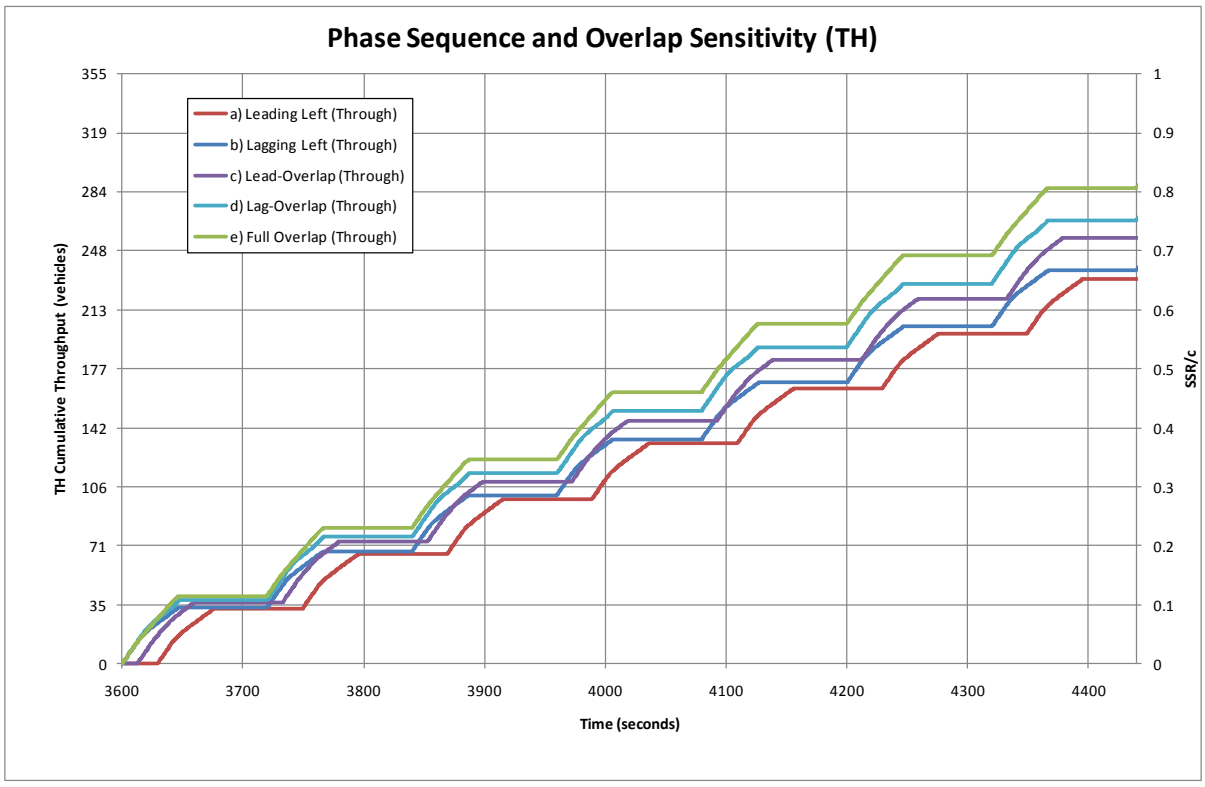

Figure 38 - Phase Sequence and Overlap Sensitivity (TH Throughput)

As expected, full overlap phasing (e) generated the highest SSR values, followed by partial overlap (c & d). This result was validated using a variety of other trials, including 5% left turn demand and 45% left turn demand, and in every case where turn pocket effects reduced the effective sustainable service rate of the approach below theoretical signal capacity, full phase overlap (e) generated the maximum SSR values for each movement. Although these findings need to be explored further, initial analysis indicates that maximizing the amount of phase overlap provides one mechanism to minimize turn pocket effects and maximize SSR relative to the theoretical signal capacity.

It is also interesting to note that lagging left phasing was slightly more efficient than a leading left phase in this particular case with 20% left turn demand, processing around 11 more total vehicles within the 15 minute time period. This is likely due to a reduction in total time spent with pocket spillback for the lagging left case, allowing greater through movement throughput with only a slight reduction in left turn throughput relative to the leading left case. In Wu's analytical models (2008), it was assumed that in oversaturated conditions with a single approach lane, there is no difference between leading and lagging left phasing. And indeed, the macroscopic simulation model generates the same values for these two phase sequences with a single through lane. When an additional through lane is introduced to the system, however, there appear to be observable differences in the efficiency of the system based on phase order. The full extent of the difference is dependent upon total g/C values, red time between phasing, and movement percentages, making generalization of the results difficult, but clearly the proposed macroscopic simulation technique enables the detection of differences not available through the use of any other macroscopic model.

5.7 Permitted Phasing

Another example of the practical applicability of the proposed macroscopic simulation approach arises when the signal timing plan includes both a protected and permitted left turn phase. With Wu's models (2008), the per-cycle signal capacity is an input variable, enabling the user to calculate the average saturation flow rate over the entire cycle for use in the equation. While this approach enables the model to deal with a combination of

a protected and permitted left turn phase, it is insensitive to the fact that queues will develop at different rates within the cycle based on the discharge rate at any given time.

The proposed model, while unable to time-varying saturation flow rates within the permitted phase, does calculate two separate values for f_{LT} based on the phase type and is therefore sensitive to protected-permitted phasing. Figure 39 demonstrates the sensitivity of the model to permitted phasing, with opposing through demand shown on the x-axis. In the example shown, the protected phase is held constant at a g/C of 0.2, but in the protected-permitted case (solid lines) the permitted phase is allowed to continue through the entire through phase (g/C 0.4).

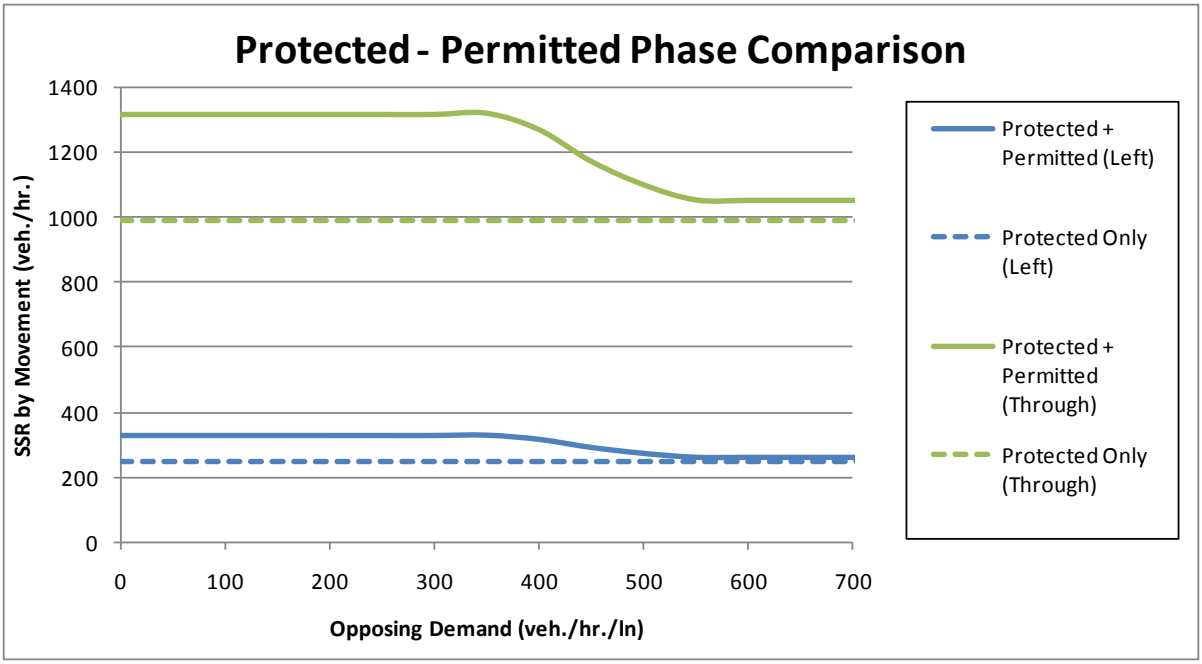

Figure 39 - Protected Only vs. Protected-Permitted Phase Sensitivity

By using the HCM 2000 approach, the model is able to take into account the effect of sneakers, as indicted by the slightly increased SSR values for the protected-permitted case

even under very high opposing demand. It should be noted that the model does not artificially increase the storage area of the pocket to account for sneakers, but by introducing a minimum saturation flow rate on the left turn pocket during the permitted phase, the model effectively reduces the impact of spillback and starvation during the permitted phase.

It should be noted that by using the HCM 2000 approach, even with zero opposing demand, f_{LT} will never equal 0.95, the assumed value within a protected phase. In fact, the maximum value for f_{LT} using the HCM 2000 procedure is approximately 0.76 due to the calculation of E_{L1}. Interestingly, however, this is not the limiting factor that generates constant output between 0 and 350 opposing vph from Figure 39. This maximum value is due to the limiting effects of a shared approach lane, where discharge from the gate (3,800 vph with 2 lanes) places a constraint on the system after the pocket clears. In other words, below a certain threshold, opposing demand is no longer a factor in limiting discharge as turn pocket effects related to the nature of the shared approach upstream of the entrance to the pocket becomes the primary constraint on throughput from the intersection.

5.8 Lane Distribution Analysis

The single greatest benefit from using the proposed macroscopic simulation tool over the analytical equations developed by Wu (2008) is the ability of the model to automatically adjust approach vehicle distribution values based on incoming demand and spillback effects. To use an equation-based analytical approach, a single vehicle distribution factor must be applied at the entrance to the system so that each approach lane may be analyzed

independently. As observed in the field, however, this value is typically not a static value that remains constant over the entire approach as through vehicles will often switch lanes to either avoid queues or prevent pocket blockage if possible.

Figure 40 provides model predictions of through vehicle lane distribution values (THVD) at three points along the approach: discharge from (1) the loading region, (2) the queue storage region, and (3) the gating region. The stop bar through vehicle distribution value is not shown, as by the nature of the model, the value would remain constant at 0.5 for two lanes as the through pocket region contains no left turning vehicles. Distance is therefore measured to the turn pocket entrance as all cells upstream of this diverge point include the influence of turning vehicles. Under a weighted equal vehicle distribution scenario ignoring turn pocket effects, approximately 37% of through vehicles would be expected to utilize the leftmost through lane, calculated as:

$$[((380 / 0.95 + 1520) / 2) - 380 / 0.95] / 1520 = \mathbf{36.8\%}$$

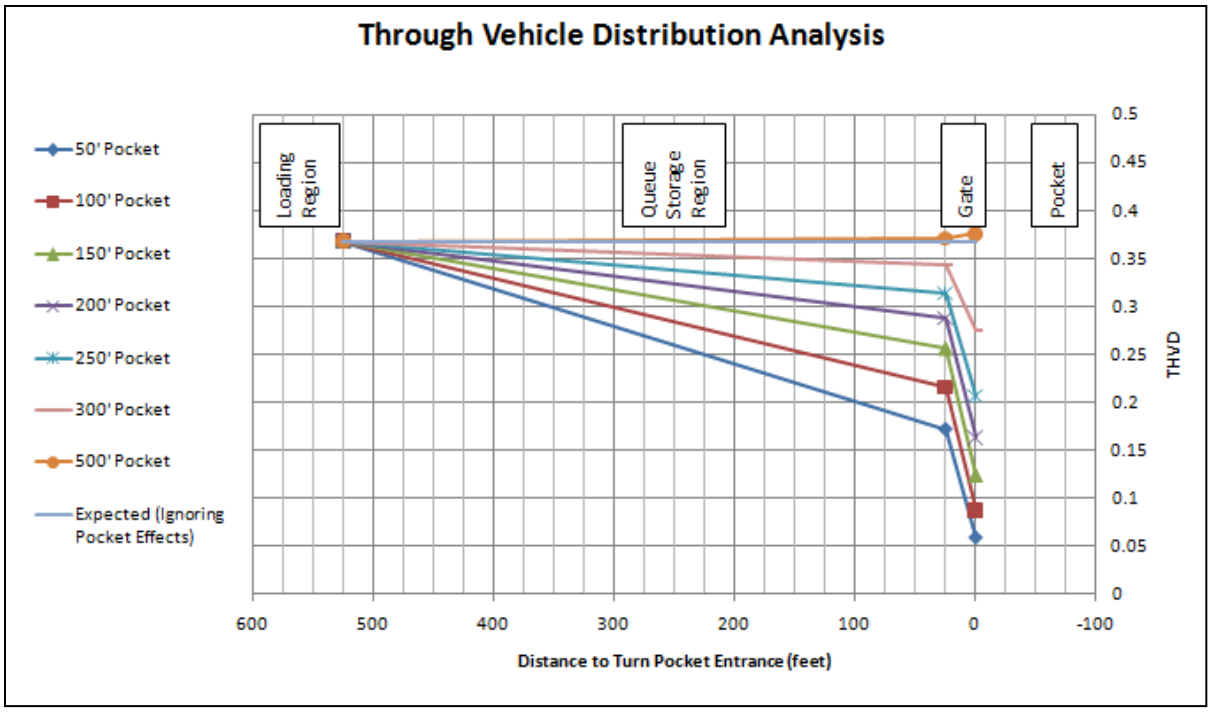

Figure 40 - Through Vehicle Lane Distribution by Distance

The figure illustrates the variability of the vehicle distribution factor and the inherent problem of applying a constant factor to the entire system. With a 50' pocket, nearly 95% of all through vehicles would use the rightmost through lane, which is strikingly higher than the 63% assumed using an adjusted equal lane distribution analysis procedure. By increasing the length of the turn pocket, however, through vehicle distribution values begin to approach the expected 37%. In fact, with a 500' pocket, this distribution is maintained over the entire approach to the turn pocket.

5.9 Phase Split Optimization

As has been shown several times throughout this analysis, the extent of short turn pocket effects are related to the signal timing plan. It therefore follows that in addition to extending the physical turn pocket or altering approach demand, modifying the allocation of existing green time between movements may alleviate at least some of throughput reductions experienced due to spillback and blockage.

Figure 41 and Figure 42 provide an example of a phase optimization procedure with a 100' left turn pocket, showing actual SSR and SSR/c on the y-axis, respectively. The basic assumption is that the total effective green time for both movements is held constant at 0.6 g/C, and total intersection throughput values are analyzed by shifting green time between movements with no phase overlap using a leading left phasing pattern (phase sequence a).

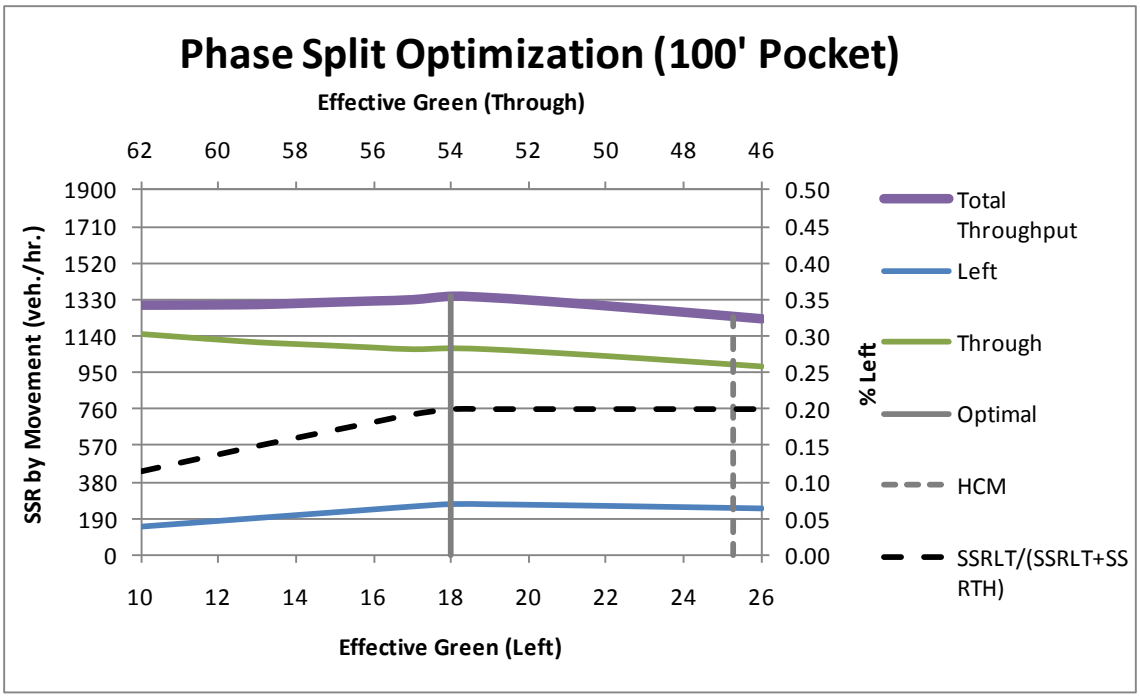

Figure 41 - Phase Split Optimization Procedure - 100' Pocket (SSR by Movement)

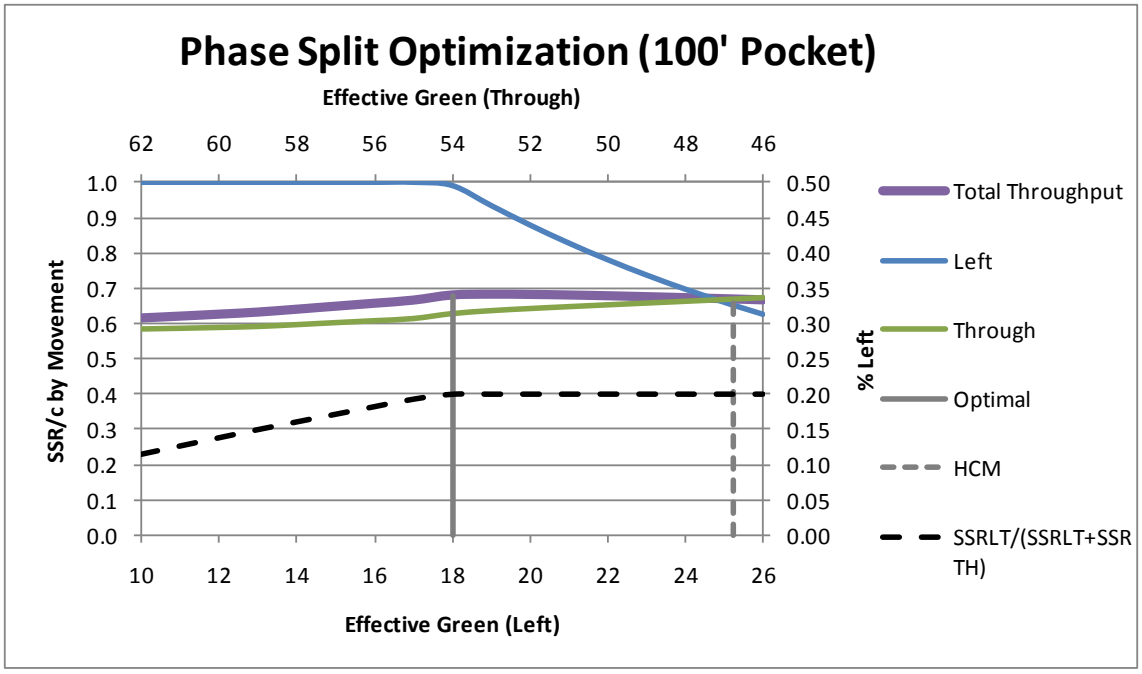

Figure 42 - Phase Split Optimization Procedure - 100' Pocket (SSR/c)

By following the purple line, which represents total approach throughput, it can be shown that overall approach operation will improve by shifting green time from the protected left phase to the through phase. With the left turning movement operating under signal capacity (≈380 vph), it may seem counterintuitive to remove green time from this movement, but in fact, much of the green time allocated to left turning vehicles is wasted. By shifting some of this time to the through movement, the total sustainable service rate of the intersection improves by around 8%.

A critical component of the analysis is the percentage output by movement (SSR_{LT} / (SSR_{LT} + SSR_{TH})), shown as the dashed black line. With fully exclusive phasing, optimization will occur when the minimum amount of green is allocated to the left turning phase while still maintaining 20% left turn output, the percentage of left turn demand. If the

output turning ratio falls below the demand turning ratio with exclusive phasing, the system becomes highly unstable. However, any additional green time allocated to the movement is simply wasted cycle time and actually reduces overall approach throughput.

While the procedure outlined provides a useful, practical tool for the practitioner, it also highlights the significance of turn pocket length when determining the optimal signal timing plan. Current HCM practice simply treats any turn pocket as a full length lane, but clearly, optimal timing plans are dependent upon the length of the turn pocket. This macroscopic simulation tool is currently the only available resource for optimizing a pre-timed control system when more than one approach lane is present, and certainly additional research is needed to investigate the critical relationship between optimal signal timing and pocket length.

5.10 Time-Dependent Demand

The final benefit of a simulation-based analysis tool over a series of analytical equations is the ability to handle time-varying demand. Figure 43 shows the input dialog that allows the user to override the fixed demand and instead input demand in 15-minute intervals. To do so, the use must simply enter a "Y" next to "Time Dependent Demand" and type values in the yellow boxes. The gray boxes show the final demand input, which are equivalent to the fixed demand entered above when the Time Dependent Demand setting is turned off.

		Time Dependent Demand?	Y
	Time Period	Demand Entry	
LT Demand	15	280	280
	30	380	380
	45	280	280
	60	150	150
	75	150	150
	90	150	150
	105	150	150
	120	150	150
TH Demand	15	1120	1120
	30	1520	1520
	45	1120	1120
	60	600	600
	75	600	600
	90	600	600
	105	600	600
	120	600	600

Figure 43 - Time-Dependent Demand Entry

Figure 44 and Figure 45 provide examples of total stop bar output using the time dependent demand setting shown above. During the initial period of heavy demand (dotted line), the system quickly reaches the sustainable service rate and maintains this discharge rate while queues build up on the approach. This queue buildup is visually represented by the separation of the lines in Figure 45. Even after demand levels drop below the SSR, the system continues to process vehicles at the sustainable service rate due to the long queue of vehicles waiting to be served. After queues clear, throughput values drop to demand levels, where all incoming vehicles are able to be served by the approach. It should be noted that the seemingly instable conditions marked by fluctuations in discharge are simply the result of a 120 second cycle, which is slightly out of sync with the 15-minute analysis periods show in the graphs.

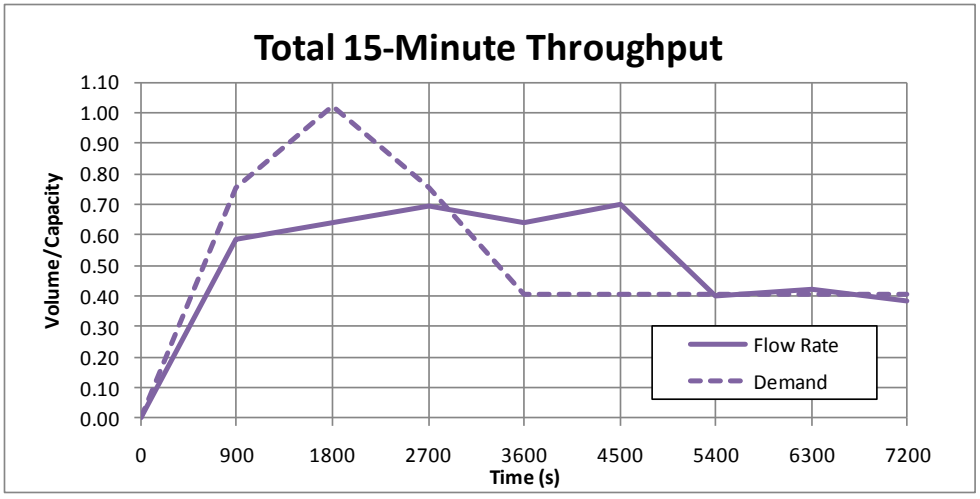

Figure 44 - Total Output with Time-Varying Demand (100' Pocket)

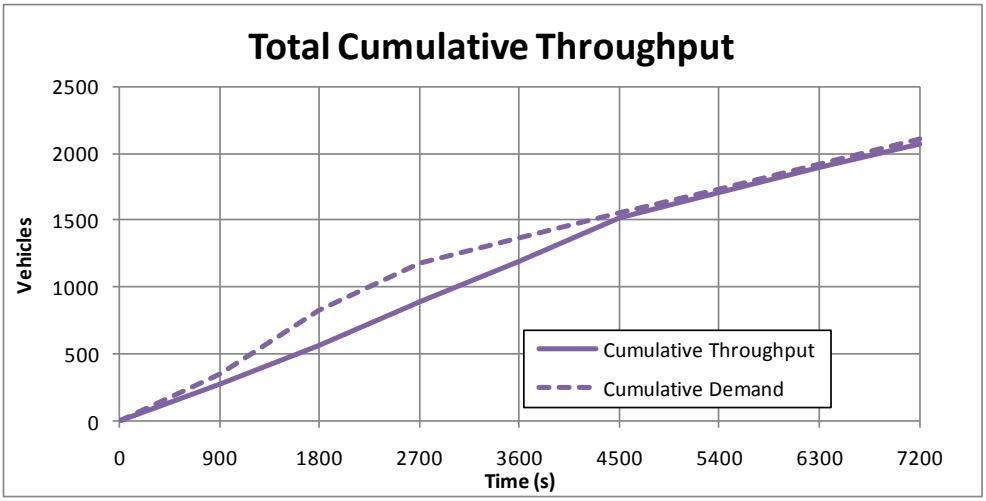

Figure 45 - Cumulative Total Output with Time-Varying Demand (100' Pocket)

5.11 Model Comparisons

For model comparison purposes, a total of 216 separate trials were performed using the proposed model, Wu's analytical macroscopic model with a weighted equal lane distribution in order to analyze the approach lanes independently, and microsimulation

(VISSIM). Table 10 provides a summary of the critical variables tested. In each case, a single left turn lane was used, with total approach demand set at 1100 vph and 1900 vph with one and two approach lanes, respectively. Each movement was allocated 0.2 g/C and 0.4 g/C respectively, with only the degree of overlap varying by trial. Note that the timing plan is slightly modified from the scenarios described above. Due to the highly oversaturated conditions generated given the assumed phase split, the 24 trials with 30% left turn demand on a two lane approach were not performed. Left turn queue buildup was simply too great to allow for reliable analysis. For both of the macroscopic models, only a single trial was run due to the deterministic nature of each. A total of 20 runs were made for each trial using VISSIM, however, and all microsimulation results reported below reflect the average hourly throughput of these 20 runs after an initial 15 minute loading period. Additionally, in order to avoid bias from vehicles attempting to merge into the pocket from the rightmost through lane, the look ahead distance was set to 10,000 feet to ensure that all left turning vehicles would even the leftmost through lane far upstream of the entrance to the turn pocket.

Table 10 - Testing Scenarios

Through Lanes	Phase Sequence	Left Turn Demand (ratio)	Pocket Length (feet)
1	Leading Left	0.10	50
2	Lagging Left	0.15	100
	Full Overlap	0.20	150
	Partial Overlap	0.25	200
		0.30	250
			500

Figure 46 and Figure 47 provide a comparison of results over multiple turn pocket lengths using each of the three models with a single approach lane and a leading left phase. Wu's macroscopic analytical models, shown in blue, include calibrated model parameters

based on simulation in VISSIM, and as a result, can be expected to match simulation values very closely when only a single approach lane is present. This is indeed the case, and slight differences with through SSR may be due to different calibration constants used for the simulation trials. The proposed macroscopic simulation tool was developed independently from microsimulation values, but still follows a very similar trend. In fact, the only difference is simply due to the initial slope of the curve, with SSR values using the proposed model increasing at a slightly greater rate relative to simulation with very short turn pockets.

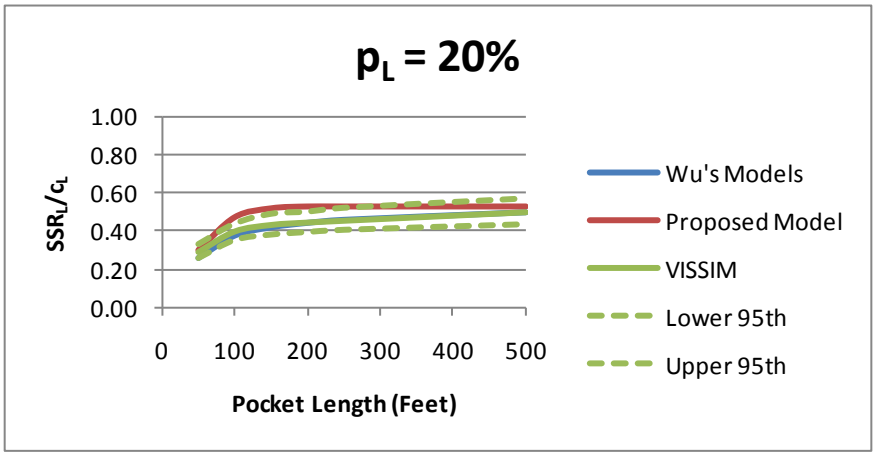

Figure 46 - Model Comparison (Left SSR with single approach lane)

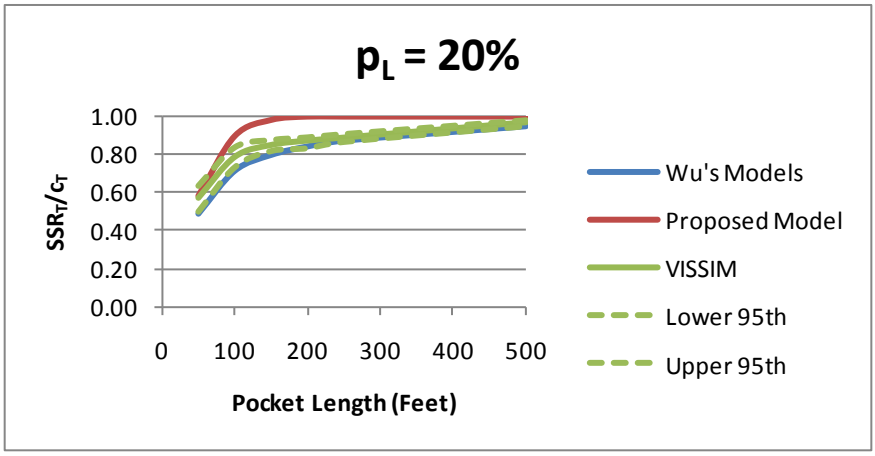

Figure 47 - Model Comparison (Through SSR with single approach lane)

The major contribution of this work is not with a single approach lane, however, as the available analytical models clearly perform very well in this context. The added benefit of using the proposed model becomes most apparent when more than one approach lane is present. Figure 48 and Figure 49 provide the results from each model under the same scenario described above, but with two approach lanes.

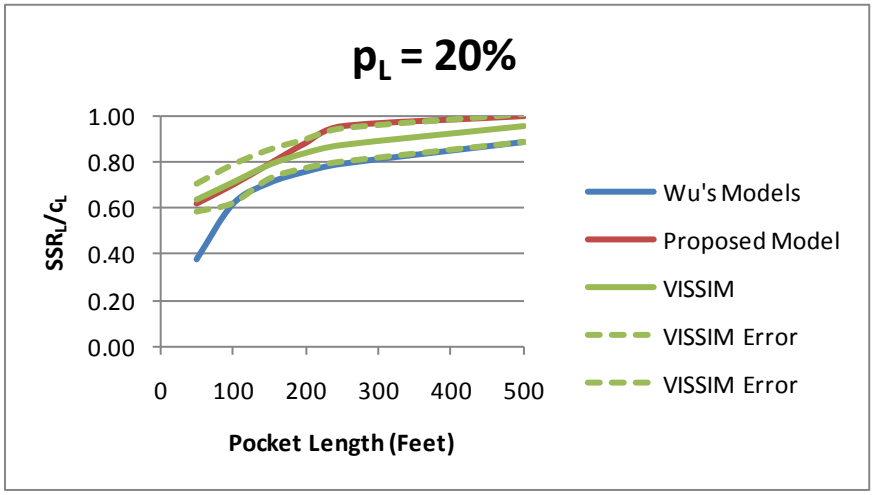

Figure 48 - Model Comparison (Left SSR with two approach lanes)

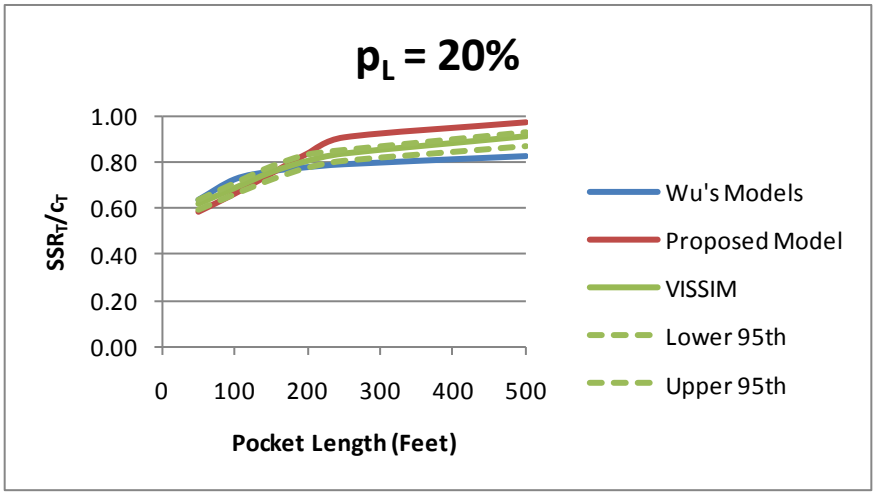

Figure 49 - Model Comparison (Through SSR with two approach lanes)

Although each model produces slightly varied results, with a very short turn pocket, the proposed model clearly follows simulation values much more closely than Wu's models. Based on the lane distribution analysis provided in section 5.8, it would be expected that the greatest difference between the models would be with very short turn pockets, as with longer turn pockets, the predicted lane distribution at the gate begins to approach the expected values used within the analytical model. This is indeed the case, and by calculating the assumed lane distribution independently from pocket length, Wu's models both underestimate left turn throughput and overestimate through vehicle throughput.

The results from each of the remaining trials are provided in Appendix B. Figure 50 and Figure 51 provide a comprehensive comparison of all 216 trials, broken out by movement. Interestingly, both macroscopic models generated similar left turn throughput values to those observed in simulation, although Wu's macroscopic model included a number of outliers with a two lane approach. In terms of through vehicle throughput, the proposed model tended to overestimate throughput, while Wu's models tended to underestimate

simulation values. Given the instability of a number of trials run using a 500' pocket, it is unsurprisingly that the proposed model was less capable of predicting through vehicle throughput values observed in simulation. It would be interesting to the test the models using a more efficiently timed signal system to reduce the effects of instability in the comparison, but such an analysis is beyond the scope of this research.

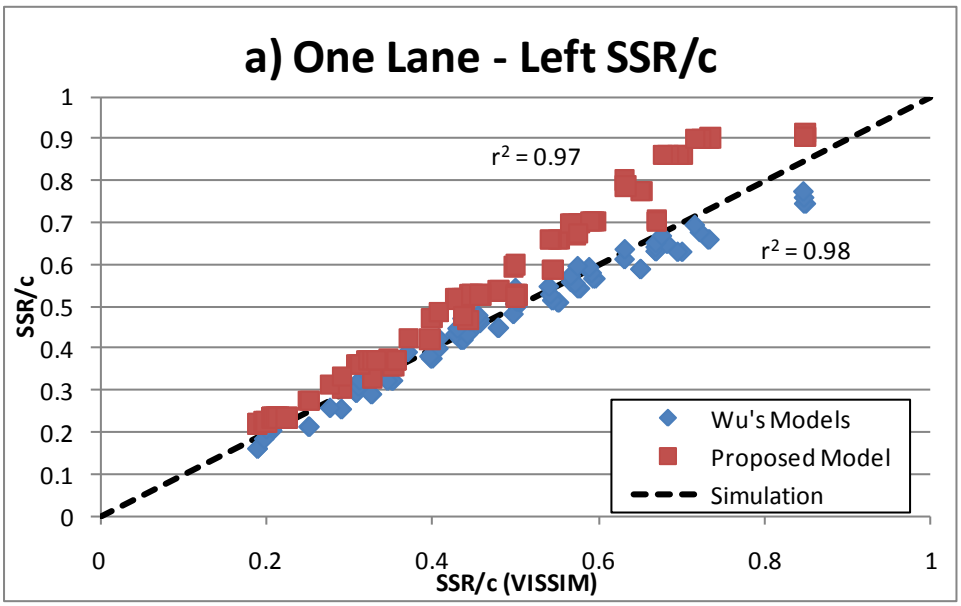

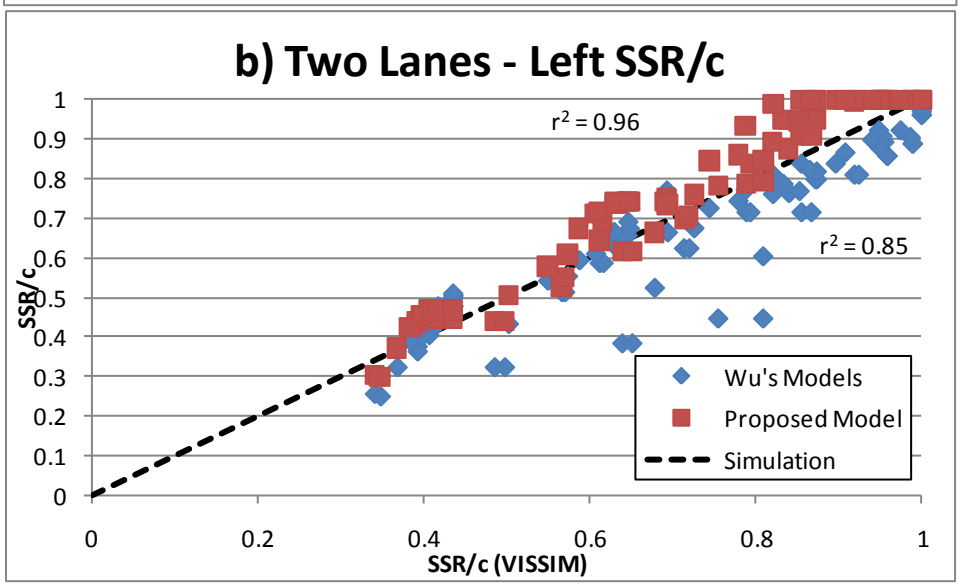

Figure 50 - SSR/c Model Comparison (Left)

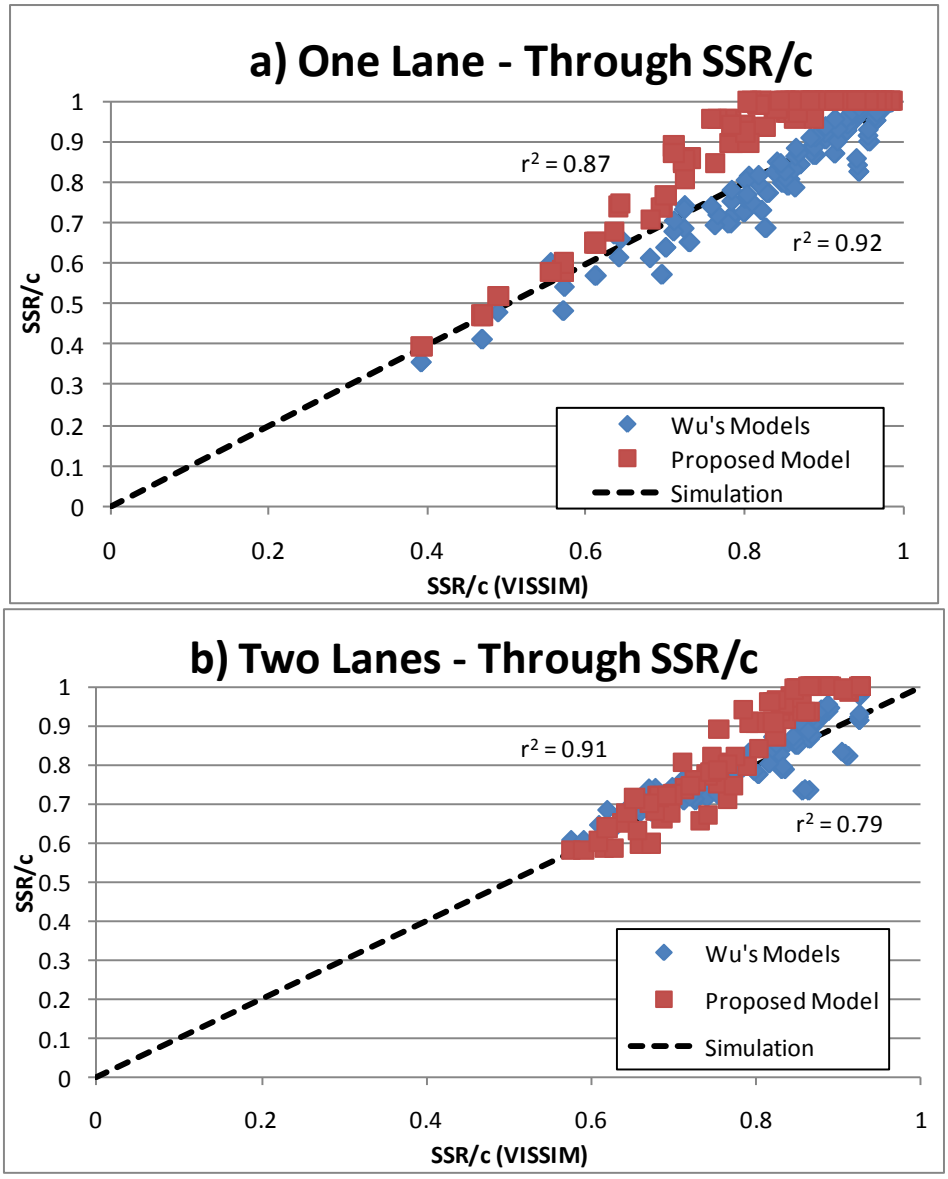

Figure 51 - SSR/c Model Comparison (Through)

The results reflected in the above figures represent all 216 trials, including the 120 trials run using a single approach lane and the 96 trials using a two lane approach. Part b of each figure highlights the discrepancies between the two macroscopic models when multiple through lanes are present. Wu's models, developed specifically for a single lane approach, follow simulation results much less closely on a two lane approach, with r^2 values of 0.85

and 0.79 by movement. The proposed model, on the other hand, maintains r^2 values of 0.96 and 0.91 by movement for these same 96 trials.

5.12 Summary

Comparison against simulation is certainly not the only measure of a model's effectiveness, as the simulation trials are themselves calibrated models intended to estimate real world data. The analysis has shown, however, that the proposed macroscopic simulation model is sensitive to each of the critical parameters outlined in the methodology section, and has demonstrated the practical applicability of the spreadsheet for scenario testing. The model is sensitive to spillback, starvation, pocket length, signal timing, as well as varying saturation flow rates. A built in lane distribution assumption by cell is able to automatically and efficiently allocate through vehicles to available lanes, which represents a step forward from previous turn pocket analysis models. Additional testing is certainly needed to validate the effectiveness of the model, but preliminary results indicate significant potential for aiding in turn pocket analysis on multi-lane approaches.

6. SUMMARY, CONCLUSIONS & RECOMMENDATIONS

6.1 Summary

The vast majority of turn pocket analysis research has focused on the probability of spillback from a turning lane in undersaturated conditions. This work provided the foundation for pocket design guidelines, which attempt to minimize the likelihood of queue buildup past the entrance to the short turn pocket. Only recently have researchers begun to investigate the effects of short turn pockets on the effective sustainable service rate of an intersection, or the maximum sustainable amount of movement throughput that is able to proceed through a signalized intersection accounting for queue interaction and blockage effects. Of the models developed that have the capability to reduce expected throughput based on turn pocket effects, none have analyzed multilane approaches. The macroscopic simulation model developed in this thesis utilizes a number of simplifying assumptions regarding through vehicle lane distribution and lane changing behavior on the approach to a congested intersection as an attempt to motivate additional research on the topic.

Preliminary results compare favorably to throughput values obtained using the microscopic simulation platform VISSIM, but the testing set included a number of unstable, time dependent results due to poor signal timing plans. It would be beneficial to test timing plans that only generate sustainable throughput values in order to remove the bias of system instability. Field data collection is difficult as the model focuses on sustainable throughput from an oversaturated intersection, but the model would benefit from a certain degree of field validation.

Despite the limitations and simplifying assumptions contained within the model, all primary objectives of the research were satisfied. Critical input variables were identified based on the literature, calibrated using field observations, and used in the development of a macroscopic simulation model sensitive to (1) spillback, (2) blockage, (3) pocket length and storage area, (4) phasing order and timing plans, (5) saturation flow rates, (6) lane changing behavior, and (7) time-dependent demand by movement. Based on the assumptions contained within Daganzo's cell-transmission model (Daganzo, 1993), the macroscopic analysis examines flow rates within discrete segments of the approach link without tracking individual vehicles explicitly, allowing for robust lane distribution analysis with minimal computational burden. Final comparison of 216 independent trials indicate that the proposed model compares favorably to microsimulation results using VISSIM, with overall r^2 values of 0.97 for the left turning movement and 0.87 for the through movement. The end result is a powerful standalone tool that can be used by practitioners and researchers alike to analyze turn pocket effects, test various signal timing strategies, perform cost-benefit analysis of physical improvements, and ultimately find the most practical option available to improve the performance of poorly operating intersections with problematic short left turn pockets on multilane approaches.

6.2 Conclusions

SSR values generated using the proposed macroscopic model provided some critical insight into the effects of short turn pockets on the operation of a multilane approach to

signalized intersections. The following list provides the primary conclusions from the research:

- SSR values by movement are highly sensitive to turn pocket length, demand by movement, phase order and phase overlap.

- Signal timing optimization is dependent upon the length of the short turn pocket(s) and demand levels by movement. Ignoring pocket length, as per the HCM 2000 methodology, may generate sub-optimal timing plans.

- With fully exclusive phasing, efficient green time allocation is accomplished by providing the left turn movement with the minimum amount of green time needed to ensure that the total percentage of left turn throughput from the approach is equivalent to the percentage of left turn demand.

- Although previous research has indicated no difference in expected SSR between leading and lagging left phasing with a single lane approach, observable difference in the phasing patterns arise when more than one through lane is present on the approach.

- Maximizing phase overlap provides one method of maximizing SSR relative to the theoretical signal capacity by limiting total blockage time.

- An increase in the total amount of time per cycle in which left turn spillback generates blockage on the leftmost through lane corresponds to a decrease in through vehicle utilization of the leftmost through lane as through vehicles avoid queue buildup.

6.3 Recommendations

For model development purposes, a number of parameters were not included in the initial version of this macroscopic simulation model. The following list provides a description of some of the critical variables not considered in this research:

6.3.1 Additional Testing Needed

Three or More Through Lanes: Although the simulation model in its current form is able to provide SSR values when more than two through lanes are present, the results have not been explored in detail, or tested against other models. Additional analysis is needed.

Heavy Vehicle Analysis: Although the user has the option to calculate passenger car equivalents offline, there was little analysis done on the effects of heavy vehicles on both spillback and blockage. Further research is needed to validate the use of passenger car equivalents with respect to heavy vehicles within this model.

6.3.2 Model Modifications Required

Courtesy Factor Analysis: In its current form, the simulation model assumes that within the gate, through vehicle drivers will shift out of the leftmost through lane, if possible, to delay the onset of pocket blockage. Alternatively, the model could assume that lane distribution within the gate follows a weighted equal lane distribution at every time interval, which would lead to additional pocket blockage. It is recommended that a user calibrated "driver courtesy factor" be added to the model in order to allow for flexibility of this behavioral assumption.

Right Turn Pocket Analysis: Current input does not allow for short right turn pocket analysis. The logic developed for short left turn pocket analysis can be easily transferred and utilized in the context of short right turn pockets, and it is recommended that the input dialog and simulation equations be modified to allow for right turn pocket analysis.

Right Turn on Red: After adding right turn pocket functionality, right turn on red can be added to the model by calculating an adjusted saturation flow rate for the red time period from the turn pocket. There is currently no easily modified way of adding right turns on red to the model in the absence of a short right turn pocket, however, as a through vehicle in the rightmost through lane at the stop bar would act as a way of blocking a right turn on red movement. Further research is needed to add RTOR to the model.

Unconventional Designs: The current model assumes that the short left turn pocket is equivalent in length to the adjacent through storage region, which is not always the case as some intersections. It is recommended that future research explore the onset of blockage when these lengths are not equivalent.

Time-Varying Signal Control: Although the use has the option to vary demand by 15-minute intervals, the pre-timed signal system is fixed throughout the entire analysis period. It may be beneficial to allow the user to modify the signal timing plan on a 15-minute basis in order to more realistically model control during the peak 15 minute period.

Actuated Control: The macroscopic simulation model currently assumes pre-timed control. Future research will be needed to explore actuated control in detail.

Other than the concept of actuated control, each of the additional parameters can be easily added to the model and tested. This list of recommendations, if implemented, has the potential to greatly improve the functionality and applicability of the model and provide practitioners with a single, easy-to-use macroscopic simulation tool for analyzing both short left and right turn pocket effects at intersections with multiple approach lanes.

Despite the limitations of the model in its current form, this single model has greater functionality for turn pocket analysis than any other macroscopic tool available. It is sensitive to pocket length, demand levels by movement, phase order, phase overlap, and permitted phasing, and includes a built-in lane distribution function that can be easily

transferred to other research on the topic. Perhaps most significantly, the model is able to clearly demonstrate that the sustainable service rate of a signalized intersection is related to the length of a turn pocket, and reallocation of green time may provide a cost-effective solution to improving the operation of a congested multilane intersection with a short left turn pocket. Results highlight both the need to include turn pocket length in signal timing equations, as well as the critical need for further research on the topic.

7. REFERENCES

Ackelik & Associates (2004). aaSIDRA User Guide, Akcelik and Associates Pty Ltd, Melbourne, Australia.

Daganzo, C. (1993). "The Cell Transmission Model. Part I: A Simple Dynamic Representation of Highway Traffic," *Transportation Research B*, Vol. 28, pp. 269–287.

Highway Capacity Manual (2000), Transportation Research Board, National Research Council, Washington D.C.

Hillier, F.S. and G.J. Lieberman (1990). Introduction to Operations Research (5th Ed.), McGraw-Hill, New York, NY, 561-930.

Kikuchi, S., P. Chakroborty, and K. Vukadinovic (1993). "Lengths of Left-Turn Lanes at Signalized Intersections," *Transportation Research Record: Journal of the Transportation Research Board, No.1385*, TRB, National Research Council, Washington, D.C., 162-171.

Kikuchi, S., M. Kii, and P. Chakroborty (2004). "Lengths of Double or Dual Left-Turn Lanes," *Transportation Research Record: Journal of the Transportation Research Board, No. 1881*, TRB, National Research Council, Washington, D.C., 72-78.

Kikuchi, S., N. Kronprasert and M. Kii (2007). "Lengths of Turn Lanes on Intersection Approaches: Three-Branch Fork Lanes- Left-Turn, Through, and Right-Turn Lanes," *Transportation Research Record: Journal of the Transportation Research Board, No. 2023*, TRB, National Research Council, Washington, D.C., 92-101.

Kikuchi, S. and N. Kronprasert (2008). "Determining the Length of the Right-Turn Lane at a Signalized Intersection," *Transportation Research Record: Journal of the Transportation Research Board, No. 2060*, TRB, National Research Council, Washington, D.C., 19-28.

Lighthill, M.J. and G.B. Whitham (1955). "On Kinematic Waves II: A Theory of Traffic Flow on Long Crowded Roads," *Proceedings of the Royal Society*, London Ser. A., 229(1178), 317-345.

Neuman, T.R. (1985). "NCHRP Report 279: Intersection Channelization Design Guide," TRB, National Research Council, Washington, D.C.

NGSIM (2009). Federal Highway Administration, U.S. Department of Transportation, <http://www.ngsim.fhwa.dot.gov>

Oppenlander, J.C. and J.E. Oppenlander (1989). "Design Lengths of Left- or Right-Turn Lanes with Separate Signal Phases," *ITE Journal*, 59(7), 23-26.

PTV AG (2008), "VISSIM," [CD-ROM], Karlsruhe, Germany.

Qi, Y., L. Yu, M. Azimi and L. Gui (2007). "Determination of Storage Lengths of Left-Turn Lanes at Signalized Intersections," *Transportation Research Record: Journal of the Transportation Research Board, No. 2023*, TRB, National Research Council, Washington, D.C., 102-111.

Reynolds, W.L., X. Zhou, N.M. Rouphail and M. Li (2010). "Estimating Sustained Service Rates at Signalized Intersections with Short Left Turn Pockets: A Mesoscopic Approach," *Transportation Research Record: Journal of the Transportation Research Board*, (pending publication), Transportation Research Board of the National Academies, Washington, D.C.

Rouphail, N.M., and R.A. Akcelik (1998). "A Preliminary Model of Queue Interaction at Signalized Paired Intersections," *Proceedings 16th ARRB Conference, Part 5,* Australian Road Research Board, Ltd., Vermont South, Victoria, Australia, 1998, pp. 325-345.

Tian, Z. and N. Wu (2006). "Probabilistic Model for Signalized Intersection Capacity with a Short Right-Turn Lane," *Journal of Transportation Engineering*, 132(3), 205-212.

Viloria, F., K. Courage and D. Avery (2000). "Comparison of Queue-Length Models at Signalized Intersections," *Transportation Research Record: Journal of the Transportation Research Board, No. 1710,* TRB, National Research Council, Washington, D.C., 222-230.

Wu, N. Total Approach Capacity at Signalized Intersections with Shared-Short Lanes – A Generalized Model Based on Simulation Study. In *Transportation Research Record: Journal of the Transportation Research Board*, No. 2027, Transportation Research Board of the National Academies, Washington, D.C., 2008, pp. 19-26.

Zhang, Y. and J. Tong (2008). "Modeling Left-Turn Blockage and Capacity at Signalized Intersection with Short Left-Turn Bay," *Transportation Research Record: Journal of the Transportation Research Board, No. 2071*, TRB, National Research Council, Washington, D.C., 71-76.

APPENDICES

APPENDIX A: SPREADSHEET IMPLEMENTATION SCREENSHOTS

Figure 52 - Parameter Calculation

Given Parameters		
u_o	30	mile/hour
Lane Width	12	feet
k_{jam} =	211.2	vhc/ml/lane
Simulation interval (dt)=	0.25	sec
	0.0000694	hr
AVS	25	feet
	0.004734848	miles
LT Demand	380	vhc/hour
TH Demand	1520	vhc/hour
Total Demand	1900	vhc/hour
Opposing Demand	0	vhc/hour
p_{LT}	0.20	ratio
p_{TH}	0.80	ratio
f_{LUo}	0.95	ratio
v_{oe}	0	vhc/hour
S_{LT}	0	vhc/ml/lane
f_W	1.00	factor
v_{olc}	0.00	vhc/hour/lane
qr_o	0.61	ratio
g_q	0.00	seconds
g_u	0.00	seconds
E_{L1}	1.32	pce/veh.
f_{min}	0.00	factor
f_m	0.00	factor
L_Q (vehicles)	20.00	vehicles
s_o	1900	vhc/hour/lane
Effective Protected Left g/C	0.21	ratio
Effective Permitted Left g/C	0.00	ratio
Effective Through g/C	0.39	ratio
Effective Opposing g/C	0.39	ratio
f_{LT}	0.95	ratio
f_{LU}	0.95	ratio
Number of left-turn pockets	1	lanes
Number of through lanes	2	lanes
Opposing Lanes	2	lanes
Segment Length	1	miles
L_{P1}	0.018939394	miles
	100	feet
L_{P2}	0	feet
Pocket Area	0.018939394	lane*miles
L_{LR}	0.881628788	miles
	4655	feet
Pocket Storage	4	vehicles
Free-flow travel time	108.0681818	seconds
Cycle Length	120	seconds
$g_{L\text{-Protected}}$ Phase	25.25	seconds
$g_{L\text{-Protected}}$ Start	0	seconds
$g_{L\text{-Protected}}$ End	25.25	seconds
$g_{L\text{-Permitted}}$ Phase	0	seconds
$g_{L\text{-Permitted}}$ Start	0	seconds
$g_{L\text{-Permitted}}$ End	0	seconds
Through Phase	46.75	seconds
Through Start	29.25	seconds
Through End	76	seconds
Opposing Phase	46.75	seconds
Opposing Start	29.25	seconds
Opposing End	76	seconds

Figure 53 - Time Step / Loading Screen

		Input								
		Signal							Capacity	
		Cycle	$Left_{Pr}$	$Left_{Pe}$	Through	Opp.	**LT Demand**	**TH Demand**	**Capacity_out_LT**	**Capacity_out_TH**
Time Interval	**Clock (sec)**	0	1	0	0	0			Service Rate*signal	Service Rate* signal
28406	7101.5	21.5	1	0	0	0	380	1520	1805	0
28407	7101.75	21.75	1	0	0	0	380	1520	1805	0
28408	7102	22	1	0	0	0	380	1520	1805	0
28409	7102.25	22.25	1	0	0	0	380	1520	1805	0
28410	7102.5	22.5	1	0	0	0	380	1520	1805	0
28411	7102.75	22.75	1	0	0	0	380	1520	1805	0
28412	7103	23	1	0	0	0	380	1520	1805	0
28413	7103.25	23.25	1	0	0	0	380	1520	1805	0
28414	7103.5	23.5	1	0	0	0	380	1520	1805	0
28415	7103.75	23.75	1	0	0	0	380	1520	1805	0
28416	7104	24	1	0	0	0	380	1520	1805	0
28417	7104.25	24.25	1	0	0	0	380	1520	1805	0
28418	7104.5	24.5	1	0	0	0	380	1520	1805	0
28419	7104.75	24.75	1	0	0	0	380	1520	1805	0
28420	7105	25	1	0	0	0	380	1520	1805	0
28421	7105.25	25.25	0	0	0	0	380	1520	1805	0
28422	7105.5	25.5	0	0	0	0	380	1520	0	0
28423	7105.75	25.75	0	0	0	0	380	1520	0	0
28424	7106	26	0	0	0	0	380	1520	0	0
28425	7106.25	26.25	0	0	0	0	380	1520	0	0
28426	7106.5	26.5	0	0	0	0	380	1520	0	0
28427	7106.75	26.75	0	0	0	0	380	1520	0	0
28428	7107	27	0	0	0	0	380	1520	0	0
28429	7107.25	27.25	0	0	0	0	380	1520	0	0
28430	7107.5	27.5	0	0	0	0	380	1520	0	0
28431	7107.75	27.75	0	0	0	0	380	1520	0	0
28432	7108	28	0	0	0	0	380	1520	0	0
28433	7108.25	28.25	0	0	0	0	380	1520	0	0
28434	7108.5	28.5	0	0	0	0	380	1520	0	0
28435	7108.75	28.75	0	0	0	0	380	1520	0	0
28436	7109	29	0	0	0	0	380	1520	0	0
28437	7109.25	29.25	0	0	1	1	380	1520	0	0
28438	7109.5	29.5	0	0	1	1	380	1520	0	3800
28439	7109.75	29.75	0	0	1	1	380	1520	0	3800
28440	7110	30	0	0	1	1	380	1520	0	3800
28441	7110.25	30.25	0	0	1	1	380	1520	0	3800
28442	7110.5	30.5	0	0	1	1	380	1520	0	3800
28443	7110.75	30.75	0	0	1	1	380	1520	0	3800
28444	7111	31	0	0	1	1	380	1520	0	3800
28445	7111.25	31.25	0	0	1	1	380	1520	0	3800
28446	7111.5	31.5	0	0	1	1	380	1520	0	3800
28447	7111.75	31.75	0	0	1	1	380	1520	0	3800
28448	7112	32	0	0	1	1	380	1520	0	3800
28449	7112.25	32.25	0	0	1	1	380	1520	0	3800
28450	7112.5	32.5	0	0	1	1	380	1520	0	3800
28451	7112.75	32.75	0	0	1	1	380	1520	0	3800
28452	7113	33	0	0	1	1	380	1520	0	3800
28453	7113.25	33.25	0	0	1	1	380	1520	0	3800
28454	7113.5	33.5	0	0	1	1	380	1520	0	3800
28455	7113.75	33.75	0	0	1	1	380	1520	0	3800
28456	7114	34	0	0	1	1	380	1520	0	3800
28457	7114.25	34.25	0	0	1	1	380	1520	0	3800
28458	7114.5	34.5	0	0	1	1	380	1520	0	3800
28459	7114.75	34.75	0	0	1	1	380	1520	0	3800
28460	7115	35	0	0	1	1	380	1520	0	3800
28461	7115.25	35.25	0	0	1	1	380	1520	0	3800
28462	7115.5	35.5	0	0	1	1	380	1520	0	3800

Figure 54 - Loading Region (Part I)

Upstream								
Demand (LT)	Demand (TH)	Demand (Total)	Percent Left	Percent Through	Vehicles (TH-Lane 1)	Density (LT)	Density (TH)	Density (Total)
749.58	2998.31	3747.88	0.20	0.80	379.94	146.22	584.86	731.08
749.60	2998.41	3748.01	0.20	0.80	379.97	146.23	584.92	731.15
749.63	2998.52	3748.15	0.20	0.80	380.01	146.24	584.97	731.21
749.66	2998.62	3748.28	0.20	0.80	380.05	146.26	585.03	731.28
749.68	2998.73	3748.41	0.20	0.80	380.08	146.27	585.08	731.35
749.71	2998.83	3748.54	0.20	0.80	380.12	146.28	585.14	731.42
749.73	2998.94	3748.67	0.20	0.80	380.16	146.30	585.20	731.49
749.76	2999.04	3748.81	0.20	0.80	380.19	146.31	585.25	731.56
749.79	2999.15	3748.94	0.20	0.80	380.23	146.33	585.31	731.63
749.81	2999.26	3749.07	0.20	0.80	380.26	146.34	585.36	731.70
749.84	2999.36	3749.20	0.20	0.80	380.30	146.36	585.42	731.78
749.87	2999.47	3749.33	0.20	0.80	380.34	146.37	585.48	731.85
749.89	2999.57	3749.47	0.20	0.80	380.38	146.38	585.53	731.92
749.92	2999.68	3749.60	0.20	0.80	380.41	146.40	585.59	731.99
749.95	2999.78	3749.73	0.20	0.80	380.45	146.41	585.65	732.06
749.97	2999.89	3749.86	0.20	0.80	380.49	146.43	585.70	732.13
750.00	2999.99	3749.99	0.20	0.80	380.52	146.44	585.76	732.20
750.02	3000.10	3750.12	0.20	0.80	380.56	146.45	585.82	732.27
750.05	3000.21	3750.26	0.20	0.80	380.60	146.47	585.88	732.35
750.08	3000.31	3750.39	0.20	0.80	380.64	146.48	585.93	732.42
750.10	3000.42	3750.52	0.20	0.80	380.67	146.50	585.99	732.49
750.13	3000.52	3750.65	0.20	0.80	380.71	146.51	586.05	732.56
750.16	3000.63	3750.78	0.20	0.80	380.75	146.53	586.11	732.63
750.18	3000.73	3750.92	0.20	0.80	380.78	146.54	586.16	732.71
750.21	3000.84	3751.05	0.20	0.80	380.82	146.56	586.22	732.78
750.24	3000.94	3751.18	0.20	0.80	380.86	146.57	586.28	732.85
750.26	3001.05	3751.31	0.20	0.80	380.90	146.58	586.34	732.92
750.29	3001.16	3751.44	0.20	0.80	380.94	146.60	586.40	733.00
750.32	3001.26	3751.58	0.20	0.80	380.97	146.61	586.45	733.07
750.34	3001.37	3751.71	0.20	0.80	381.01	146.63	586.51	733.14
750.37	3001.47	3751.84	0.20	0.80	381.05	146.64	586.57	733.21
750.39	3001.58	3751.97	0.20	0.80	381.09	146.66	586.63	733.29
750.42	3001.68	3752.10	0.20	0.80	381.12	146.67	586.69	733.36
750.45	3001.79	3752.24	0.20	0.80	381.16	146.69	586.75	733.43
750.47	3001.89	3752.37	0.20	0.80	381.20	146.70	586.80	733.50
750.50	3002.00	3752.50	0.20	0.80	381.24	146.72	586.86	733.58
750.53	3002.11	3752.63	0.20	0.80	381.20	146.70	586.80	733.50
750.55	3002.21	3752.76	0.20	0.80	381.16	146.69	586.74	733.43
750.58	3002.32	3752.90	0.20	0.80	381.12	146.67	586.68	733.35
750.61	3002.42	3753.03	0.20	0.80	381.08	146.66	586.62	733.28
750.63	3002.53	3753.16	0.20	0.80	381.04	146.64	586.56	733.20
750.66	3002.63	3753.29	0.20	0.80	381.00	146.63	586.50	733.13
750.68	3002.74	3753.42	0.20	0.80	380.97	146.61	586.44	733.05
750.71	3002.84	3753.56	0.20	0.80	380.93	146.60	586.38	732.98
750.74	3002.95	3753.69	0.20	0.80	380.89	146.58	586.32	732.90
750.76	3003.06	3753.82	0.20	0.80	380.85	146.57	586.26	732.83
750.79	3003.16	3753.95	0.20	0.80	380.81	146.55	586.20	732.75
750.82	3003.27	3754.08	0.20	0.80	380.77	146.54	586.14	732.68
750.84	3003.37	3754.22	0.20	0.80	380.73	146.52	586.08	732.61
750.87	3003.48	3754.35	0.20	0.80	380.69	146.51	586.02	732.53
750.90	3003.58	3754.48	0.20	0.80	380.65	146.49	585.96	732.46
750.92	3003.69	3754.61	0.20	0.80	380.62	146.48	585.90	732.38
750.95	3003.79	3754.74	0.20	0.80	380.58	146.46	585.84	732.31
750.97	3003.90	3754.87	0.20	0.80	380.54	146.45	585.78	732.23
751.00	3004.01	3755.01	0.20	0.80	380.50	146.43	585.72	732.16
751.03	3004.11	3755.14	0.20	0.80	380.46	146.42	585.67	732.08
751.05	3004.22	3755.27	0.20	0.80	380.42	146.40	585.61	732.01

Figure 55 - Loading Region (Part II)

Vehicles (LT)	Vehicles (TH)	Vehicles (Total)	Out Flow (LT)	Out Flow (TH)	Out Flow (Total	Out Veh. (LT)	Out Veh. (TH)	Out Veh. (TH-Lane 1)	Out Veh. (Total)
					Min[Sat.Flow*lns, k_{us}*s*lns, (k_{jam}-k_{ds})*s*l_{ds}/dt				
257.82	1031.26	1289.08	29.00	116.02	145.02	491.74	1966.95	724.66	2458.68
257.84	1031.36	1289.20	28.01	112.06	140.07	491.74	1966.96	724.67	2458.69
257.86	1031.46	1289.32	27.06	108.23	135.28	491.74	1966.96	724.67	2458.70
257.89	1031.55	1289.44	26.13	104.53	130.66	491.74	1966.97	724.67	2458.71
257.91	1031.65	1289.57	25.24	100.95	126.19	491.74	1966.98	724.68	2458.72
257.94	1031.75	1289.69	24.37	97.49	121.87	491.75	1966.98	724.68	2458.73
257.96	1031.85	1289.81	23.54	94.15	117.69	491.75	1966.99	724.68	2458.74
257.99	1031.95	1289.94	22.73	90.93	113.66	491.75	1967.00	724.68	2458.75
258.01	1032.05	1290.06	21.95	87.81	109.76	491.75	1967.00	724.69	2458.75
258.04	1032.15	1290.18	21.20	84.80	106.00	491.75	1967.01	724.69	2458.76
258.06	1032.25	1290.31	20.47	81.89	102.36	491.75	1967.01	724.69	2458.77
258.09	1032.35	1290.43	19.77	79.08	98.85	491.75	1967.02	724.69	2458.77
258.11	1032.45	1290.56	19.09	76.36	95.45	491.76	1967.03	724.69	2458.78
258.14	1032.55	1290.68	18.43	73.74	92.17	491.76	1967.03	724.70	2458.79
258.16	1032.65	1290.81	17.80	71.20	89.00	491.76	1967.04	724.70	2458.79
258.19	1032.75	1290.94	17.19	68.76	85.94	491.76	1967.04	724.70	2458.80
258.21	1032.85	1291.06	16.60	66.39	82.99	491.76	1967.04	724.70	2458.81
258.24	1032.95	1291.19	16.03	64.11	80.13	491.76	1967.05	724.70	2458.81
258.26	1033.05	1291.31	15.47	61.90	77.37	491.76	1967.05	724.70	2458.82
258.29	1033.15	1291.44	14.94	59.77	74.71	491.76	1967.06	724.71	2458.82
258.31	1033.25	1291.57	14.43	57.71	72.14	491.77	1967.06	724.71	2458.83
258.34	1033.36	1291.69	13.93	55.72	69.65	491.77	1967.07	724.71	2458.83
258.36	1033.46	1291.82	13.45	53.80	67.25	491.77	1967.07	724.71	2458.84
258.39	1033.56	1291.95	12.99	51.95	64.93	491.77	1967.07	724.71	2458.84
258.42	1033.66	1292.08	12.54	50.16	62.70	491.77	1967.08	724.71	2458.85
258.44	1033.76	1292.20	12.11	48.43	60.53	491.77	1967.08	724.71	2458.85
258.47	1033.86	1292.33	11.69	46.76	58.45	491.77	1967.08	724.71	2458.85
258.49	1033.97	1292.46	11.29	45.14	56.43	491.77	1967.09	724.72	2458.86
258.52	1034.07	1292.59	10.90	43.58	54.48	491.77	1967.09	724.72	2458.86
258.54	1034.17	1292.72	10.52	42.08	52.60	491.77	1967.09	724.72	2458.86
258.57	1034.27	1292.84	10.16	40.63	50.78	491.77	1967.09	724.72	2458.87
258.59	1034.38	1292.97	9.81	39.22	49.03	491.77	1967.10	724.72	2458.87
258.62	1034.48	1293.10	9.47	37.87	47.34	491.77	1967.10	724.72	2458.87
258.65	1034.58	1293.23	9.14	36.56	45.70	491.78	1967.10	724.72	2458.88
258.67	1034.69	1293.36	8.82	35.30	44.12	491.78	1967.10	724.72	2458.88
258.70	1034.79	1293.49	760.00	3040.00	3800.00	491.83	1967.32	724.80	2459.15
258.67	1034.68	1293.35	760.00	3040.00	3800.00	491.88	1967.53	724.88	2459.41
258.64	1034.58	1293.22	760.00	3040.00	3800.00	491.93	1967.74	724.96	2459.67
258.62	1034.47	1293.09	760.00	3040.00	3800.00	491.99	1967.95	725.03	2459.94
258.59	1034.37	1292.96	760.00	3040.00	3800.00	492.04	1968.16	725.11	2460.20
258.57	1034.26	1292.83	760.00	3040.00	3800.00	492.09	1968.37	725.19	2460.46
258.54	1034.16	1292.70	760.00	3040.00	3800.00	492.15	1968.58	725.27	2460.73
258.51	1034.05	1292.56	760.00	3040.00	3800.00	492.20	1968.79	725.35	2460.99
258.49	1033.95	1292.43	760.00	3040.00	3800.00	492.25	1969.00	725.42	2461.26
258.46	1033.84	1292.30	760.00	3040.00	3800.00	492.30	1969.22	725.50	2461.52
258.43	1033.73	1292.17	760.00	3040.00	3800.00	492.36	1969.43	725.58	2461.78
258.41	1033.63	1292.04	760.00	3040.00	3800.00	492.41	1969.64	725.66	2462.05
258.38	1033.52	1291.90	760.00	3040.00	3800.00	492.46	1969.85	725.73	2462.31
258.35	1033.42	1291.77	760.00	3040.00	3800.00	492.52	1970.06	725.81	2462.58
258.33	1033.31	1291.64	760.00	3040.00	3800.00	492.57	1970.27	725.89	2462.84
258.30	1033.21	1291.51	760.00	3040.00	3800.00	492.62	1970.48	725.97	2463.10
258.28	1033.10	1291.38	760.00	3040.00	3800.00	492.67	1970.69	726.05	2463.37
258.25	1033.00	1291.24	760.00	3040.00	3800.00	492.73	1970.90	726.12	2463.63
258.22	1032.89	1291.11	760.00	3040.00	3800.00	492.78	1971.12	726.20	2463.90
258.20	1032.78	1290.98	760.00	3040.00	3800.00	492.83	1971.33	726.28	2464.16
258.17	1032.68	1290.85	760.00	3040.00	3800.00	492.88	1971.54	726.36	2464.42
258.14	1032.57	1290.72	760.00	3040.00	3800.00	492.94	1971.75	726.43	2464.69

Figure 56 - Queue Storage Region (Part I)

Queue Region									
Density (LT)	Density (TH)	Density (Total)	Vehicles (LT)	Vehicles (TH)	Percent Left	Percent Through	Vehicles (TH-Lane 1)	Vehicles (Total)	Density (Lane 1)
148.96	136.67	211.15	14.11	25.88	0.35	0.65	5.52	39.99	207.23
148.91	136.70	211.15	14.10	25.89	0.35	0.65	5.52	39.99	207.23
148.86	136.72	211.15	14.10	25.89	0.35	0.65	5.53	39.99	207.23
148.81	136.75	211.15	14.09	25.90	0.35	0.65	5.53	39.99	207.24
148.76	136.77	211.15	14.09	25.90	0.35	0.65	5.54	39.99	207.24
148.71	136.80	211.16	14.08	25.91	0.35	0.65	5.54	39.99	207.24
148.67	136.82	211.16	14.08	25.91	0.35	0.65	5.55	39.99	207.24
148.63	136.84	211.16	14.07	25.92	0.35	0.65	5.55	39.99	207.25
148.59	136.87	211.16	14.07	25.92	0.35	0.65	5.56	39.99	207.25
148.55	136.89	211.16	14.07	25.93	0.35	0.65	5.56	39.99	207.25
148.51	136.91	211.16	14.06	25.93	0.35	0.65	5.56	39.99	207.25
148.47	136.93	211.16	14.06	25.93	0.35	0.65	5.57	39.99	207.26
148.44	136.95	211.17	14.06	25.94	0.35	0.65	5.57	39.99	207.26
148.40	136.97	211.17	14.05	25.94	0.35	0.65	5.57	39.99	207.26
148.37	136.98	211.17	14.05	25.94	0.35	0.65	5.58	39.99	207.26
148.34	137.00	211.17	14.05	25.95	0.35	0.65	5.58	39.99	207.26
148.30	137.02	211.17	14.04	25.95	0.35	0.65	5.58	39.99	207.27
148.28	137.03	211.17	14.04	25.95	0.35	0.65	5.59	39.99	207.27
148.25	137.05	211.17	14.04	25.96	0.35	0.65	5.59	39.99	207.27
148.22	137.06	211.17	14.04	25.96	0.35	0.65	5.59	39.99	207.27
148.19	137.08	211.17	14.03	25.96	0.35	0.65	5.59	39.99	207.27
148.17	137.09	211.17	14.03	25.96	0.35	0.65	5.60	40.00	207.28
148.14	137.11	211.18	14.03	25.97	0.35	0.65	5.60	40.00	207.28
148.12	137.12	211.18	14.03	25.97	0.35	0.65	5.60	40.00	207.28
148.09	137.13	211.18	14.02	25.97	0.35	0.65	5.60	40.00	207.28
148.07	137.14	211.18	14.02	25.97	0.35	0.65	5.61	40.00	207.28
148.05	137.15	211.18	14.02	25.98	0.35	0.65	5.61	40.00	207.28
148.03	137.17	211.18	14.02	25.98	0.35	0.65	5.61	40.00	207.28
148.01	137.18	211.18	14.02	25.98	0.35	0.65	5.61	40.00	207.29
147.99	137.19	211.18	14.01	25.98	0.35	0.65	5.62	40.00	207.29
147.97	137.20	211.18	14.01	25.98	0.35	0.65	5.62	40.00	207.29
147.95	137.21	211.18	14.01	25.99	0.35	0.65	5.62	40.00	207.29
147.93	137.22	211.18	14.01	25.99	0.35	0.65	5.62	40.00	207.29
147.92	137.23	211.18	14.01	25.99	0.35	0.65	5.62	40.00	207.29
147.90	137.23	211.18	14.01	25.99	0.35	0.65	5.62	40.00	207.29
146.91	136.35	209.81	13.91	25.82	0.35	0.65	5.59	39.74	205.94
146.48	136.57	209.81	13.87	25.87	0.35	0.65	5.63	39.74	205.95
146.04	136.79	209.81	13.83	25.91	0.35	0.65	5.67	39.74	205.96
145.61	137.00	209.81	13.79	25.95	0.35	0.65	5.72	39.74	205.97
145.18	137.21	209.81	13.75	25.99	0.35	0.65	5.76	39.74	205.99
144.76	137.43	209.81	13.71	26.03	0.34	0.66	5.80	39.74	206.00
144.34	137.64	209.81	13.67	26.07	0.34	0.66	5.84	39.74	206.01
143.92	137.85	209.81	13.63	26.11	0.34	0.66	5.88	39.74	206.02
143.50	138.06	209.81	13.59	26.15	0.34	0.66	5.92	39.74	206.03
143.09	138.26	209.81	13.55	26.19	0.34	0.66	5.96	39.74	206.04
142.68	138.47	209.81	13.51	26.22	0.34	0.66	6.00	39.74	206.05
142.27	138.67	209.81	13.47	26.26	0.34	0.66	6.04	39.74	206.06
141.87	138.87	209.81	13.43	26.30	0.34	0.66	6.08	39.74	206.07
141.46	139.07	209.81	13.40	26.34	0.34	0.66	6.12	39.74	206.08
141.07	139.27	209.81	13.36	26.38	0.34	0.66	6.16	39.74	206.09
140.67	139.47	209.81	13.32	26.42	0.34	0.66	6.20	39.74	206.10
140.28	139.67	209.81	13.28	26.45	0.33	0.67	6.23	39.74	206.12
139.88	139.86	209.81	13.25	26.49	0.33	0.67	6.27	39.74	206.13
139.50	140.06	209.81	13.21	26.53	0.33	0.67	6.31	39.74	206.14
139.11	140.25	209.81	13.17	26.56	0.33	0.67	6.35	39.74	206.15
138.73	140.44	209.81	13.14	26.60	0.33	0.67	6.39	39.74	206.16
138.35	140.63	209.81	13.10	26.63	0.33	0.67	6.42	39.74	206.17

Figure 57 - Queue Storage Region (Part II)

Spillback Flag	Blockage Flag	Out Flow (LT)	Out Flow (TH)	Out Flow (Total)	Out Veh. (LT)	Out Veh. (TH)	Out Veh. (TH-Lane 1)	Out Veh. (Total)
0.00	0.00	100.69	39.38	140.07	477.64	1941.06	430.78	2418.69
0.00	0.00	97.21	38.07	135.28	477.64	1941.06	430.78	2418.70
0.00	0.00	93.85	36.81	130.66	477.65	1941.06	430.79	2418.71
0.00	0.00	90.61	35.58	126.19	477.66	1941.07	430.79	2418.72
0.00	0.00	87.48	34.39	121.87	477.66	1941.07	430.79	2418.73
0.00	0.00	84.45	33.24	117.69	477.67	1941.07	430.79	2418.74
0.00	0.00	81.54	32.12	113.66	477.67	1941.07	430.79	2418.75
0.00	0.00	78.72	31.05	109.76	477.68	1941.07	430.79	2418.75
0.00	0.00	75.99	30.00	106.00	477.68	1941.08	430.79	2418.76
0.00	0.00	73.37	28.99	102.36	477.69	1941.08	430.79	2418.77
0.00	0.00	70.83	28.02	98.85	477.69	1941.08	430.79	2418.77
0.00	0.00	68.38	27.07	95.45	477.70	1941.08	430.79	2418.78
0.00	0.00	66.01	26.16	92.17	477.70	1941.08	430.79	2418.79
0.00	0.00	63.73	25.28	89.00	477.71	1941.09	430.79	2418.79
0.00	0.00	61.52	24.42	85.94	477.71	1941.09	430.79	2418.80
0.00	0.00	59.39	23.60	82.99	477.72	1941.09	430.79	2418.81
0.00	0.00	57.34	22.80	80.13	477.72	1941.09	430.79	2418.81
0.00	0.00	55.35	22.02	77.37	477.72	1941.09	430.79	2418.82
0.00	0.00	53.44	21.28	74.71	477.73	1941.09	430.79	2418.82
0.00	0.00	51.59	20.55	72.14	477.73	1941.10	430.79	2418.83
0.00	0.00	49.80	19.85	69.65	477.73	1941.10	430.79	2418.83
0.00	0.00	48.07	19.18	67.25	477.74	1941.10	430.79	2418.84
0.00	0.00	46.41	18.53	64.93	477.74	1941.10	430.79	2418.84
0.00	0.00	44.80	17.89	62.70	477.74	1941.10	430.79	2418.85
0.00	0.00	43.25	17.28	60.53	477.75	1941.10	430.79	2418.85
0.00	0.00	41.75	16.70	58.45	477.75	1941.10	430.79	2418.85
0.00	0.00	40.30	16.13	56.43	477.75	1941.10	430.79	2418.86
0.00	0.00	38.91	15.57	54.48	477.76	1941.11	430.79	2418.86
0.00	0.00	37.56	15.04	52.60	477.76	1941.11	430.79	2418.86
0.00	0.00	36.26	14.53	50.78	477.76	1941.11	430.80	2418.87
0.00	0.00	35.00	14.03	49.03	477.76	1941.11	430.80	2418.87
0.00	0.00	33.79	13.55	47.34	477.77	1941.11	430.80	2418.87
0.00	0.00	32.61	13.09	45.70	477.77	1941.11	430.80	2418.88
0.00	0.00	31.48	12.64	44.12	477.77	1941.11	430.80	2418.88
0.00	0.00	1355.63	2444.37	3800.00	477.86	1941.28	430.83	2419.15
0.00	0.00	1355.41	2444.59	3800.00	477.96	1941.45	430.87	2419.41
0.00	0.00	1351.30	2448.70	3800.00	478.05	1941.62	430.91	2419.67
0.00	0.00	1347.23	2452.77	3800.00	478.15	1941.79	430.94	2419.94
0.00	0.00	1343.18	2456.82	3800.00	478.24	1941.96	430.98	2420.20
0.00	0.00	1339.16	2460.84	3800.00	478.33	1942.13	431.02	2420.46
0.00	0.00	1335.17	2464.83	3800.00	478.42	1942.30	431.06	2420.73
0.00	0.00	1331.21	2468.79	3800.00	478.52	1942.48	431.10	2420.99
0.00	0.00	1327.28	2472.72	3800.00	478.61	1942.65	431.13	2421.26
0.00	0.00	1323.37	2476.63	3800.00	478.70	1942.82	431.17	2421.52
0.00	0.00	1319.49	2480.51	3800.00	478.79	1942.99	431.21	2421.78
0.00	0.00	1315.64	2484.36	3800.00	478.88	1943.16	431.25	2422.05
0.00	0.00	1311.81	2488.19	3800.00	478.98	1943.34	431.29	2422.31
0.00	0.00	1308.01	2491.99	3800.00	479.07	1943.51	431.33	2422.58
0.00	0.00	1304.24	2495.76	3800.00	479.16	1943.68	431.37	2422.84
0.00	0.00	1300.50	2499.50	3800.00	479.25	1943.86	431.41	2423.10
0.00	0.00	1296.78	2503.22	3800.00	479.34	1944.03	431.45	2423.37
0.00	0.00	1293.08	2506.92	3800.00	479.43	1944.20	431.49	2423.63
0.00	0.00	1289.41	2510.59	3800.00	479.52	1944.38	431.54	2423.90
0.00	0.00	1285.77	2514.23	3800.00	479.61	1944.55	431.58	2424.16
0.00	0.00	1282.16	2517.84	3800.00	479.69	1944.73	431.62	2424.42
0.00	0.00	1278.56	2521.44	3800.00	479.78	1944.90	431.66	2424.69
0.00	0.00	1275.00	2525.00	3800.00	479.87	1945.08	431.70	2424.95

Figure 58 - Gate (Part I)

Gate							
Density (LT)	Density (TH)	Density (Total)	Vehicles (LT)	Vehicles (TH)	Vehicles (TH-Lane 1)	Vehicles (Total)	Receiving Density (Lane 1)
14.94	202.70	210.17	0.07	1.92	0.92	1.99	209.15
14.43	202.99	210.21	0.07	1.92	0.93	1.99	209.22
13.94	203.27	210.24	0.07	1.92	0.93	1.99	209.28
13.46	203.54	210.27	0.06	1.93	0.93	1.99	209.35
13.01	203.80	210.31	0.06	1.93	0.93	1.99	209.41
12.56	204.06	210.34	0.06	1.93	0.93	1.99	209.47
12.13	204.30	210.37	0.06	1.93	0.94	1.99	209.53
11.72	204.53	210.40	0.06	1.94	0.94	1.99	209.59
11.32	204.76	210.42	0.05	1.94	0.94	1.99	209.65
10.93	204.98	210.45	0.05	1.94	0.94	1.99	209.70
10.56	205.20	210.48	0.05	1.94	0.95	1.99	209.75
10.20	205.40	210.50	0.05	1.95	0.95	1.99	209.80
9.85	205.60	210.52	0.05	1.95	0.95	1.99	209.85
9.51	205.79	210.55	0.05	1.95	0.95	1.99	209.89
9.19	205.98	210.57	0.04	1.95	0.95	1.99	209.94
8.87	206.16	210.59	0.04	1.95	0.95	1.99	209.98
8.57	206.33	210.61	0.04	1.95	0.96	1.99	210.02
8.27	206.50	210.63	0.04	1.96	0.96	1.99	210.07
7.99	206.66	210.65	0.04	1.96	0.96	1.99	210.10
7.72	206.81	210.67	0.04	1.96	0.96	1.99	210.14
7.45	206.96	210.69	0.04	1.96	0.96	2.00	210.18
7.19	207.11	210.71	0.03	1.96	0.96	2.00	210.21
6.95	207.25	210.72	0.03	1.96	0.96	2.00	210.25
6.71	207.39	210.74	0.03	1.96	0.97	2.00	210.28
6.48	207.52	210.76	0.03	1.97	0.97	2.00	210.31
6.25	207.64	210.77	0.03	1.97	0.97	2.00	210.34
6.04	207.77	210.79	0.03	1.97	0.97	2.00	210.37
5.83	207.88	210.80	0.03	1.97	0.97	2.00	210.40
5.63	208.00	210.81	0.03	1.97	0.97	2.00	210.43
5.44	208.11	210.83	0.03	1.97	0.97	2.00	210.46
5.25	208.22	210.84	0.02	1.97	0.97	2.00	210.48
5.07	208.32	210.85	0.02	1.97	0.97	2.00	210.51
4.89	208.42	210.86	0.02	1.97	0.97	2.00	210.53
4.72	208.51	210.88	0.02	1.97	0.98	2.00	210.55
4.56	181.05	183.33	0.02	1.71	0.85	1.74	155.47
23.75	171.46	183.33	0.11	1.62	0.75	1.74	155.47
40.01	163.33	183.33	0.19	1.55	0.67	1.74	155.47
53.71	156.48	183.33	0.25	1.48	0.61	1.74	155.47
65.24	150.71	183.33	0.31	1.43	0.55	1.74	155.47
74.93	145.87	183.33	0.35	1.38	0.50	1.74	155.47
83.06	141.80	183.33	0.39	1.34	0.46	1.74	155.47
89.86	138.40	183.33	0.43	1.31	0.43	1.74	155.47
95.55	135.56	183.33	0.45	1.28	0.40	1.74	155.47
100.29	133.19	183.33	0.47	1.26	0.38	1.74	155.47
104.23	131.22	183.33	0.49	1.24	0.36	1.74	155.47
107.50	129.58	183.33	0.51	1.23	0.35	1.74	155.47
110.20	128.23	183.33	0.52	1.21	0.33	1.74	155.47
112.42	127.12	183.33	0.53	1.20	0.32	1.74	155.47
114.24	126.21	183.33	0.54	1.20	0.31	1.74	155.47
115.71	125.48	183.33	0.55	1.19	0.31	1.74	155.47
116.90	124.88	183.33	0.55	1.18	0.30	1.74	155.47
117.85	124.41	183.33	0.56	1.18	0.30	1.74	155.47
118.59	124.04	183.33	0.56	1.17	0.29	1.74	155.47
119.17	123.75	183.33	0.56	1.17	0.29	1.74	155.47
119.60	123.54	183.33	0.57	1.17	0.29	1.74	155.47
119.90	123.38	183.33	0.57	1.17	0.29	1.74	155.47
120.11	123.28	183.33	0.57	1.17	0.28	1.74	155.47

Figure 59 - Gate (Part II)

Spillback Flag	Blockage Flag	Out Flow (LT)	Out Flow (TH)	Out Flow (Total)	Out Veh. (LT)	Out Veh. (TH)	Out Veh. (TH-Lane 1)	Out Veh. (Total)
0.00	0.00	135.28	0.00	135.28	477.57	1939.14	183.07	2416.70
0.00	0.00	130.66	0.00	130.66	477.58	1939.14	183.07	2416.71
0.00	0.00	126.19	0.00	126.19	477.59	1939.14	183.07	2416.72
0.00	0.00	121.87	0.00	121.87	477.59	1939.14	183.07	2416.73
0.00	0.00	117.69	0.00	117.69	477.60	1939.14	183.07	2416.74
0.00	0.00	113.66	0.00	113.66	477.61	1939.14	183.07	2416.75
0.00	0.00	109.76	0.00	109.76	477.62	1939.14	183.07	2416.75
0.00	0.00	106.00	0.00	106.00	477.62	1939.14	183.07	2416.76
0.00	0.00	102.36	0.00	102.36	477.63	1939.14	183.07	2416.77
0.00	0.00	98.85	0.00	98.85	477.64	1939.14	183.07	2416.77
0.00	0.00	95.45	0.00	95.45	477.65	1939.14	183.07	2416.78
0.00	0.00	92.17	0.00	92.17	477.65	1939.14	183.07	2416.79
0.00	0.00	89.00	0.00	89.00	477.66	1939.14	183.07	2416.79
0.00	0.00	85.94	0.00	85.94	477.66	1939.14	183.07	2416.80
0.00	0.00	82.99	0.00	82.99	477.67	1939.14	183.07	2416.81
0.00	0.00	80.13	0.00	80.13	477.68	1939.14	183.07	2416.81
0.00	0.00	77.37	0.00	77.37	477.68	1939.14	183.07	2416.82
0.00	0.00	74.71	0.00	74.71	477.69	1939.14	183.07	2416.82
0.00	0.00	72.14	0.00	72.14	477.69	1939.14	183.07	2416.83
0.00	0.00	69.65	0.00	69.65	477.70	1939.14	183.07	2416.83
0.00	0.00	67.25	0.00	67.25	477.70	1939.14	183.07	2416.84
0.00	0.00	64.93	0.00	64.93	477.70	1939.14	183.07	2416.84
0.00	0.00	62.70	0.00	62.70	477.71	1939.14	183.07	2416.85
0.00	0.00	60.53	0.00	60.53	477.71	1939.14	183.07	2416.85
0.00	0.00	58.45	0.00	58.45	477.72	1939.14	183.07	2416.85
0.00	0.00	56.43	0.00	56.43	477.72	1939.14	183.07	2416.86
0.00	0.00	54.48	0.00	54.48	477.73	1939.14	183.07	2416.86
0.00	0.00	52.60	0.00	52.60	477.73	1939.14	183.07	2416.86
0.00	0.00	50.78	0.00	50.78	477.73	1939.14	183.07	2416.87
0.00	0.00	49.03	0.00	49.03	477.74	1939.14	183.07	2416.87
0.00	0.00	47.34	0.00	47.34	477.74	1939.14	183.07	2416.87
0.00	0.00	45.70	0.00	45.70	477.74	1939.14	183.07	2416.88
0.00	0.00	44.12	0.00	44.12	477.75	1939.14	183.07	2416.88
0.00	0.00	42.60	3757.40	3800.00	477.75	1939.40	183.20	2417.15
0.00	0.00	47.31	3752.69	3800.00	477.75	1939.66	183.33	2417.41
0.00	0.00	246.98	3553.02	3800.00	477.77	1939.90	183.45	2417.67
0.00	0.00	417.02	3382.98	3800.00	477.80	1940.14	183.55	2417.94
0.00	0.00	560.96	3239.04	3800.00	477.84	1940.36	183.64	2418.20
0.00	0.00	682.54	3117.46	3800.00	477.88	1940.58	183.72	2418.46
0.00	0.00	785.01	3014.99	3800.00	477.94	1940.79	183.80	2418.73
0.00	0.00	871.18	2928.82	3800.00	478.00	1940.99	183.87	2418.99
0.00	0.00	943.49	2856.51	3800.00	478.06	1941.19	183.94	2419.26
0.00	0.00	1004.03	2795.97	3800.00	478.13	1941.39	184.00	2419.52
0.00	0.00	1054.57	2745.43	3800.00	478.21	1941.58	184.06	2419.78
0.00	0.00	1096.66	2703.34	3800.00	478.28	1941.76	184.11	2420.05
0.00	0.00	1131.58	2668.42	3800.00	478.36	1941.95	184.16	2420.31
0.00	0.00	1160.45	2639.55	3800.00	478.44	1942.13	184.21	2420.58
0.00	0.00	1184.21	2615.79	3800.00	478.53	1942.31	184.26	2420.84
0.00	0.00	1203.66	2596.34	3800.00	478.61	1942.49	184.31	2421.10
0.00	0.00	1219.46	2580.54	3800.00	478.69	1942.67	184.35	2421.37
0.00	0.00	1232.20	2567.80	3800.00	478.78	1942.85	184.40	2421.63
0.00	0.00	1242.36	2557.64	3800.00	478.87	1943.03	184.44	2421.90
0.00	0.00	1250.34	2549.66	3800.00	478.95	1943.21	184.49	2422.16
0.00	0.00	1256.48	2543.52	3800.00	479.04	1943.38	184.53	2422.42
0.00	0.00	1261.09	2538.91	3800.00	479.13	1943.56	184.57	2422.69
0.00	0.00	1264.41	2535.59	3800.00	479.21	1943.74	184.62	2422.95
0.00	0.00	1266.63	2533.37	3800.00	479.30	1943.91	184.66	2423.21

Figure 60 - Pocket

Downstream						Left	Through
Density (LT)	Density (TH)	Vehicles (LT)	Vehicles (TH)	Out Flow (LT)	Out Flow (TH)	Out Veh. (LT)	Out Veh. (TH)
7.36	211.20	0.14	8.00	220.75	0.00	477.43	1931.14
7.04	211.20	0.13	8.00	211.35	0.00	477.45	1931.14
6.75	211.20	0.13	8.00	202.47	0.00	477.46	1931.14
6.47	211.20	0.12	8.00	194.08	0.00	477.48	1931.14
6.20	211.20	0.12	8.00	186.14	0.00	477.49	1931.14
5.95	211.20	0.11	8.00	178.61	0.00	477.50	1931.14
5.72	211.20	0.11	8.00	171.46	0.00	477.51	1931.14
5.49	211.20	0.10	8.00	164.68	0.00	477.53	1931.14
5.27	211.20	0.10	8.00	158.22	0.00	477.54	1931.14
5.07	211.20	0.10	8.00	152.08	0.00	477.55	1931.14
4.87	211.20	0.09	8.00	146.22	0.00	477.56	1931.14
4.69	211.20	0.09	8.00	140.64	0.00	477.57	1931.14
4.51	211.20	0.09	8.00	135.31	0.00	477.58	1931.14
4.34	211.20	0.08	8.00	130.21	0.00	477.58	1931.14
4.18	211.20	0.08	8.00	125.34	0.00	477.59	1931.14
4.02	211.20	0.08	8.00	120.68	0.00	477.60	1931.14
3.87	211.20	0.07	8.00	0.00	0.00	477.60	1931.14
4.16	211.20	0.08	8.00	0.00	0.00	477.60	1931.14
4.43	211.20	0.08	8.00	0.00	0.00	477.60	1931.14
4.70	211.20	0.09	8.00	0.00	0.00	477.60	1931.14
4.95	211.20	0.09	8.00	0.00	0.00	477.60	1931.14
5.20	211.20	0.10	8.00	0.00	0.00	477.60	1931.14
5.44	211.20	0.10	8.00	0.00	0.00	477.60	1931.14
5.67	211.20	0.11	8.00	0.00	0.00	477.60	1931.14
5.89	211.20	0.11	8.00	0.00	0.00	477.60	1931.14
6.10	211.20	0.12	8.00	0.00	0.00	477.60	1931.14
6.31	211.20	0.12	8.00	0.00	0.00	477.60	1931.14
6.51	211.20	0.12	8.00	0.00	0.00	477.60	1931.14
6.70	211.20	0.13	8.00	0.00	0.00	477.60	1931.14
6.89	211.20	0.13	8.00	0.00	0.00	477.60	1931.14
7.07	211.20	0.13	8.00	0.00	0.00	477.60	1931.14
7.24	211.20	0.14	8.00	0.00	0.00	477.60	1931.14
7.41	211.20	0.14	8.00	0.00	3800.00	477.60	1931.40
7.57	204.23	0.14	7.74	0.00	3800.00	477.60	1931.66
7.73	204.16	0.15	7.73	0.00	3800.00	477.60	1931.93
7.90	204.07	0.15	7.73	0.00	3800.00	477.60	1932.19
8.81	203.62	0.17	7.71	0.00	3800.00	477.60	1932.46
10.34	202.85	0.20	7.68	0.00	3800.00	477.60	1932.72
12.39	201.82	0.23	7.64	0.00	3800.00	477.60	1932.98
14.89	200.57	0.28	7.60	0.00	3800.00	477.60	1933.25
17.77	199.13	0.34	7.54	0.00	3800.00	477.60	1933.51
20.97	197.54	0.40	7.48	0.00	3800.00	477.60	1933.77
24.43	195.81	0.46	7.42	0.00	3800.00	477.60	1934.04
28.11	193.96	0.53	7.35	0.00	3800.00	477.60	1934.30
31.98	192.03	0.61	7.27	0.00	3800.00	477.60	1934.57
36.00	190.02	0.68	7.20	0.00	3800.00	477.60	1934.83
40.15	187.95	0.76	7.12	0.00	3800.00	477.60	1935.09
44.40	185.82	0.84	7.04	0.00	3800.00	477.60	1935.36
48.74	183.65	0.92	6.96	0.00	3800.00	477.60	1935.62
53.16	181.44	1.01	6.87	0.00	3800.00	477.60	1935.89
57.63	179.21	1.09	6.79	0.00	3800.00	477.60	1936.15
62.15	176.95	1.18	6.70	0.00	3800.00	477.60	1936.41
66.70	174.67	1.26	6.62	0.00	3800.00	477.60	1936.68
71.29	172.38	1.35	6.53	0.00	3800.00	477.60	1936.94
75.89	170.07	1.44	6.44	0.00	3800.00	477.60	1937.21
80.52	167.76	1.52	6.35	0.00	3800.00	477.60	1937.47
85.15	165.44	1.61	6.27	0.00	3800.00	477.60	1937.73

APPENDIX B: ADDITIONAL MODEL COMPARISON RESULTS

Figure 61 - Model Comparison (Single Through Lane - Phase a)

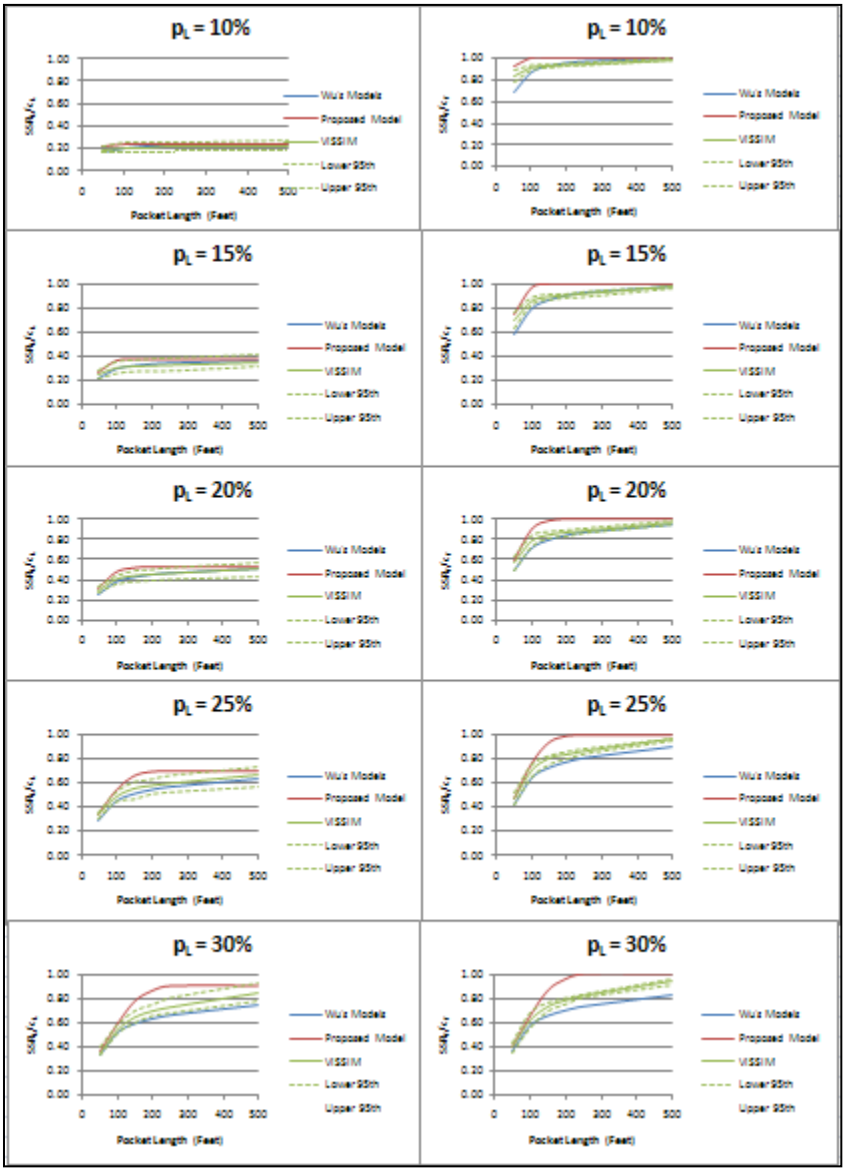

Figure 62 - Model Comparison (Two Through Lanes - Phase a)

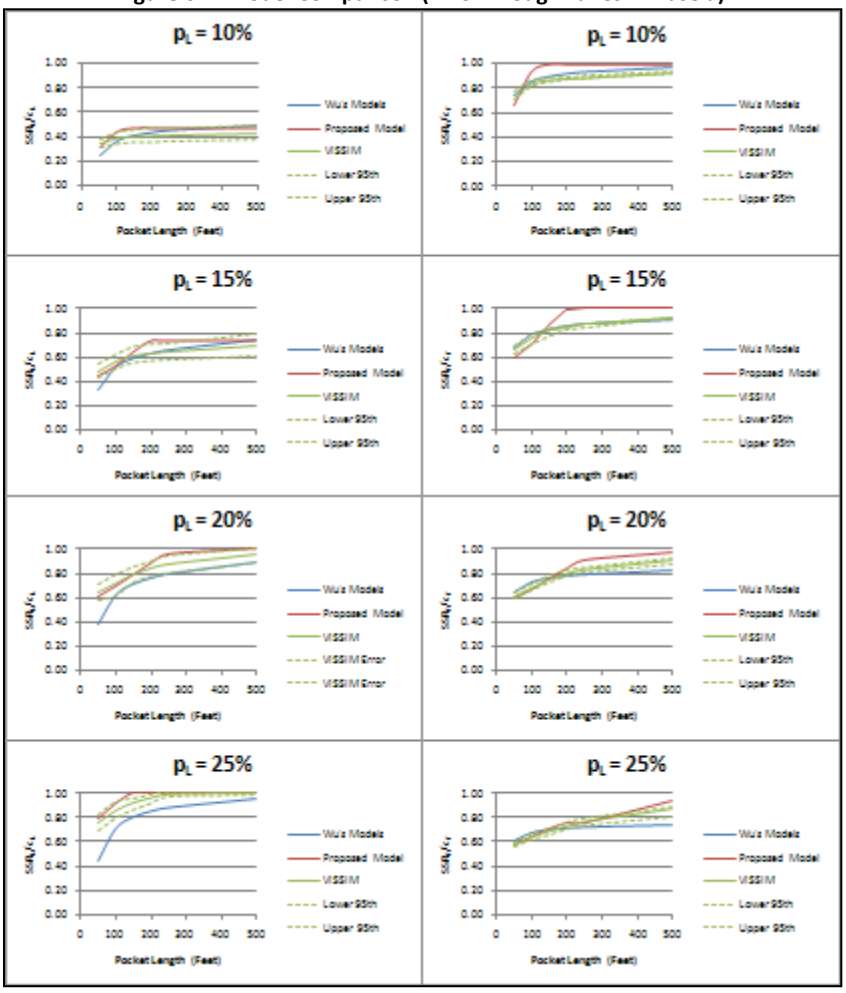

Figure 63 - Model Comparison (Single Through Lane - Phase b)

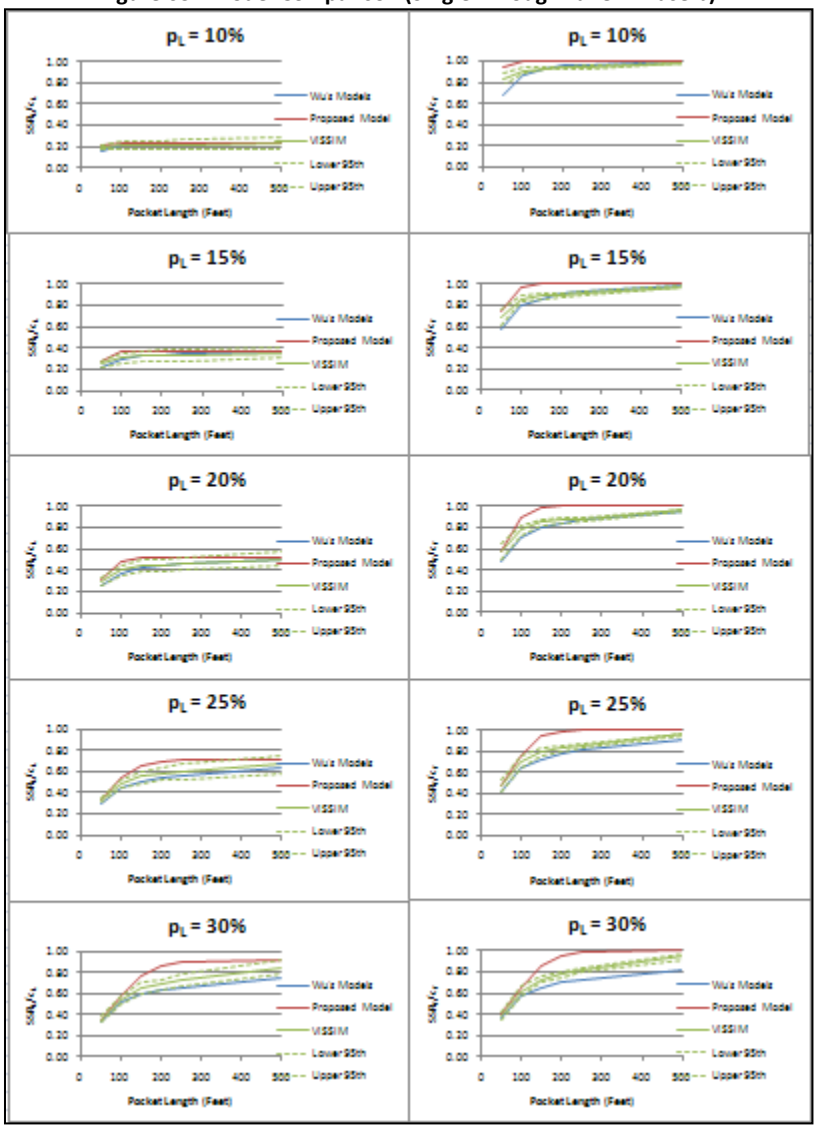

Figure 64 - Model Comparison (Two Through Lanes - Phase b)

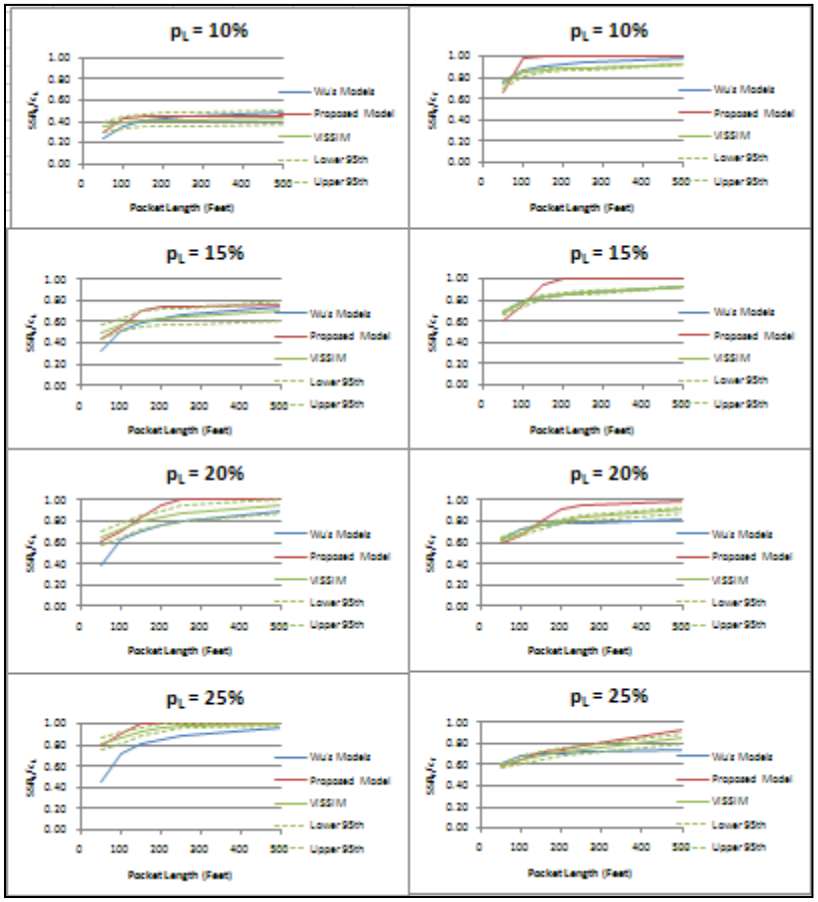

Figure 65 - Model Comparison (Single Through Lane - Phase c)

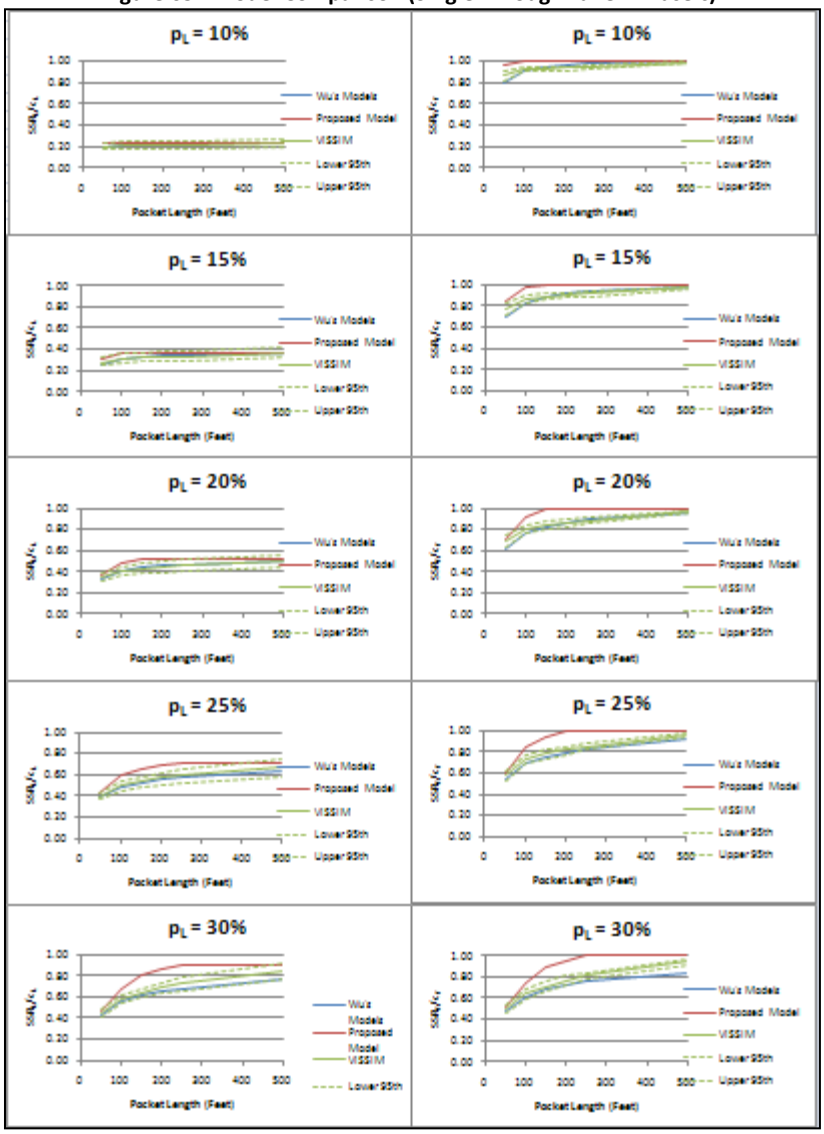

Figure 66 - Model Comparison (Two Through Lanes - Phase c)

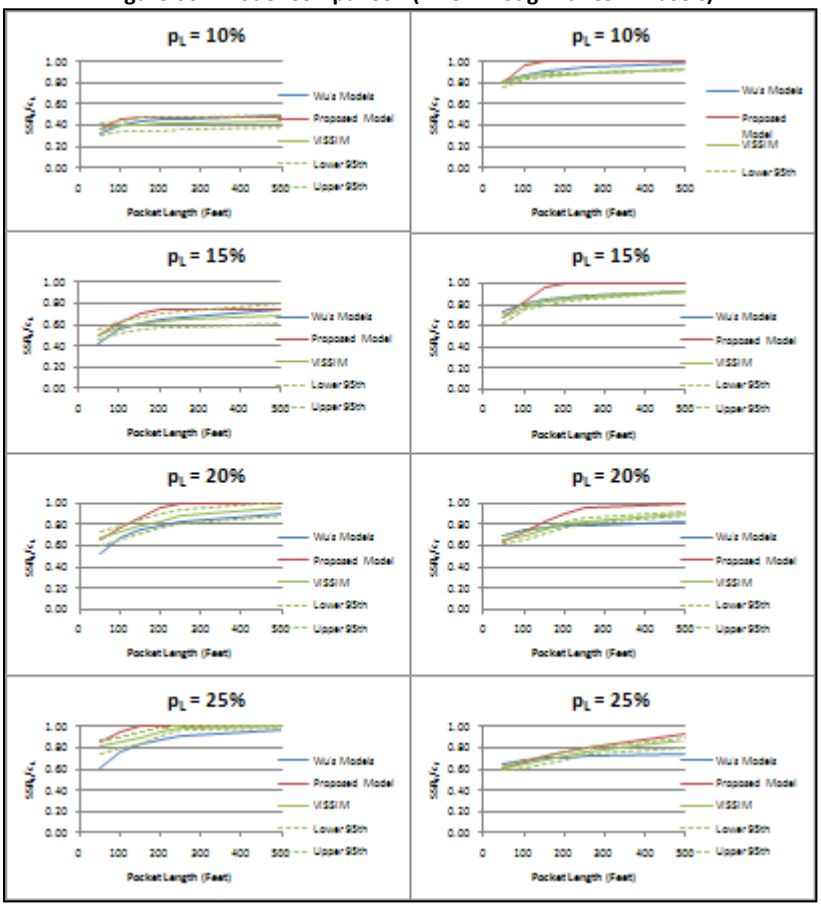

Figure 67 - Model Comparison (Single Through Lanes - Phase e)

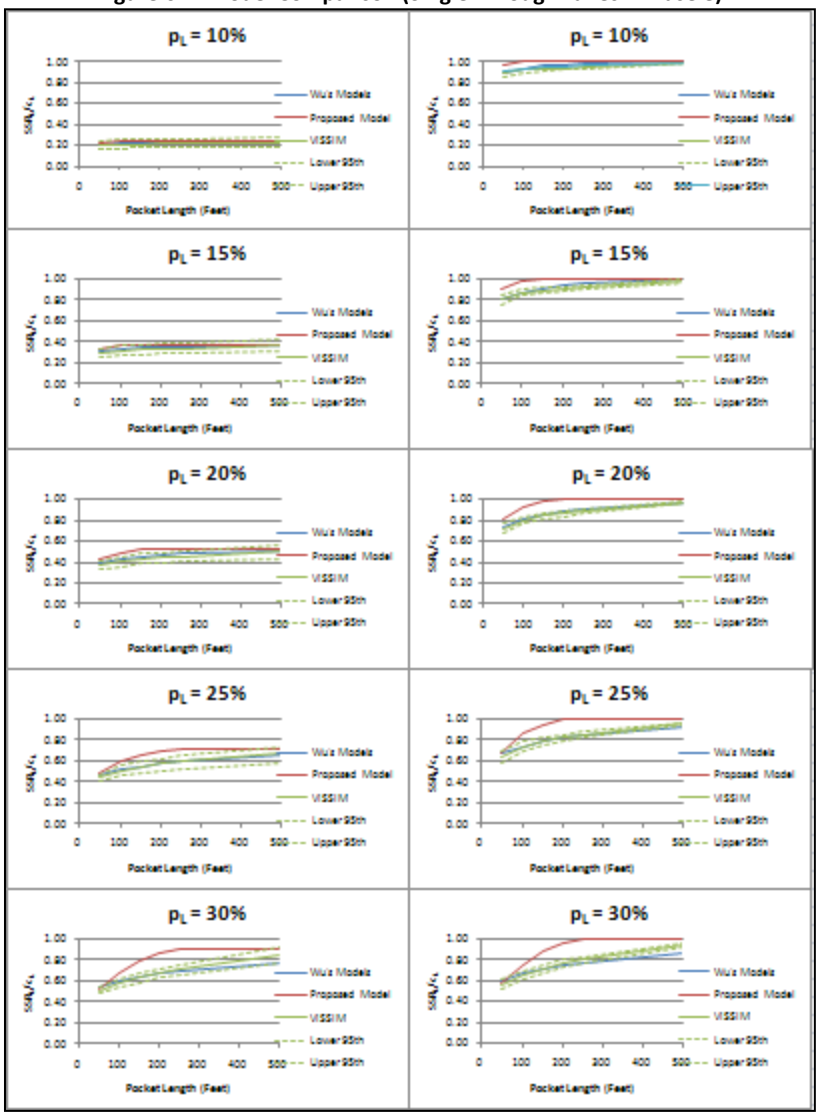

Figure 68 - Model Comparison (Two Through Lanes - Phase e)